

THESIS

WATER QUALITY BENEFITS OF WETLANDS UNDER HISTORIC AND POTENTIAL
FUTURE CLIMATE IN THE SPRAGUE RIVER WATERSHED, OREGON

Submitted by

Rosemary M. Records

Department of Geosciences

In partial fulfillment of the requirements

For the Degree of Master of Science

Colorado State University

Fort Collins, Colorado

Fall 2013

Master's Committee:

Advisor: Steven Fassnacht
Co-Advisor: Mazdak Arabi

Walter Duffy
Greg Butters

Copyright by Rosemary Records 2013

All Rights Reserved

ABSTRACT

WATER QUALITY BENEFITS OF WETLANDS UNDER HISTORIC AND POTENTIAL FUTURE CLIMATE IN THE SPRAGUE RIVER WATERSHED, OREGON

An understanding of potential climate-induced changes in stream sediment and nutrient fluxes is important for the long-term success of regulatory programs such as the Total Maximum Daily Load and sustainability of aquatic ecosystems. Such changes are still not well characterized, particularly in the Pacific Northwest, although shifts in stream flow associated with warming temperatures have already been observed in the region. Conservation practices such as wetland restoration are often regarded as important in watershed-scale management of water quality. However, the potential of wetland gains or losses to alter future stream water quality conditions has received relatively little study.

The primary goal of this research is to assess the basin-scale regulation of sediment, nitrogen and phosphorus provided by variable wetland extent under current climate and potential mid-21st century climate. Specific objectives of the study are (1) to evaluate the effects of present-day wetlands on stream water quality under current climate; (2) to identify direction and magnitude of potential changes in stream flow, sediment, and nutrient loads under present-day wetlands and potential future climate; and (3) to determine how wetland gain or loss might exacerbate or ameliorate climate-induced changes in future water quality.

These objectives are investigated with the Soil and Water Assessment Tool (SWAT) hydrologic model in the Sprague River watershed in southern Oregon, United States, which has been historically snowmelt dominated and where elevated nutrient loads in the 20th century have contributed to decline of fish species downstream. Results suggest that present-day wetlands under current climate may result in substantially lower nitrogen and phosphorus loads at the Sprague River watershed outlet. SWAT

simulations forced with precipitation and temperature from six General Circulation Model (GCM) derived climate projections for 2030-2059 suggest uncertainty in magnitude and direction of both precipitation and stream flow changes on an average annual and monthly basis. Under present-day wetland extent, long-term average annual runoff for 2030-2059 decreased by 4% under one projection relative to a baseline period of 1954-2005, but increased by 6-31% under other projections. However, change in future annual runoff was statistically different from baseline for only two of six climate projections.

Late spring and summer stream flow was lower in all simulations but significantly different from baseline in only some cases; for simulations driven with wetter future climate projections average monthly flow increased significantly from approximately October through March, and peak average monthly flow increased from 3-36% but timing did not alter. A simulation driven with a drier future climate projection showed decreases in average flow for most months, but was not significantly different from baseline. Simulated average annual sediment and nutrient loads generally tracked flow seasonality and decreased by 6% (sediment), 8% (TN) and 11% (TP) under one projection, but increased from 7-52% (sediment), 4-37% (TN) and 1-38% (TP) under other projections. Findings suggest that nutrient loads at the Sprague River outlet under future climate and scenarios of wetland change could vary significantly from baseline, or could be similar to the historic period. However, a threshold of wetland loss may exist beyond which large increases in nutrient loads could occur, and wetland gain might do little to ameliorate climate impacts to stream water quality in the Sprague River watershed.

ACKNOWLEDGEMENTS

I would like to thank the U.S. Department of Agriculture Conservation Effects Assessment Project (CEAP-Wetlands), the California Cooperative Fish and Wildlife Research Unit, and Humboldt and Colorado State Universities for their financial and administrative support of this research. This work was made possible through the guidance and input of many people, particularly of my co-advisers Mazdak Arabi and Steven Fassnacht, my committee member Walter Duffy, and the CEAP-Wetlands Director Bill Effland. Katherine Hegewisch, University of Idaho, provided the downscaled climate projections used in this study, undertook bias-correction of projections to meteorological stations, and offered prompt and thorough guidance in use and application of the data. Sharon Kahara, Michael Hughes, Joseph Quansah, Steven Faulkner, Susan Marshall and Andre Lehre encouraged graduate research in the topics discussed here and provided invaluable feedback, data and technical assistance. Soil and Water Assessment Tool (SWAT) developers, staff and users offered swift technical support and modeling advice. The North Central Climate Science Center and the Northwest Climate Science Center made possible my attendance at an informative workshop for early career climate impact researchers.

I am very appreciative of the generosity of Klamath Basin agencies and individuals with their time, data, and expertise, including but not limited to Larry Dunsmoor and Kris Fischer of the Klamath Tribes for data used in calibration and testing of this model; Chantell Royer and members of the Klamath Basin Monitoring Program; Marshall Gannett, John Risley and other U.S. Geological Survey researchers; David Ferguson, Natural Resources Conservation Service Klamath Falls Service Center; Shannon Peterson and the Klamath Basin Rangeland Trust; Graham Matthews and Cort Pryor of Graham Matthews and Associates; and Amy Gowan and Richard Ford of Fremont-Winema National Forest.

I greatly appreciate the assistance and friendship of members of the Arabi, Fassnacht, Roesner, and Gates labs at Colorado State University. In particular, Mehdi Ahmadi and Haw Yen developed and

refined many of the tools used to calibrate the model and helped overcome technical difficulties; Tyler Wible and Jeff Ditty provided coding assistance; and Meagan Smith, Niah Venable and their families offered everything from proof-reading to moving assistance. Leslie Farrar's administrative support and advice have been invaluable.

Finally, I would like to thank my family for their encouragement and support.

TABLE OF CONTENTS

TABLE OF CONTENTS	vi
LIST OF TABLES	viii
LIST OF FIGURES	xiii
CHAPTER 1. INTRODUCTION	1
1.1. SUMMARY	1
1.2. STUDY AREA	3
CHAPTER 2. METHODS.....	6
2.1. HYDROLOGIC MODEL	6
2.2. HISTORIC CLIMATE DATA	9
2.3. LAND MANAGEMENT	11
2.4. MODEL CALIBRATION AND TESTING	12
2.5. FUTURE CLIMATE PROJECTIONS	13
2.6. WETLAND SCENARIOS.....	15
2.7. STATISTICAL ANALYSES	17
CHAPTER 3. RESULTS AND DISCUSSION.....	20
3.1. MODEL PERFORMANCE.....	20
3.2. EFFECTS OF WETLAND LOSS AND GAIN UNDER PRESENT-DAY CLIMATE ...	21
3.3. BIAS-CORRECTED PROJECTED CLIMATE.....	24
3.4. PROJECTED HYDROLOGY AND WATER QUALITY UNDER BASELINE WETLANDS	25
3.5. EFFECTS OF WETLAND LOSS AND GAIN UNDER FUTURE CLIMATE.....	29
3.6. ASSUMPTIONS AND LIMITATIONS	31
3.7. IMPLICATIONS AND FUTURE WORK.....	33
CHAPTER 4. CONCLUSIONS	37
TABLES	39
FIGURES	42
REFERENCES	49
APPENDIX I: DETAILED METHODS FOR CALIBRATION AND TESTING	73

APPENDIX II: DETAILED METHODS FOR DOWNSCALING OF FUTURE CLIMATE PROJECTIONS	78
APPENDIX III: LITERATURE REVIEW OF ROLE OF WETLANDS IN NUTRIENT CYCLING IN THE UPPER KLAMATH RIVER BASIN	80
APPENDIX IV: SUPPLEMENTARY TABLES	82
APPENDIX V: SUPPLEMENTARY FIGURES	104
LIST OF ABBREVIATIONS.....	121

LIST OF TABLES

Table 1. General Circulation Models (GCMs) and Representative Concentration Pathways (RCPs) used in scenario analysis using the Coupled Model Intercomparison Project 5 (CMIP5) Multivariate Adapted Constructed Analogs (MACA) of University of Idaho. Absolute change in average annual temperature (“ ΔT ”) and percent change in average annual total precipitation (“% Change P”) are shown between the future period 2030-2059 and historic period (1950-2005). Values are averaged from daily 4 km gridded data over the entire Sprague River watershed.....39

Table 2. Depressional wetland model parameters, equations and sources. “Parameter” is the parameter name in the SWAT pond (.pnd) file. “Wetlands database” refers to Oregon Natural Heritage Information Center and the Wetlands Conservancy (2009), U.S. Department of Agriculture Natural Resources Conservation Service (2011), U.S. Fish and Wildlife Service (2011), and U.S. Geological Survey (2011).40

Table 3. Calibration (C) and testing (T) statistics for Sprague River tributaries and mainstem. The calibration period is 2001-2006 and the testing period is 2007-2010, except for flow (Q) at the South Fork of the Sprague River, where calibration is for even years from October 1992 to September 2003, and testing is for odd years for the same period. All statistics are monthly except sediment and nutrient statistics for the South Fork of the Sprague River, which are daily. Numbers following tributary name correspond to numbered flow (first) and water quality sampling location (second) shown in Figure 1. Information on stream flow gages and water quality sampling locations is shown in Appendix IV, Table 13. PBIAS = percent bias; a negative (positive) value denotes an overestimate (underestimate). R^2 = coefficient of determination; and NS = Nash-Sutcliffe coefficient.....41

Table 4. Flow characteristics for calibration and testing periods at Sprague tributary and mainstem gages. Calibration (testing) periods are 2001-2006 (2007-2010), with the exception of South Fork of the Sprague River at Brownsworth, which was calibrated (tested) for even (odd) years of the period 1992-2003. Site numbers correspond to numbers in Figure 1 and in Appendix IV, Table 13. “SD” = standard deviation; “Avg” = mean.83

Table 5. Attributes of meteorological stations used in the SWAT hydrologic model. “Lat” = latitude; “Long” = longitude. “NCDC” = National Climatic Data Center, Global Historical Climatology Network (GHCN); “SNOTEL” = Natural Resources Conservation Service Snow Telemetry.....84

Table 6. Results of chi-square goodness-of-fit test of daily observed precipitation data following data gap in-filling. The chi-square goodness-of-fit test was used to test the null hypothesis, h_0 , that the cumulative gamma distributions fitted to unfilled precipitation data for each calendar month are a random sample from a cumulative gamma distribution fitted to filled precipitation data for the same calendar month. The test was performed for filled and unfilled daily precipitation data

for the period January 1, 1950 to December 31, 2010. The test result, h , is unity if the null hypothesis can be rejected at the 5% significance level and 0 if the null hypothesis cannot be rejected. Significance level of the test is denoted by p . Station abbreviations and attributes are noted in Appendix IV, Table 5. The data in-filling procedure is described in the text.85

Table 7. Results of the two-sample Kolmogorov-Smirnov test for daily observed precipitation data following data gap in-filling. The two-sample Kolmogorov-Smirnov test was used to test the null hypothesis, h , that filled and unfilled precipitation data are from the same continuous distribution for each calendar month. The test was performed for filled and unfilled daily precipitation data for the period January 1, 1950 to December 31, 2010. The test result, h , is unity if the null hypothesis can be rejected at the 5% significance level and 0 if the null hypothesis cannot be rejected. Significance level of the test is denoted by p . Station abbreviations and attributes are noted in Appendix IV, Table 5. The data in-filling procedure is described in the text.....86

Table 8. Results of the two-sample Kolmogorov-Smirnov test for daily observed minimum temperature data following data gap in-filling. The two-sample Kolmogorov-Smirnov test was used to test the null hypothesis, h , that filled and unfilled data are from the same continuous distribution for each calendar month. The test was performed for filled and unfilled daily minimum temperature data for the period January 1, 1950 to December 31, 2010. The test result, h , is unity if the null hypothesis can be rejected at the 5% significance level and 0 if the null hypothesis cannot be rejected. Significance level of the test is denoted by p . Station abbreviations and attributes are noted in Appendix IV, Table 5. The data in-filling procedure is described in the text.....87

Table 9. Results of the two-sample Kolmogorov-Smirnov test for daily observed maximum temperature data following data gap in-filling. The two-sample Kolmogorov-Smirnov test was used to test the null hypothesis, h , that filled and unfilled data are from the same continuous distribution for each calendar month. The test was performed for filled and unfilled daily minimum temperature data for the period January 1, 1950 to December 31, 2010. The test result, h , is unity if the null hypothesis can be rejected at the 5% significance level and 0 if the null hypothesis cannot be rejected. Significance level of the test is denoted by p . Station abbreviations and attributes are noted in Appendix IV, Table 5. The data in-filling procedure is described in the text.....88

Table 10. Pond model parameters, equations and sources. “Parameter” is the parameter name in the SWAT pond (.pnd) file. “Wetlands database” refers to Oregon Natural Heritage Information Center and the Wetlands Conservancy (2009), U.S. Department of Agriculture Natural Resources Conservation Service (2011), U.S. Fish and Wildlife Service (2011), and U.S. Geological Survey (2011).....89

Table 11. Performance of LOADEST model for predicting monthly loads at Sprague River water quality observation locations. Site numbers correspond to locations in Figure 1 and in Appendix IV, Table 13. 2 = Sprague River at Power Plant; 4 = Sycan River at Drew’s Road; 5 = North

Fork of the Sprague River at #3411 Rd. LOADEST model numbers are described by Runkel et al. (2004). PPPC = probability plot correlation coefficient. A value of 1 indicates a perfect linear relation between the log-transformed load and model residuals. The coefficient of determination (R^2) shows the percent of variation in log load that can be explained by the model regression equation.90

Table 12. Water quality characteristics for calibration and testing periods at Sprague River tributary and mainstem sampling locations. All values are in mg L^{-1} . “NF” = North Fork; “SF” = South Fork. Sampling locations are shown in Figure 1 and in Appendix IV, Table 13. Calibration (testing) periods are 2001-2006 (2007-2010). “Avg” = mean; “SD” = standard deviation.91

Table 13. Stream flow gage and water quality sampling locations in the Sprague River watershed. “USGS” = U.S. Geological Survey; “OWRD” = Oregon Water Resources Department; “USFS” = Fremont Winema National Forest. Drainage areas are those calculated by the SWAT model; water quality monitoring locations are within 2 river km of a stream gage except in the case of site 6 (see explanation in section 2.4). “Q” = Stream flow gage; “WQ” = water quality monitoring location. “C” = calibration period; “T” = testing period. Numbers (“No.”) correspond to labels in Figure 1.92

Table 14. Calibrated model parameters and values for Sprague River tributaries and mainstem (“Main”).93

Table 15. Change in downscaled and bias-corrected projected precipitation and temperature, 1954-2005 and 2030-2059. Differences between historic and future climate from a given General Circulation Model (GCM) and Representative Concentration Pathway (RCP) are calculated separately for eight meteorological stations and averaged across all stations.96

Table 16. Average annual simulated runoff and loads of sediment, total nitrogen and total phosphorus at the Sprague River outlet for the period 2001-2010 under scenarios of depressional and riparian wetland extent (scenarios defined in section 2.6) and observed precipitation and temperature. “Base” represents baseline wetland extent under present-day conditions. Scenarios of +/-25, 50, 75 and 100% are applied to all wetlands in the Sprague watershed and represent a change in width for riparian buffers and a change in surface area and volume for depressional wetlands. “10 m min” shows a scenario of a riparian buffer of a minimum 10 m width throughout the watershed, with depressional wetland extent unaltered from baseline. “Diff” and “% Change” show absolute and percent change between a given wetland scenario and baseline wetland extent utilizing the same climate forcings for 2001-2010. “Avg” = mean; “SD” = standard deviation. .97

Table 17. Summary of annual runoff 1954-2005 ($n = 52$) observed at the U.S. Geological Survey gauge 1150100, Sprague River near Chiloquin, Oregon (“Obs”), and simulated by the calibrated and tested model using precipitation and temperature forcings under three General Circulation Models (CanESM2, INMCM4, and MIROC5) and two Representative Concentration Pathways (RCPs). Values shown are in mm; “Avg” = mean; “SD” = standard deviation; and “Diff” = the observed average less the simulated average.98

Table 18. Simulated thirty-year average annual runoff, sediment and nutrient loads for the period 2030-2059 at the outlet of the Sprague River forced with precipitation and temperature data from three General Circulation Models (GCMs) and two Representative Concentration Pathways (RCPs). Absolute and percent differences are differences between the 52-year annual average for 1954-2005 and the 30-year annual average for 2030-2059, where the hydrologic model is forced with the same GCM and RCP for both time periods. Unshaded values indicate positive differences, while shaded values indicate negative differences. Bold values marked with an asterisk show future fluxes that are significantly different from the historic baseline under a Mann-Whitney-Wilcoxon two-tailed test ($\alpha = 0.1$). “Avg” = mean; “SD” = standard deviation. 99

Table 19. Percent difference in monthly flow (“Q”), sediment load (“S”), TN load (“N”), and TP load (“P”) simulated for 30 years between 2030-2059 and 52 years between 1954-2005 under three General Circulation Models (GCMs) and two Representative Concentration Pathways (RCPs). Differences are between the 52-year annual average for the historic period and the 30-year annual average for the future period, where the hydrologic model is forced with the same GCM and RCP for both time periods. Unshaded values indicate positive differences, while shaded values indicate negative differences. Bold values marked with an asterisk show future fluxes that are significantly different from the historic baseline under a Mann-Whitney-Wilcoxon two-tailed test ($\alpha = 0.1$). 100

Table 20. Results of Mann-Kendall test for trend and Sen’s slope estimator for 2030-2059 monthly average daily stream flow (“Q”, in $\text{m}^3 \cdot \text{s}^{-1}$), total sediment load (“S”, in $\text{tons} \cdot \text{month}^{-1}$), total nitrogen load (“N”, in $\text{kg} \cdot \text{month}^{-1}$), and total phosphorus load (“P”, in $\text{kg} \cdot \text{month}^{-1}$) simulated under three General Circulation Models (GCMs) and two Representative Concentration Pathways (RCPs). Blank cells are not significant; unshaded values indicate significant positive trends, while shaded values indicate significant negative trends ($\alpha = 0.1$); $n = 30$ for each month. Values show Sen’s slope estimate of rate of change (units are described above), and superscript symbol shows significance level. + = 0.1; * = 0.05; and ** = 0.01. Annual Q, S, N and P showed significant trends only for P under CanESM2 (RCP 4.5 and 8.5) ($1033 \text{ kg} \cdot \text{year}^{-1}$ and $1484 \text{ kg} \cdot \text{year}^{-1}$, respectively, $\alpha = 0.05$), and MIROC5 (RCP 8.5, $1049 \text{ kg} \cdot \text{year}^{-1}$, $\alpha = 0.01$). 101

Table 21. Average annual simulated runoff and loads of sediment, TN and TP at the Sprague River for the period 2030-2059 under scenarios of depressional and riparian wetland extent (scenarios defined in section 2.6) and two General Circulation Models (RCP 8.5). “Base” represents baseline wetland extent under present-day conditions. Scenarios of +/- 50 and -100% are applied to all wetlands in the Sprague watershed as a change in width for riparian buffers and in surface area and volume for depressional wetlands. “Fut. Change” and “Fut % Change” are between a given wetland scenario and baseline wetland extent utilizing the same General Circulation Model forcing for 2030-2059; “Hist. Diff” and “Hist % Change” are between the 2030-2059 scenario and 1954-2005 baseline wetland extent. “Avg” = mean; “SD” = standard deviation. 102

Table 22. Percent of riparian wetland area within a 30 m buffer of streams in the Sprague River watershed, sorted by Strahler stream order (Knighton, 1998). Riparian wetlands areas are from a wetlands database (Oregon Natural Heritage Information Center and the Wetlands Conservancy (2009), U.S. Department of Agriculture Natural Resources Conservation Service, 2011; U.S. Fish and Wildlife Service, 2011; U.S. Geological Survey 2011). Stream orders are based on classification of a high-resolution stream network (U.S. Geological Survey, 2010b). Where multi-thread channels occurred, side channels were assigned the stream order of the main channel. “Not classified” indicates canals, ditches and some bifurcating side channels where order could not be determined (most of the latter are near the confluence of the South Fork of the Sprague River with the Sprague River mainstem). Disappearing streams occur throughout the study area because of high soil permeability (Gannett et al., 2007).103

LIST OF FIGURES

Figure 1. Sprague River watershed, Oregon, USA. Numbers of calibration and testing sites (circles) correspond to site information in Table 3 and Appendix IV, Table 13. Wetlands are derived from four Oregon wetlands databases: Oregon Natural Heritage Information Center and the Wetlands Conservancy (2009), U.S. Department of Agriculture Natural Resources Conservation Service (2011), U.S. Fish and Wildlife Service (2011), and U.S. Geological Survey (2011). Irrigated sites are those designated for agricultural irrigation by the Oregon Water Resources Department (2008). In the upper inset map, the Sprague River watershed (entire Klamath River Basin) is shown in black (green). In the lower map, the study area is denoted by a star.42

Figure 2. Schematic of SWAT hydrologic model setup and scenario analysis.....43

Figure 3. Time series of monthly calibration (2001-2006) and testing (2007-2010) periods for the mainstem of the Sprague River for stream flow. Stream flow time series is at the U.S. Geological Survey gauge Sprague River near Chiloquin, Oregon (site 1 in Figure 1 and Table 3; and in Appendix IV, Table 13).....44

Figure 4. Simulated percent change in 2001-2010 average monthly and annual TP and TN loads at the outlet of the Sprague River, Oregon under scenarios of loss and gain of riparian and depressional wetlands. “Base” represents baseline wetland extent under present-day conditions. Scenarios of +/-25, 50, 75 and +100% are applied to all wetlands in the Sprague watershed and represent a change in width for riparian buffers and a change in surface area and volume for depressional wetlands. “10 m min” shows a scenario of a riparian buffer of a minimum 10 m width throughout the watershed, with depressional wetland extent unaltered from baseline.45

Figure 5. As for Figure 4, but only for a scenario of 100% loss of riparian and depressional wetlands.....46

Figure 6. Annual and monthly average warming and percent change in precipitation, stream flow, sediment and nutrients for two climate projections. The two projections represent extremes in temperature and precipitation change from baseline for the six climate projections utilized in this study. Length of bars in (a) and (f) show percent change in precipitation from baseline, while colors of bars show change in average temperature, rounded to the nearest 0.5°C. Percent change is shown for stream flow (b and g) in blue; sediment (c and h) in brown; total nitrogen (d and i) in green; and total phosphorus (e and j) in purple. Percent changes are between averages for 2030-2059 and 1954-2005. Historic and future averages are also shown as mean monthly discharge and loads in Appendix V, Figure 13.....47

Figure 7. Change in average annual total phosphorus load between 2030-2059 relative to 1954-2005 averages under scenarios of loss and gain of riparian and depressional wetlands for Representative Concentration Pathway (RCP) 8.5, General Circulation Models (GCMs)

CanESM2 and INMCM4. These GCMs and RCP represent extremes in precipitation and temperature changes for the six climate projections utilized in this study. The central mark of the box is the median; box lower (upper) edges represent the 25th and 75th percentiles, respectively, whiskers extend to the most extreme data points not considered outliers, and outliers are plotted individually as red crosses. Base” represents baseline wetland extent under present-day conditions. Scenarios of +/- 50 and -100% change are applied to all wetlands in the Sprague watershed and represent a change in width for riparian buffers and a change in surface area and volume for depressional wetlands. As precipitation decreased under INMCM4 (RCP 8.5), only scenarios of wetland loss were simulated for this GCM and RCP. The red line denotes a 40% reduction in annual TP loads (the targeted condition for total phosphorus external loads to Upper Klamath Lake in the Lake’s Total Maximum Daily Load), using GCM-driven simulations of 1954-2005 annual average loads as reference.48

Figure 8. Map of example riparian wetland width and maximum depressional wetland volume used in SWAT model wetland scenarios. Figures 8a, c and e show riparian wetland width (FILTERW parameter in SWAT .mgt file) in m under 50% decrease in baseline width (a); baseline width (c) and 50% increase in baseline width (e). Dark grey = 0; yellow = 1 – 5; green = 6 – 10; pale blue = 11 – 20; medium blue = 21 – 30; and dark blue ≥ 30. Figures 8b, d and f show the maximum depressional wetland volume (WET_MXVOL parameter in SWAT .pnd file) in 104 m³ under 50% decrease (b); baseline extent (d) and 50% increase (f). Grey = 0; yellow = 1 -25; green = 26 – 50; and pale blue ≥ 50..... 105

Figure 9. Time series and analysis of calibration (2001-2006) and testing (2007-2010) periods for the mainstem of the Sprague River for sediment. Time series is at site 2 (Figure 1; Table 3; Appendix IV, Table 13)..... 106

Figure 10. Time series and analysis of calibration (2001-2006) and testing (2007-2010) periods for the mainstem of the Sprague River for total nitrogen. Time series is at site 2 (Figure 1; Table 3; Appendix IV, Table 13)..... 107

Figure 11. Time series and analysis of calibration (2001-2006) and testing (2007-2010) periods for the mainstem of the Sprague River for total phosphorus. Time series is at site 2 (Figure 1; Table 3; Appendix IV, Table 13)..... 108

Figure 12. Time series and analysis of calibration (2001-2006) and testing (2007-2010) periods for the North Fork of the Sprague River for stream flow. Time series is at site 6 (Figure 1; Table 3; Appendix IV, Table 13)..... 109

Figure 13. Time series and analysis of calibration (2001-2006) and testing (2007-2010) periods for the North Fork of the Sprague River for sediment. Time series is at site 5 (Figure 1; Table 3; Appendix IV, Table 13)..... 110

Figure 14. Time series and analysis of calibration (2001-2006) and testing (2007-2010) periods for the North Fork of the Sprague River for total nitrogen. Time series is at site 5 (Figure 1; Table 3; Appendix IV, Table 13)..... 111

Figure 15. Time series and analysis of calibration (2001-2006) and testing (2007-2010) periods for the North Fork of the Sprague River for total phosphorus. Time series is at site 5 (Figure 1; Table 3; Appendix IV, Table 13)..... 112

Figure 16. Time series and analysis of calibration (2001-2006) and testing (2007-2010) periods for the Sycan River for stream flow. Time series is at site 3 (Figure 1; Table 3; Appendix IV, Table 13)..... 113

Figure 17. Time series and analysis of calibration (2001-2006) and testing (2007-2010) periods for the Sycan River for sediment. Time series is at site 4 (Figure 1; Table 3; Appendix IV, Table 13). 114

Figure 18. Time series and analysis of calibration (2001-2006) and testing (2007-2010) periods for the Sycan River for total nitrogen. Time series is at site 4 (Figure 1; Table 3; Appendix IV, Table 13)..... 115

Figure 19. Time series and analysis of calibration (2001-2006) and testing (2007-2010) periods for the Sycan River for total phosphorus. Time series is at site 4 (Figure 1; Table 3; Appendix IV, Table 13)..... 116

Figure 20. Time series and analysis of calibration (and testing periods for the South Fork of the Sprague River for stream flow. Calibration is for even calendar years from 1992 – 2003; testing is for odd years for the same period. Time series is at site 8 (Figure 1; Table 3; Appendix IV, Table 13)..... 117

Figure 21. Time series of daily sediment, TN and TP calibration and testing periods for the South Fork of the Sprague River. Time series are at site 7 (Figure 1; Table 3; Appendix IV, Table 13). 118

Figure 22. Graph of average monthly stream flow, 1954-2005 simulated by the SWAT hydrologic model at the Sprague River outlet using precipitation and temperature forcings from the three General Circulation Models used in this study. Averages of observations for the same time period near the Sprague River outlet at the U.S. Geological Survey stream flow gauge, Sprague River near Chiloquin, Oregon, are shown in black. 119

Figure 23. Simulated average monthly stream flow, sediment, and nutrient fluxes at the Sprague River outlet under the historic period (1954-2005, shown in black) and future period (2030-2059, shown in blue) under two climate projections. Figures 23a, 23b, 23c, and 23d show stream flow, sediment load, TN load and TP load, respectively under the CanESM2 RCP 8.5 projection. Figures 23e, 23f, 23g, and 23h show the same constituents for the INMCM4 RCP 8.5 projection. 120

CHAPTER 1. INTRODUCTION

1.1. SUMMARY

An understanding of potential stream water quality conditions under future climate is critical for the long-term success of regulatory programs such as the Total Maximum Daily Load and the European Water Framework Directive; protection of drinking water quality and human health; and sustainability of ecosystems (Solheim et al., 2010; Mulholland and Sale, 2011). Possible drivers of stream water quality changes under future climate are numerous, and include increases in water temperature and chemical reaction rates, leading to more rapid nutrient cycling; greater stream power, erosion and thus geomorphologic alterations under more extreme floods; and increases in concentration of contaminants under lower flows and higher evapotranspiration (Whitehead et al., 2009). However, while numerous studies have characterized potential changes in stream flow under future climate projections (Lettenmaier et al., 1999; Wood et al., 2004; Hay et al., 2011), relatively few have evaluated potentially severe climate-induced changes in sediment and nutrients fluxes, particularly of phosphorus (Murdoch et al., 2000; Jeppesen et al., 2007; Solheim et al., 2010; Ahmadi et al., 2013).

Although the majority of assessments of pollutant fluxes under future climate and the impact of conservation practices on such fluxes has been conducted in heavily cultivated watersheds in the American Midwest, the Western United States is likely to be particularly vulnerable to hydroclimatic change in the 21st century (Diffenbaugh et al., 2012). The region has one of the fastest-growing populations in the United States, yet is already challenged to meet current water demand (Serreze et al., 1999; Colorado River Basin Water Supply and Demand Study Team, 2011; Mackun et al., 2011). Furthermore, the West has shown trends toward lower snowpack and earlier spring flow associated with warming in the latter half of the 20th century (Mote, 2003; Stewart et al., 2005) —effects which may be exacerbated under continued regional warming, and with potential to impact sensitive aquatic species such as Pacific salmon (Mote et al., 2003; Barnett et al., 2008; Diffenbaugh et al., 2012). Several recent

studies have addressed impacts of climate change in American Western watersheds on stream temperature (Beechie et al., 2012; Ficklin et al., 2013; Wade et al., 2013) or sediment (e.g., Naik and Jay, 2011; Ficklin et al., 2013). However, to the authors' knowledge no studies have yet assessed potential effects of future climate on nutrient fluxes in watersheds where shifts from snowmelt dominated to rainfall-dominated hydrology may occur in the 21st century.

The Intergovernmental Panel on Climate Change (IPCC) has concluded that current management practices may be insufficient to address climate-induced changes in water quality (Bates et al., 2008). However, relatively few studies have evaluated the impact of existing or potential management or conservation practices on sediment and nutrient fluxes under future climate (Whitehead et al., 2006; Parker et al., 2008; Woznicki et al., 2011; Van Liew et al., 2012; Ahmadi et al., 2013). Even fewer studies have evaluated impacts of wetland conservation or restoration, which has been cited as critical in watershed scale management of nutrients (Verhoeven et al., 2006). Previous research evaluating the impacts of conservation practices (such as wetlands) aimed at ameliorating water quality conditions under future climate has generally assumed that the practice will persist under future conditions (e.g., Whitehead et al., 2006; Woznicki et al., 2011; Van Liew et al., 2012). However, relatively small changes in wetland water balance under future climate may cause expansion or contraction of wetland extent, shifts in wetland type, or conversion of wetlands to dry land; and altered future hydroclimatic conditions may induce changes in land use (Meyer et al., 1999; Burkett and Kusler, 2000; Candela et al., 2009; Moradkhani et al., 2010; Praskievicz and Chang, 2011).

The primary goal of this study is to assess the basin-scale regulation of water quality provided by variable wetland extent under current and future climatic conditions in a Pacific Northwest watershed for the mid-21st century. Specific objectives of the study are (1) to evaluate the effects of wetland loss and gain under present-day climate on stream water quality at the watershed scale; (2) to identify direction and magnitude of potential changes in stream flow, sediment, and nutrient loads under future climate and baseline wetland conditions; and (3) to determine how wetland gain or loss might exacerbate or

ameliorate climate-induced changes in future water quality. These objectives are investigated in the semi-arid Sprague River watershed in southern Oregon, in the Western United States. Assessment of the separate and combined impacts of future climate and wetland loss or gain on water quality in this watershed can yield novel insight into how flow and nutrient fluxes in other historically snowmelt-dominated American Western watersheds may respond to projected shifts in temperature and precipitation.

1.2. STUDY AREA

The Sprague River watershed drains an area of about 4000 km² in the Upper Klamath River Basin of southern Oregon, USA. The watershed lies in the rainshadow of the Cascade Mountains and is semi-arid. The Sprague River is supplied by three major tributaries: The South and North Forks, which join to form the Sprague River mainstem near Beatty, Oregon, and the larger Sycan River, which reaches the mainstem about 20 km downstream of this confluence (Figure 1). The Sprague River is the largest tributary to the Williamson River. The Sprague and Williamson Rivers are two of the three largest tributaries to the large, shallow Upper Klamath Lake and contribute over half of the lake's inflow. The third main tributary to Upper Klamath Lake, the Wood River, lies to the west of the Sprague and Williamson Rivers (Figure 1).

Mean annual precipitation and temperature ranges from 340 mm and 10°C at the Snow Telemetry (SNOTEL) station Summer Lake approximately 15 km northeast of the watershed boundary, to 950 mm and 4°C at the SNOTEL Crazyman Flat in the headwaters of the Sycan River (1981-2010 averages obtained from <http://www.wcc.nrcs.usda.gov/snotel/Oregon/oregon.html>). The majority of precipitation occurs between October and March. January is typically coldest, while July is typically warmest (-3°C and 15°C mean minimum and maximum monthly temperatures, respectively at Summer Lake; -2°C and 14°C at Crazyman Flat).

Elevation ranges from about 1270 to 2600 m above sea level (U.S. Geological Survey, 2009). The Upper Klamath River Basin geology generally consists of lava flows, volcanic rocks, or volcanic vents interbedded with sedimentary and volcanoclastic material (Gannett et al., 2007). The region's volcanic-derived soils are generally naturally rich in phosphorus (P) and highly permeable in much of the watershed, particularly in young volcanic areas (Cahoon, 1985; Graham et al., 2005; Gannett et al., 2007). The majority of the watershed is covered in coniferous forest dominated by Ponderosa and Lodgepole pine (*Pinus ponderosa* and *Pinus contorta*) (Rabe and Calonje, 2009). Other land cover is mostly rangeland, wetlands, and irrigated cattle pasture (Homer et al., 2007).

Annual peak flows at the Sprague River outlet near Chiloquin, Oregon generally occur between the months of February and June and are associated with snowmelt (Mayer and Naman, 2011; U.S. Geological Survey, 2012). Groundwater discharge to streams is approximately 3 to $4 \text{ m}^3 \cdot \text{s}^{-1}$ in the North Fork of the Sprague River and in the lower Sprague River Valley, but only about $1 \text{ m}^3 \cdot \text{s}^{-1}$ in reaches of the Sycan River and the South Fork (Gannett et al., 2007).

Total phosphorus (TP) loads to Upper Klamath Lake have increased in the last century above background levels already high from regional volcanic geology (Boyd et al., 2002). Elevated TP loads are associated with large blooms and die-offs of phytoplankton in Upper Klamath Lake, which cause extremes in pH and oxygen concentration that may be lethal to federally listed endangered fish species (Boyd et al., 2002). The Klamath River begins downstream of Upper Klamath Lake at the lake's dam-controlled outlet, from which the river flows some 400 km to the Pacific Ocean in California (Thorsteinson et al., 2011; Eldridge et al., 2012a) (Figure 1). Upper Klamath Lake water quality can contribute to poor water quality downstream in the Klamath River by export of high nutrient and organic matter loads, which may also favor growth of liver-toxin producing cyanobacteria (Thorsteinson et al., 2011; Eldridge et al., 2012b). While internal loading from lake sediments comprises the majority of TP sources to Upper Klamath Lake, external sources account for approximately a third of the total load. Of this third, approximately 50% is believed to be from the Williamson and Sprague rivers, with

anthropogenic sources attributed primarily to increased runoff in the Williamson and Sprague watersheds, wetland drainage, and associated oxidation of organic matter and loss of sequestered nutrients from wetlands (Risley and Laenen, 1999; Boyd et al., 2002).

Historically, wetlands and riparian zones were extensive in the Upper Klamath Basin, including the Sprague River watershed. However, an estimated 90% or more of wetlands in the Upper Klamath River Basin have been lost to diking and draining for agriculture (Gearheart et al., 1995). Today, wetlands comprise less than 8% of the Sprague River basin (Oregon Natural Heritage Information Center and the Wetlands Conservancy, 2009; U.S. Geological Survey, 2010a; U.S. Department of Agriculture Natural Resources Conservation Service, 2011; U.S. Fish and Wildlife Service, 2011). The Total Maximum Daily Load (TMDL) targeted condition for Upper Klamath Lake is a 40% reduction in external TP loads to the lake (Boyd et al., 2002). Previous research suggests that wetland restoration is one of the most effective means to reduce TP loads in the Upper Klamath Basin, and conservation efforts have focused particularly on restoration of large lakeside wetlands (Gearheart et al., 1995; Anderson, 1998; McCormick and Campbell, 2007).

However, much of the Upper Klamath River Basin is in a transitional elevation zone where the form of precipitation (rain or snow) is sensitive to relatively slight changes in temperature. The hydroclimatology of Upper Klamath Basin has shown warming, decreases in snow water equivalent, and earlier spring melt since the 1950s similar to changes observed elsewhere in the American West (Mote, 2003; Mayer and Naman, 2011; Risley et al., 2012). While it appears quite possible that such trends will continue, the potential effects on the basin's water quality are not well understood.

CHAPTER 2. METHODS

2.1. HYDROLOGIC MODEL

The Soil and Water Assessment Tool (SWAT) model was developed by the U.S. Department of Agriculture (USDA) to assess land management impacts on hydrology and water quality over long time periods, and has been used successfully in hundreds of water resources studies globally (Arnold et al., 1998; Gassman et al., 2007). SWAT is a continuous, distributed-parameter model that operates on a daily or more frequent time-step. The model delineates a basin into subwatersheds, which are further divided into hydrologic response unit (HRUs), unique combinations of soil type, land cover, and slope class (Arnold et al., 2011).

We set up four separate SWAT models for the Sycan, North and South Forks of the Sprague River, and the Sprague River mainstem using ArcSWAT version 2009.93.7b (U.S. Department of Agriculture Agricultural Research Service, 2011). Setup inputs were a 30 m National Elevation Dataset (NED) raster, a stream layer derived from a National Hydrography Dataset (NHD)-High flow line, a National Land Cover Dataset (NLCD) 2001, and U.S. General Soil Map (STATSGO) (Homer et al., 2004; U.S. Geological Survey, 2010b; U.S. Department of Agriculture Agricultural Research Service, 2011). Each irrigated field designated for agricultural use by the Oregon Water Resources Department (OWRD) was modeled as a separate HRU of the dominant NLCD 2001 land cover type within the field boundary (Oregon Water Resources Department, 2008). We then forced the SWAT model with historic climate data and wetland scenarios for a historic period and with future climate projections and wetland scenarios for a future period (described below). The total number of HRUs for each of the four models was 442 (Sycan River); 236 (North Fork of the Sprague River); 452 (South Fork of the Sprague River); and 640 (Sprague River mainstem).

Wetland representation in the SWAT model

In the current SWAT model, wetlands are typically represented by two means. Riparian wetlands or buffers are represented as a filter strip, and a trapping efficiency is calculated based on the strip width. For sediment and nutrients in surface runoff, this is calculated as

$$Trap_{eff} = 0.367 \cdot (width)^{0.2967} \quad \text{Eqn. 1}$$

For nutrients in subsurface runoff, the trapping efficiency is calculated as

$$Trap_{eff} = \frac{[2.1661 \cdot (width) - 5.1302]}{100} \quad \text{Eqn. 2}$$

The trapping efficiency is allowed to reach a maximum of 1. Sediment and nutrient loads contributed from an HRU are reduced by the trapping efficiency for that HRU, as

$$Load_{new} = Load_{old} \cdot (1 - Trap_{eff}) \quad \text{Eqn. 3}$$

Depressional wetlands and ponds are represented by impoundment routines in SWAT, in which water body surface areas, estimated volumes, and percent contributing drainage area are aggregated to a single value per subwatershed (Neitsch et al., 2009). In SWAT, a percentage of overland flow and associated sediment and nutrient loads from each HRU within the subwatershed are delivered to depressional wetlands and ponds based on the fraction of each subwatershed draining to water bodies within the catchment. The wetland or pond water balance accounts for inflow, direct precipitation on the water body surface, evaporation, seepage, storage, and outflow, which is delivered to the stream reach. Sediments and

nutrients in depressional water bodies are modeled with a mass balance, incorporating apparent settling rates for nutrients, trapping efficiencies, equilibrium concentrations above which settling will occur, and mean particle size. Filter strip and depressional wetland calculations are detailed in Neitsch et al. (2005) and Neitsch et al. (2009).

Previous applications of SWAT to wetlands and water resources

A number of previous studies have used the SWAT model to assess the role of wetlands in flow and water quality regulation. All studies discussed below have been conducted for watersheds in the United States, except where noted. For riparian wetlands, Cho et al. (2010b) predicted water quality effects of conservation practices targeting erosion and nutrients, including riparian forest buffers, in the Little River Experimental Watershed in Georgia. Additionally, Cho et al. (2010a) determined that the degree of watershed subdivision selected during SWAT model setup could impact nutrient and sediment yields under riparian buffer scenarios in the Little River Experimental Watershed. Moriasi et al. (2006) assessed the impacts of riparian forest and bermudagrass filter strips in an Oklahoma watershed by altering parameters governing channel erosion and using the SWAT filter strip routine, respectively. Sahu and Gu (2009) compared nitrate reductions mediated by filter strips adjacent to streams to reductions by filter strips located mid-slope in an Iowa watershed.

Several studies have also demonstrated amendments to SWAT riparian wetland representation. Liu et al. (2007) integrated SWAT and the Riparian Ecosystem Management Model to assess reductions in sediment and TP mediated by riparian buffers in a southern Ontario watershed, Canada. Subsequently, utilizing the same study area, Liu et al. (2008) developed a SWAT extension module for riparian wetlands, including lateral connectivity of riparian wetlands with the channel. In an earlier work, Hattermann et al. (2006) assessed the impact of integration of riparian zones and wetlands into the Soil and Water Integrated Model (SWIM) on discharge and nitrate yields in agricultural German catchment. The SWIM model has a number of similarities with the SWAT model. The main amendments to SWIM

were addition of daily groundwater fluctuations at the HRU scale and uptake by plants of water and nutrients within wetlands, as well as N retention in subsurface water. The latter is included in the present version of the SWAT model.

SWAT studies assessing water quality impacts of depressional wetlands include Almendinger et al. (2012), who demonstrated that SWAT depressional wetland and ponds modules were well suited to represent hydrology of two Midwestern watersheds, and that depressional features influence hydrology and sediment delivery in these basins. Wang et al. (2010) compared the impacts of depressional wetland conservation and restoration scenarios on flow, sediment, TN and TP in two Minnesota watersheds.

Previous applications of SWAT to climate impacts to water resources

The SWAT model has been used extensively in hydrologic modeling of climate change impacts. Gassman et al. (2007) reported 30 separate such studies had been conducted by the mid-2000s and noted that approximately two thirds of this research had examined only hydrologic impacts of climate change, with less than a third assessing impacts on pollutants. The authors also provided a detailed literature review of these studies. More recently, the SWAT model has been used for assessment of climate change impacts on hydrology, water quality, or both in diverse watersheds in the American Midwest (Ahmadi et al., 2013; Chaplot, 2007; Van Liew et al., 2012; Woznicki et al., 2011); San Joaquin River valley (Ficklin et al., 2010) and the Sierra Nevada mountains, California, United States (Ficklin et al., 2013); Canada (Shrestha et al., 2012); southern China (Li et al., 2011); Korea (Park et al., 2011); and Iran (Abbaspour et al., 2010).

2.2. HISTORIC CLIMATE DATA

Historic climate data input to the SWAT model were drawn from two daily datasets: the Global Historical Climatology Network (GHCN) from the National Climatic Data Center (NCDC) and Snow

Telemetry (SNOTEL) from the Natural Resources Conservation Service (NRCS). The NCDC extensively quality assures and quality controls GHCN data prior to data release (Durre et al., 2010), and we conducted no further quality control besides removal of flagged data. Since SNOTEL precipitation data are recorded as cumulative values for the water year (October 1 to September 30), incremental daily values are especially sensitive to errors (Serreze et al., 1999). Therefore, we performed additional pre-processing of the SNOTEL cumulative precipitation and temperature data following methods outlined by Serreze et al. (1999). Additionally, where precipitation or temperature data were lacking for a given day at a station, data were selected from a surrogate station with the highest coefficient of determination (R^2) value and the data gap was in-filled by multiplying precipitation or adding temperature data at the surrogate station, using the calculated ratio (for precipitation) or difference (for temperature) between the station with missing data and the surrogate station. When an observation was absent at all stations, or where R^2 values of the station with missing data and surrogate stations were less than 0.2, data gaps were filled by the SWAT weather data generator developed by Nicks (1971). The SWAT weather generator was also used to generate solar radiation, relative humidity, and windspeed for the model. Effects of data in-filling on precipitation and temperature datasets were quantified using the chi-square goodness-of-fit test and the Kolmogorov-Smirnov test (Appendix IV, Tables 6-9). However, it should be noted that in most years, most meteorological stations contained fewer than 30-40 days with data gaps and rarely contained sequential gaps of more than two to three days.

Data from the meteorological station closest to each subwatershed centroid were used as precipitation and temperature inputs for that subwatershed. Each subwatershed was divided into ten bands representing an equal change in elevation using code developed by Mazdak Arabi at Colorado State University. Precipitation and temperature lapse rates with elevation were calculated from Parameter-elevation Regressions on Independent Slopes Model (PRISM) 1981-2010 800 m gridded climate normals and a 30 m NED raster dataset and calibrated within a 95% confidence interval around the resulting

regression slopes (U.S. Geological Survey, 2009; PRISM Climate Group at Oregon State University, 2012).

2.3. LAND MANAGEMENT

The primary land uses in the Sprague River watershed are grazing of beef cattle in irrigated bottom land in the Sprague River valley and timber harvest (Rabe and Calonje, 2009; U.S. Department of Agriculture Natural Resources Conservation Service, 2009). The majority of pasture in the Sprague River valley watershed is grazed from spring to fall and is flood irrigated from surface water sources (U.S. Department of Agriculture Natural Resources Conservation Service, 2009). Stocking rates for irrigated lands are not documented, but were assumed to equal $2 \text{ head} \cdot \text{ac}^{-1}$ ($4.9 \text{ head} \cdot \text{ha}^{-1}$) (David Ferguson, Natural Resources Conservation Service Klamath Falls Service Center, Klamath Falls, Oregon office, personal communication, 2012). Grazing rotations were assigned only to irrigated lands designated for agricultural use by the Oregon Water Resources Department (2008). Beef cattle were grazed on tall fescue (the default pasture crop in the SWAT model) from 1 April to 30 September, consuming $29.5 \text{ kg} \cdot \text{ha}^{-1} \cdot \text{day}^{-1}$ in dry biomass, trampling the same amount, and depositing $7.7 \text{ kg} \cdot \text{ha}^{-1} \cdot \text{day}^{-1}$. Autoirrigation was applied starting 1 June for the duration of the growing season and was based on plant water demand with an assumed maximum depth of 382 mm after published flood irrigation depths for the Wood River Valley; irrigation efficiency fraction (which accounts for losses between irrigation source and the location applied, including evaporation and conveyance losses) assumed = 1 due to lack of local information on conveyance losses); and surface runoff fraction = 0.58. Grazing parameters were derived from regional literature, correspondence with NRCS staff, and literature equations relating cattle mass to forage consumption and manure production (Ciotti, 2005; American Society of Agricultural and Biological Engineers, 2006; U.S. Department of Agriculture Natural Resources Conservation Service, 2009; David Ferguson, Natural Resources Conservation Service Klamath Falls Service Center, Klamath Falls, Oregon office, personal communication, 2012).

The Chiloquin wastewater treatment plant, the sole point source recognized in the Upper Klamath Lake TMDL, was input to the SWAT model with the following average daily flow, organic P, and soluble P for the year: $378.5 \text{ m}^3 \cdot \text{day}^{-1}$, $0.94 \text{ kg} \cdot \text{day}^{-1}$, and $0.57 \text{ kg} \cdot \text{day}^{-1}$, respectively. Flow and TP loadings were derived from Boyd et al. (2002) and fractions of TP loadings comprised of organic and mineral phosphorus from Gu et al. (2011). The plant is located in the town of Chiloquin, Oregon, shown in Figure 1.

2.4. MODEL CALIBRATION AND TESTING

The SWAT model was calibrated and tested using stream flow, sediment, total nitrogen (TN), and TP data at four stream flow gages and four water quality observation locations sampled by the Klamath Tribes (Figure 1; Appendix IV, Table 13) (Klamath Tribes, 2008).

Calibration and testing periods were 2001-2006 and 2007-2010, respectively, with the exception of stream flow in the South Fork of the Sprague River. This tributary was instead calibrated for flow for even years from 1992-2003 and tested for odd years during the same time period as long-term data for the 2000s were not available. At sampling locations on the Sycan River, North Fork of the Sprague River, and Sprague River mainstem, sediment and nutrient grab sample observations were converted to monthly load estimates with the LOADEST tool prior to use as calibration and testing data (Runkel et al., 2004). The percent of variation in the log load explained by the model regression equation (R^2) exceeded 0.90 for most cases, and 0.70 for all cases. (Regression models used and load estimation performance is summarized in Appendix IV, Table 11.)

As continuous daily flow observations from nearby stream flow gages required for LOADEST estimates were not available at the South Fork of the Sprague River, at this location we calibrated and tested for daily stream flow, sediment and nutrients loads estimated from water quality grab samples and instantaneous discharge observations made during sample collection. Calibration parameters were

selected from a Morris sensitivity analysis for all four constituents for 2001-2010 using the statistical measures of percent bias and Nash-Sutcliffe coefficient to evaluate model sensitivity. Additional parameters were identified from the SWAT literature (Morris, 1991; Moriasi et al., 2007). We autocalibrated the model with Dynamically Dimensioned Search (DDS) algorithms, employing manual calibration where necessary to fine-tune model performance using tools developed by Mehdi Ahmadi at Colorado State University (Tolson and Shoemaker, 2007). Model calibration and testing steps are detailed in Appendix I. Model calibration parameters and final calibrated values are shown in Appendix IV, Table 14.

Sprague River tributaries and mainstem have unique hydrologic characteristics that cannot be accurately represented using fixed values for SWAT basin-level (global) parameters (Boyd et al., 2002; Lind, 2009; Mayer and Naman, 2011; Gannett et al., 2012) (Appendix IV, Table 4, Tables 12-13). Therefore, we calibrated and tested three separate SWAT models for the Sycan, North and South Forks of the Sprague River. The daily tributary outputs from each calibrated and tested tributary model were read as inlet data to a separate model for the Sprague River mainstem, which was then calibrated and tested using these tributary inputs.

2.5. FUTURE CLIMATE PROJECTIONS

The 2040s is a useful planning horizon for the Pacific Northwest, and is the period when General Circulation Model (GCM) projections begin to markedly diverge from each other (Salathé et al., 2007; Mote and Salathé Jr., 2010). Climate scientists recommend assessing 30-year averages centered on the future period of interest, so in this study the term “2040s” refers to the period 2030-2059 (Salathé et al., 2007; Mote and Salathé Jr., 2010). We assessed 14 candidate climate projections derived from General Circulation Model (GCMs) and representing a range in future precipitation and temperature changes across the Sprague River watershed between 2030-2059 and the historic period generated by the GCMs,

1950-2005 (K. Hegewisch, Department of Geography, University of Idaho, personal communication, 2013). GCM projections were drawn from the Coupled Model Intercomparison Project 5 (CMIP5) Multivariate Adapted Constructed Analogs (MACA) 4 km gridded data available from the University of Idaho, United States (<http://nimbus.cos.uidaho.edu/MACA/>) and described by Abatzoglou and Brown (2012) and Abatzoglou (2013). Projections included two Representative Concentration Pathways (RCPs 4.5 and 8.5), climate scenarios incorporating plausible greenhouse gas emission rates and mitigation efforts (Taylor et al., 2012). An RCP of 8.5 denotes an increase of approximately $8.5 \text{ W} \cdot \text{m}^{-2}$ in global radiative forcing by 2100 (Taylor et al., 2012). In SWAT, users may specify atmospheric CO_2 concentrations, but the model does not allow concentrations to vary with time as would be expected for a 30-year simulation period; therefore CO_2 levels in the hydrologic model were held constant with time.

All projections showed warming in the Sprague River watershed for the 2040s relative to 1950-2005. However, roughly the same number of GCMs under both RCPs projected decreases in average annual precipitation as projected increases. We selected three GCMs representative of extremes in projected precipitation and temperature changes under the 14 candidate projections (Table 1). The INMCM4 model is slightly warmer and drier than the historic period; the CanESM2 model is substantially warmer and wetter; and the MIROC5 model represents moderate increases in both temperature and precipitation. Both RCPs were used for each of the three GCMs, yielding a total of six distinct climate projections used in this study.

While CMIP5 MACA data are available at a 4 km grid resolution, hydrologic models such as SWAT require daily inputs of precipitation and minimum and maximum temperature at a set of points (meteorological stations). Bias correction from the gridded data described above to meteorological stations was performed by Katherine Hegewisch of the University of Idaho after methods described in Vrac et al. (2012) (detailed in Appendix II).

2.6. WETLAND SCENARIOS

Baseline wetlands

Regional wetland and water body spatial databases were used to identify the area and type of wetlands and lakes within the Sprague River basin under current (baseline) conditions (Oregon Natural Heritage Information Center and the Wetlands Conservancy, 2009; U.S. Geological Survey, 2010a; b; U.S. Department of Agriculture Natural Resources Conservation Service, 2011; U.S. Fish and Wildlife Service, 2011). Mapped wetlands adjacent to streams and rivers, which comprise the majority of wetland area in the Sprague watershed, were classified as riparian. Following methods of Cho et al. (2010b), we created a 30 m buffer to all streams within a high-resolution network (NHD-High flow line) (U.S. Geological Survey, 2010b) of the Sprague River watershed, and then calculated the fraction of the buffer comprised of riparian wetlands within each subwatershed. We then multiplied this fraction by 30 to estimate riparian wetland width in m for each subwatershed, and set the filter strip width in m (FILTERW parameter in the corresponding SWAT management file) to this value.

Wetlands that were not adjacent to rivers and streams were designated as depressional using the SWAT impoundment routines described above. Pond and wetland geometries were derived from the regional geospatial data described above and surface-area to volume equations from SWAT and regional literature values for water bodies, while drainage area was estimated using the ArcGIS Desktop Spatial Analyst Hydrology tools (ArcGIS Desktop: Release 9.3., Environmental Systems Research Institute, Redlands, CA). Wetland geometry equations are shown in Table 2; pond geometry equations are in Appendix IV, Table 10.

Sycan Marsh is a large (approximately 1000 ha) surface-water dominated wetland in the headwaters of the Sycan River (Figure 1). Because it both buffers the riparian corridor and attenuates floodwater in the Sycan River headwaters, it was represented as both a riparian and a depressional wetland within the model.

Wetland scenarios

The baseline and hypothetical wetland loss and gain scenarios were as follows, and were applied equally to all wetlands in the Sprague River watershed:

- 1) Baseline wetland extent: Described above.
- 2) 25, 50, 75, and 100% wetland loss: Riparian wetland buffer widths (the FILTERW parameter in the SWAT .mgt file) were reduced by 25, 50, 75 or 100%. Depressional wetland normal and maximum surface areas and volumes were reduced by the same percentage as riparian wetland widths.
- 3) 25, 50, 75 and 100% wetland gain: Riparian wetland buffer widths and depressional wetland parameters were increased by 25, 50, 75 or 100%.
- 4) 10 m minimum riparian wetland buffer: The FILTERW parameter was set equal to

$$\max\{ 10\text{ m}, \text{Baseline width (m)} \} \quad \text{Eqn. 4}$$

The 10 m width is based on NRCS recommended minimum buffer strip widths for water quality improvements (Moriassi et al., 2006).

To elucidate the sensitivity of annual and monthly flow, sediment and nutrient fluxes to changes in wetlands throughout the entire Sprague River watershed and water quality benefits provided by present wetlands, we simulated the baseline and all wetland scenarios (+/-25, +/-50, +/-75, +/-100%, and a 10 m minimum riparian buffer) using observed precipitation and temperature for 2001-2010.

To explore how potential climate-induced change in wetlands might ameliorate or exacerbate climate change effects on future stream water quality, we simulated one wetland baseline scenario and

two to three scenarios of wetland loss or gain for 2030-2059 with two GCMs for RCP 8.5 representing extremes in temperature and precipitation change (CanESM2 and INMCM4 models, Table 1). Both GCMs project future warming, with a 1.4°C temperature increase under INMCM4 RCP 8.5 and a 3.1°C increase under CanESM2 RCP 8.5 (values are for downscaled gridded data, prior to station bias-correction). However, INMCM4 RCP 8.5 projects a decrease in precipitation of 3.5% over the study area, while CanESM2 RCP 8.5 projects an 11.1% increase (section 2.5). While variables controlling wetland occurrence and persistence across a landscape are complex (Arora, 2002; Merot et al., 2003), we considered scenarios of wetland gain (either climate-induced or anthropogenic) to be implausible under a warmer and drier climate (INMCM4 RCP 8.5); therefore, only scenarios of wetland loss (50% and 100%) were simulated under this climate projection. Conversely, depending on local water balance and landscape controls, wetlands could potentially decrease, expand, or change little under a warmer and wetter climate (CanESM2 RCP 8.5); therefore, scenarios of both wetland loss (50% and 100%) and gain (50%) were simulated under this climate projection. (Examples of scenarios of riparian wetland buffer width and depressional wetland volume are shown in Appendix V, Figure 8). While scenarios of wetland losses or gains exceeding 50% or even 25% may not be likely, such hypothetical simulations can yield insight into important watershed-scale controls on water quality under current and future climate.

2.7. STATISTICAL ANALYSES

As in other hydrologic modeling studies, the potential impacts of conservation practices and of climate change on sediment and nutrient loads were reported as a percent change in average conditions on an annual or monthly basis; this allows for ready comparisons between this study and previous research. The period 1950-2005 is recommended for comparisons between historic conditions and future hydroclimatic changes with the MACA dataset, as the downscaling process matches precipitation and temperature statistics between observed and modeled historic data for this entire period (K. Hegewisch, Department of Geography, University of Idaho, personal communication, 2013). However, since the

calibrated SWAT model requires a four-year warm-up and historic GCM data were not available until 1950, SWAT simulations for 2030-2059 using the six climate projections were compared to a baseline period of 1954-2005. Since GCMs simulate the historic period differently, comparisons between historic and future conditions were made utilizing simulations for both periods with the same GCM and RCP. For example, reported percent changes in TP for MIROC5 RCP 4.5 are comparisons between the 52-year average annual TP load for 1954-2005 and the 30-year average annual TP load for 2030-2059 simulated by the hydrologic model forced with MIROC5 RCP 4.5 precipitation and temperature data.

We assessed simulations of future hydrology and water quality for significant differences from the historic period and for trend, although such analyses do not appear to be common in hydrologic modeling studies of future climate impacts (Foy, 2010; Hay et al., 2011; Ahmadi et al., 2013 being exceptions). We used a two-tailed Mann-Whitney-Wilcoxon test to assess whether flow, sediment, TN and TP simulated at the Sprague River outlet for 2030-2059 ($n = 30$) under a given GCM, RCP and wetland scenario at the $\alpha = 0.1$ significance level differed from fluxes simulated under the same GCM, RCP and baseline wetlands for 1954-2005 ($n = 52$). The Mann-Whitney-Wilcoxon test is a non-parametric alternative to the independent-sample t -test and may be more appropriate for water resources data, which often cannot be assumed to be normally distributed (Helsel and Hirsch, 2002). We assessed total annual runoff and loads as well as average monthly stream flow and total loads for each calendar month to determine significance of seasonal changes. Analysis was performed using Minitab 16 Statistical Software (Minitab Inc., State College, PA).

We selected the α significance level of 0.1 because we considered it more important to identify potential trends or differences from the historic period in future data than to have a small probability of a type I error in test results. This significance level was used for all other statistical analyses described below.

We utilized the Mann-Kendall test, a non-parametric test for a monotonic trend, to test for trends in annual total runoff and loads, as well as monthly average stream flow and total monthly loads of sediment, TN and TP for each calendar month (Helsel and Hirsch, 2002) ($n = 30$). Where a trend existed, we used Sen's nonparametric estimator of slope to quantify the rate and direction of change. Both tests were performed using the MAKESENS spreadsheet application developed by the Finnish Meteorological Institute (Helsinki). The application is available at <http://en.ilmatieteenlaitos.fi/makesens> and is described by Salmi et al. (2002).

Finally, we used the Friedman test to assess whether future nutrient loads differed among wetland scenarios under the CanESM2 and INMCM4 (RCP 8.5) projections. This non-parametric test determines whether the median for two or more related groups of data are identical (Helsel and Hirsch, 2002).

CHAPTER 3. RESULTS AND DISCUSSION

3.1. MODEL PERFORMANCE

Model performance during the calibration period was considered acceptable at a monthly timestep if Nash-Sutcliffe coefficient (NS) ≥ 0.5 and percent bias (PBIAS) was within recommended thresholds: $\leq \pm 25\%$ (stream flow), $\leq \pm 55\%$ (sediment), and $\leq \pm 70\%$ (TN and TP) (Moriassi et al., 2007). The NS statistic ranges from $-\infty$ to 1.0, with 1.0 indicating a perfect fit between observed and simulated data plotted on a 1:1 line. Values ≤ 0 indicate that the mean of observations is a better predictor than the model. The PBIAS statistic measures the average tendency of simulated values to be lesser or greater than the corresponding observed values. Positive (negative) values indicate a model bias to underestimation (overestimation) (Moriassi et al., 2007).

Generally, model performance criteria for the testing or validation period should not be as strict as for the calibration period, and performance criteria are similarly less strict for a daily than a monthly timestep (Moriassi et al., 2007; Engel et al., 2007). Model monthly performance during the testing period and model daily performance during calibration and testing were considered acceptable if NS equaled or exceeded 0.2 and PBIAS was within the same ranges described for monthly calibration above. This is within the range of reported model performance for similar applications of the SWAT model (Santhi et al., 2001; Bracmort et al., 2006; Jha et al., 2007; Bosch, 2008; Sahu and Gu, 2009; Cho et al., 2010b; Lam et al., 2011).

Model performance utilizing these criteria was generally acceptable for stream flow, sediment and TP at the four calibration and testing locations (Table 3), although stream flow PBIAS at the North Fork of the Sprague River was slightly outside the acceptable range (31% overestimation of observed stream flow values). For monthly TN loads at the Sycan River during the testing period and daily TN loads at the South Fork of the Sprague River during calibration and testing, PBIAS and NS were outside the above thresholds. TN model performance at the Sprague River mainstem was acceptable; however,

tributary performance for TN should be taken into account when considering the TN results presented below, as should the model tendency to estimate a somewhat high mineral fraction for TN and TP. Santhi et al. (2001) reported that a SWAT model calibrated for the Bosque River watershed in Texas underestimated organic N yields during peak flows, which they attributed to low simulated sediment yields in the watershed. The SWAT model calculates organic N and P loads as a function of upland erosion, which in the Sprague River watershed is relatively low (Graham Matthews & Associates, 2007) and may lead to a lower simulated organic nutrient fraction in SWAT. However, return flow and runoff from flood irrigated pastures adjacent to streams, as well as cattle access to waterways could provide seasonally important sources of N and P not accounted for in the current SWAT model (e.g., Ciotti, 2005), as might periodic exports of dissolved nutrients from Sycan Marsh reported in some seasons and years (Wong and Bienz, 2011, as cited in CH2MHill, 2012). Time series of flow, sediment, TN and TP near the Sprague River mainstem outlet are shown in Figure 3 and in Appendix V (Figures 9-20) for the North and South Forks of the Sprague River and the Sycan River. Statistical measures of performance during calibration and testing periods are summarized in Table 3.

3.2. EFFECTS OF WETLAND LOSS AND GAIN UNDER PRESENT-DAY CLIMATE

In the historic period (2001-2010), scenarios of wetland loss and gain had little to no impact on average annual runoff (<1% change relative to baseline wetland extent). Wetland loss (gain) resulted in increases (decreases) in sediment, TN and TP, but the sensitivity to change in wetlands varied by flux. In general, any scenario but that of 100% wetland loss caused relatively little change in annual or monthly sediment and nutrient loads. Changes in average annual sediment load were small; 100% loss of wetlands resulted in sediment load increases of only 9.3%; a 10 m minimum riparian wetland buffer reduced sediment loads by 4.1%; and all other scenarios of wetland change varied average annual sediment loads by less than +/- 2.5%.

The minimal impact of wetlands on runoff in this study is not surprising, as riparian buffer strips in SWAT attenuate sediment and nutrients but do not impact flow (Neitsch et al., 2009). Depressional wetlands do impact flow in SWAT, but their extent in the Sprague River watershed is limited (Oregon Natural Heritage Information Center and the Wetlands Conservancy, 2009; U.S. Geological Survey, 2010a; U.S. Department of Agriculture Natural Resources Conservation Service, 2011; U.S. Fish and Wildlife Service, 2011).

Sediment removal rates in Sprague River wetlands are not documented. However, other hydrologic modeling studies have typically shown somewhat greater rates than those reported in this work, ranging from approximately 20-70% (Vaché et al., 2003; Moriasi et al., 2006; Cho et al., 2010b). This difference might be attributed to the importance of bank erosion relative to upslope erosion as a sediment source in the Sprague River watershed (Graham Matthews & Associates, 2007; NewFields River Basin Services and Kondolf, 2012). As is common in many SWAT applications, riparian wetlands were represented only with the riparian buffer width (FILTERW) parameter; however, a study obtained after model setup indicates prevalence of bank erosion and slumping in the Sprague River and tributaries as well as efficacy of riparian wetlands in the watershed in bank stabilization (NewFields River Basin Services and Kondolf, 2012). Therefore, the results presented here indicate that riparian wetlands in the Sprague River do mediate sediment contributed to the reach from upslope sources, but may not fully reflect the role of the riparian zone in bank stabilization in this watershed.

While scenarios of up to +/-75% wetland loss or gain had modest impact on nutrient fluxes, a hypothetical scenario of 100% wetland loss resulted in a 27% and 42% increase, respectively, in mean annual TN and TP loads (Figures 4-5; Appendix IV, Table 16). The greatest decrease in annual nutrient loads afforded by wetland gains was 9% (8%) for TN (TP) under 100% increase in wetlands (10 m minimum riparian buffer). In a review of field studies of wetlands, Fisher and Acreman (2004) reported average reductions in outflow of N and P species of 67% and 58%, respectively, which is greater than percent reductions afforded by wetland gains or percent increases induced by wetland losses in this study.

However, these studies were at the field scale and may not “scale up” to the watershed level used in this study. Cho et al. (2010b), using SWAT, reported that conservation of current riparian forest extent in the Little River Experimental Watershed, Georgia, United States, resulted in annual stream TN and TP load reductions similar to those reported here when compared to a hypothetical 100% loss of riparian cover, and additionally noted that percent increases in nutrient fluxes under total loss of present-day riparian forest were greater than nutrient reductions afforded by a hypothetical scenario of restoration to an intact 14 m riparian corridor. Similarly, in another SWAT modeling study, Wang et al. (2010) suggested that depression wetland conservation may be more efficient in reducing nutrient loads than wetland restoration in a northwestern Minnesota watershed.

In this study, changes in nutrient fluxes under wetland loss and gain also varied seasonally (Figures 4-5). Johnston et al. (1990) used GIS-derived watershed variables with principle component analysis and multiple linear regression to determine cumulative effects of wetlands on water quality in Minnesota, USA. Results indicated that during high flows wetlands were more effective in removal of suspended solids, TP, and ammonia, but were more effective at nitrate removal during low flow periods. Impacts of wetland loss on TN loads in this study are greatest from August through November, when base flow is dominant and the most prevalent form of N is nitrate; the timing of maximum increases in TP load under wetland loss is nearly opposite to that of TN, occurring from December through March during the high flow season when wetland-mediated P removal may be most efficient.

The loss of Upper Klamath Lake littoral wetlands is believed to have substantially increased nutrient loading to the lake, and to date most research and restoration effort has focused on these wetlands (e.g., Gearheart et al., 1995; Snyder and Morace, 1997; Anderson, 1998; Duff et al., 2009; Wong et al., 2011). The results of this study suggest that present-day tributary riparian wetlands also play an important role in mediating TN and TP loads to Upper Klamath Lake. However, field data are necessary to verify model parameterization of wetland nutrient cycling in the Upper Klamath River Basin, which past research indicates is complex (Appendix III).

3.3. BIAS-CORRECTED PROJECTED CLIMATE

General Circulation Model (GCM) projections represent a “partial sampling” of possible changes in future climate (Brown and Wilby, 2012), but should be regarded as plausible future scenarios rather than forecasts. Long-term changes in gridded projected climate data are shown in Table 1.

This section briefly describes changes in 1954-2005 and 2030-2059 in data bias-corrected to meteorological stations. Monthly and annual averages for total precipitation and daily temperature were calculated separately for each of eight stations for the two time periods. Percent change was then computed separately for each station; the change averaged across the eight stations is reported here.

Annual average daily temperature increased under all models and RCPs, from 0.8-3.1 °C (1.1-3.1 °C) for minimum (maximum) daily temperature. Most models and RCPs showed the greatest warming in June or July (Appendix IV, Table 15), as has been reported in previous climate projections for the Pacific Northwest (Mote and Salathé Jr., 2010).

Downscaled average annual precipitation decreased by 3% under INMCM4 RCP 8.5, but increased by 0.1-11% for INMCM4 RCP 4.5 and CanESM2 and MIROC5 for both RCPs. The greatest percent changes in average monthly precipitation generally occurred in June, July or August (decreases of 15-19% under INMCM4 RCPs, and increases of 18-51% under CanESM2 and MIROC5 RCPs) (Appendix IV, Table 15). The sign and magnitude of GCM projections of changes in precipitation are generally more uncertain than projections of changes in temperature (Mote and Salathé Jr., 2010), and this uncertainty propagates through the hydrologic modeling framework to the simulated magnitude and sign of changes in future stream flow and loads of sediment and nutrients (below).

3.4. PROJECTED HYDROLOGY AND WATER QUALITY UNDER BASELINE

WETLANDS

As future simulations were compared to a historic period simulated with the corresponding GCM data, model performance for 1954-2005 is of note. The hydrologic model driven with the GCM data for this period simulated observed historic stream flow fairly well. The 52-year average annual runoff for GCM-driven simulations was 6% (MIROC5) to 9% (INMCM4) greater than the average for the same period of observed runoff at the U.S Geological Survey gauge at Sprague River near Chiloquin, Oregon (station 1 in Figure 1) and standard deviations were similar between simulations and observed data. These findings may be explained by the slight wet bias for the historic period in the Pacific Northwest under the CMIP5 GCMs (Rupp et al., 2013; Sheffield et al., 2013). Long-term peak average monthly stream flow observations ($39 \text{ m}^3 \cdot \text{s}^{-1}$) agreed well with simulations ($37\text{-}42 \text{ m}^3 \cdot \text{s}^{-1}$), but occurred one month earlier in simulations (March) (Appendix IV, Table 17; Appendix V, Figure 22). Simulations generally generated somewhat higher historic average monthly flows from January through March than observations, but agreed closely throughout the rest of the year (Appendix V, Figure 22).

Annual and monthly changes in flow, sediment and nutrients for climate projections representing extremes in warming and change in precipitation (CanESM2 and INMCM4, RCP 8.5) are shown in Figure 6 as percent change from baseline and in Appendix V, Figure 23 as historic and simulated future time series (for simulations under all climate projections and significance in differences between the historic and future period, see Appendix IV, Tables 18-19).

Five climate projections projected increases in average annual total precipitation and in average annual runoff for 2030-2059 relative to 1954-2005, with INMCM4 (RCP 8.5) being the sole exception (climate values here are calculated from data downscaled, bias-corrected to stations, and averaged across stations for 1954-2005; see section 3.3). However, changes in annual runoff were significant only under

CanESM2 (RCP 4.5, $p < 0.05$, and RCP 8.5, $p < 0.001$), and changes in INMCM4 (RCP 8.5), were generally negative but not significant on an annual or monthly basis.

Interannual variability (standard deviation) in the future period was relatively high for flow, sediment and nutrients (Appendix IV, Table 18), and monthly changes were of a greater magnitude than annual shifts. All climate projections simulated decreases in average monthly stream flow from April through early to late summer, and with the exception of INMCM4 (RCP 8.5), simulated stream flow increases from October through March (Figure 6; Appendix IV, Tables 18-19; Appendix V, Figure 23). Decreases in some spring and summer months were only significant under the MIROC5 projections, while increases in at least some winter months were significant under all projections but INMCM4 (RCP 8.5).

Despite some significant differences between the historic and future periods, a Mann-Kendall test over the period 2030-2059 did not show significant trends in annual stream flow, and few trends in average monthly stream flow or loads of sediment and nutrients (Appendix IV, Table 20). A relatively small number of water resources climate impact studies has used trend analysis tests on simulated future time series of stream flow. One such study was by Hay et al. (2011), who used regression analysis on the mean of a moving 12-year window averaged by GCM emission scenario for the period 2001-2099. Where the regression was significant, they reported the trend (slope of the regression). Results of this study for the Sprague River were detailed by Risley et al. (2012), who did not report significant trends in mean annual stream flow but noted significant positive trends in mean annual surface runoff under higher emissions scenarios. However, while Risley et al. projected a change in the timing of peak average monthly stream flow from April to March, our study projected no such change, possibly because even during the baseline period all GCMs and RCPs simulated peak average monthly stream flow in March (Appendix V, Figure 22). Peak average monthly flow decreased by 1% under INMCM4 (RCP 8.5) and increased from 3-36% for all other GCMs and RCPs. In contrast to a study of historic Upper Klamath Lake stream flow trends from the 1940s to the mid-2000s (Mayer and Naman, 2011), this study showed

few significant trends in average monthly stream flow in the future period, and significant negative monthly trends were projected only under the INMCM4 (RCP 8.5) model for some months of the year (Appendix IV, Table 20).

The greatest simulated increases in mean monthly flow for any given GCM and RCP in this study ranged from 16-115% and generally occurred from October through March, within the range of simulated changes in winter runoff reported for the Western Cascades for the 2050s (Waibel et al., 2013). While the greatest percent increases in precipitation generally occurred in summer, this was typically a small absolute increase and all models projected decreases in stream flow from April through as late as August (Appendix IV, Table 15 and Table 19). Decreases in April flow, although not statistically significant, could be attributed to more snow melt occurring earlier in the season and a lower snow pack, as observed in other studies in the Western United States, particularly as the Sprague River watershed spans elevations where snow accumulation and persistence are reported to be especially sensitive to small changes in temperature (Mote, 2003; Hamlet et al., 2007; Jefferson, 2011; Risley et al., 2012; Diffenbaugh et al., 2012; Sproles et al., 2013).

Under present-day wetland extent, simulated average annual sediment and nutrient loads decreased by 6% (sediment), 8% (TN) and 11% (TP) under INCM4 RCP 8.5, but increased from 7-52% (sediment), 4-37% (TN) and 1-38% (TP) under other projections (Figure 6; Appendix IV, Tables 18-19). Annual and monthly patterns of significance in sediment, TN and TP changes from the historic period were similar to those for flow and are detailed in Appendix IV, Tables 18-19. Percent changes in average sediment, TN and TP loads showed the same sign as changes in flow on a monthly and annual basis for almost all months under almost all climate projections. Greatest percent increases generally occurred from October through March and ranged from 26-242% (sediment), 13-121% (TN), and 8-97% (TP); and the greatest percent decreases from April through September for sediment (4-44%), and April through June for TN (reductions of 4-41%) and TP (7-33%). Previous climate impact modeling studies have estimated increases in sediment loads of 20-146% for several American Midwestern watersheds with increasing

future stream flow (Woznicki et al., 2011; Van Liew et al., 2012), and decreases in sediment concentration with decreasing stream flow in the historically snow-melt dominated American Sierra Nevada mountains (Ficklin et al., 2013).

The magnitude of percent change in average sediment loads for a given month was greater than the corresponding change in flow under most projections, whereas this was frequently but not always the case for TN or TP loads (Figure 6; Appendix IV, Tables 18-19). Sediment loads typically increase logarithmically with stream flow, which may partly explain this result (Novotny, 2003; Naik and Jay, 2011). In SWAT, this is reflected in the simplified Bagnold equation, in which the maximum concentration of sediment that may be transported within the reach increases exponentially with peak stream flow. However, the greater percent change in sediment relative to stream flow could also be related to future climate. Under a warmer future climate in the Pacific Northwest a precipitation phase change from snow to rain and a decrease in protective snow cover on the soil surface may be expected (Mote, 2003; Nolin and Daly, 2006; Sproles et al., 2013). In contrast to runoff from snow melt, runoff from rain has more erosive power (in the SWAT model, snowmelt has no erosive power) (Neitsch et al., 2009). Ficklin et al. (2013) reported a significantly negative correlation between simulated future snowmelt and sediment concentration in the American Sierra Nevada. A shift in precipitation from snow to rain is likely to simultaneously decrease soil cover and increase the area contributing to erosion, while increasing rainfall impact and the runoff volume and magnitude of peak runoff. In SWAT, erosion calculated with the modified universal soil loss equation varies exponentially with the latter two hydrologic variables, and linearly with soil erodibility and cover (Neitsch et al., 2009).

Changes in average nutrient loads reported here are within literature ranges of 5 to 88% for TN and -6 to 74% for TP, although such changes can be expected to vary widely by region, time period modeled, and choice of climate forcing data (Bouraoui et al., 2002; Ficklin et al., 2010; Woznicki et al., 2011; Van Liew et al., 2012).

While changes in loads under wetter future climate projections are clearly related to stream flow changes, transport of nutrients could also be altered under some of the same mechanisms described above for sediment. This is especially the case for organic N and P and for mineral P adsorbed to sediment, and transport of these nutrient fractions in the SWAT model is calculated from upland erosion and reach sediment concentration (Neitsch et al., 2009). Soluble P is typically entrained from the uppermost soil layers in surface runoff, and so may be mobilized more frequently under higher-magnitude flows such as those observed in winter under wetter climate projections (Neitsch et al., 2009). Additionally, hydroclimatic shifts may alter not only nutrient transport but also biogeochemical cycling. Warmer future climate may extend the growing season and the period of microbially-mediated upland and in-stream nutrient transformations (Whitehead et al., 2009). Rates of N and P cycling (including decomposition, mineralization, nitrification and denitrification) are strongly influenced by temperature and moisture, and so may either accelerate or decrease depending on degree and timing of future warming and water availability (Baron et al., 2009; Solheim et al., 2010; Ahmadi et al., 2013).

3.5. EFFECTS OF WETLAND LOSS AND GAIN UNDER FUTURE CLIMATE

This section summarized the combined effects on water quality of changes in wetlands and future climate under the two extreme climate projections noted in section 2.6, IMCM4 and CanESM2 (RCP 8.5). Simulated changes in flow, sediment and nutrients under a given wetland scenario relative to fluxes under baseline wetland extent for the same time period were of a similar magnitude between 2030-2059 and 2001-2010 (reported in section 3.2). An exception was the impact of 100% wetland loss on average annual TP fluxes; this scenario resulted in 64-70% increases for 2030-2059 above a baseline wetland scenario for the 2040s, but only a 42% increase for 2001-2010 relative to a baseline wetland scenario for the 2000s (Appendix IV, Table 16, Table 21). Median annual load of TN and TP differed among wetland scenarios for CanESM2 (Friedman test, $\chi^2(3) = 90.0, p < 0.001$) and for INMCM4 ($\chi^2(2) = 60.0, p < 0.00$).

Comparisons of future fluxes under wetland scenarios to fluxes under baseline wetland extent from 1954-2005 showed the combined impact of changing climate and wetland loss or gain. Under baseline wetland extent, future TN and TP loads were significantly different from historic loads for CanESM2, but not for INMCM4 (section 3.4). This was also the case under most scenarios of wetland change. One notable exception was TP load under total loss of wetlands for the INMCM4 projection, which was significantly different from historic TP load. Where future loads were significantly different from historic under the Mann-Whitney-Wilcoxon test, the *p*-value is shown in parentheses following the percent change between the historic and future period (reported below).

When comparing simulations of 100% wetland loss for 2030-2059 to baseline wetland extent for the period 1954-2005, average annual TN load increased 68% (CanESM2 RCP 8.5, *p* <0.001) and 15% (INMCM4 RCP 8.5) as compared to 37% increase (CanESM2 RCP 8.5, *p* <0.001) and 8% decrease (INMCM4 RCP 8.5) between the historic and future periods with no wetland loss.

Similarly, average annual TP loads increased 135% (CanESM2 RCP 8.5, *p* <0.001) and 47% (INMCM4 RCP 8.5, *p* <0.001) under simulations of 100% wetland loss relative to the historic period, as compared to a future 38% increase (*p* <0.001) and 11% decrease, for CanESM2 and INMCM4 respectively, under no wetland loss. Load increases of TN and TP under 50% wetland loss were generally much more modest than under total loss of wetlands (Appendix IV, Table 21).

Despite the large impact of 100% loss on simulated future TP loads, wetland gains in most years were insufficient to reach a 40% reduction in external TP loads at the Sprague River outlet, when compared to 1954-2005 average annual loads under a baseline wetland extent (Figure 7). Forty percent reduction is the Total Maximum Daily Load (TMDL) targeted condition for Upper Klamath Lake, to which the combined flow of the Sprague and Williamson Rivers drains (Boyd et al., 2002).

3.6. ASSUMPTIONS AND LIMITATIONS

As in other studies of climate change impacts, this study incorporates multiple sources of uncertainty, including hydrologic model uncertainty, measurement uncertainty in calibration data, and uncertainty in future climate forcings. The latter include uncertainty in global forcings such as future greenhouse gas levels; the physical response of the climate system in the GCM formulation; and internal model variability of the GCMs (Rupp et al., 2013). While we acknowledge the value of a detailed uncertainty analysis in interpreting results presented here, such an analysis is beyond the scope of the current study.

Aspects of the hydrologic model framework that might influence study results and interpretation include: Representation of riparian buffer strips within the SWAT model; channel connectivity with the floodplain and representation of riparian wetlands; and time-invariant parameters. These components will impact both future simulations and the simulated historic baselines to which they are compared.

In the current SWAT model, riparian wetlands trap sediment and nutrients from upslope sources prior to routing to the reach. Trapping efficiencies of sediment and nutrients in surface runoff increase non-linearly with buffer width (Equation 1). Therefore within the modeling framework, loss of all riparian wetlands could be expected to have a greater proportional impact on nutrient and sediment loads than loss of only some of the existing buffer. Similarly, additional riparian restoration where a buffer of several meters already exists would result in a smaller proportional reduction in nutrient loads.

In this study we have represented the hypothetical impact of future climatic or anthropogenic impacts on wetlands simply via changes in wetland geometry. However, future climate and possible climate-induced changes in flood duration (noted above) could also alter riparian water availability, plant composition, and nutrient cycling (Perry et al., 2012)—all of which might serve to alter future stream water quality.

Additionally, we applied percent changes in wetland scenarios to all wetlands within the Sprague River watershed. However, changes in wetlands under future climate could vary spatially. For example, shorter flowpath groundwater systems such as those supplying baseflows to headwater streams could be more impacted by climate-related changes in groundwater recharge than larger streams (Waibel et al., 2013). A large percentage of riparian wetlands in the Sprague River watershed are adjacent to such headwater streams (Appendix IV, Table 22). Future modeling could assess the sensitivity of Sprague River water quality to spatially varying wetland loss—such as losses only for wetlands adjacent to headwater streams.

The SWAT riparian buffer model filters surface and subsurface runoff contributed from uplands to the reach. Overbank flooding from the channel into the riparian zone and resulting decreased flow velocities and attenuation or re-entrainment of sediment and nutrients in the floodplain is not modeled, and neither are transformations between nutrient fractions within riparian wetlands (Neitsch et al., 2009). Although leveed in sections, much of the Sprague River mainstem and the Sycan River still overflow their banks at higher discharges, and scouring of volcanically-deposited floodplain material may be an important component of the Sprague River sediment budget (Rasmussen, 2011; NewFields River Basin Services and Kondolf, 2012). This suggests that floodplain connectivity could play an important role not apparent in this study in mediating climate-induced flow increases simulated under some climate projections, as well as stream sediment and nutrient loads. Future work would benefit from detailed field data on Sprague River wetland removal efficiencies of sediment and nutrients and riparian buffer impacts on stream water quality.

Several parameters and processes that are time-invariant in SWAT could in reality be expected to vary temporally. These include CO₂ concentrations (noted above); land cover and land use; lapse rates of precipitation and temperature with elevation; channel morphology and planform; and nutrient processes within the riparian zone (Neitsch et al., 2009). This study assumes a static channel cross-section and planform over time; however, channel adjustments to climate-induced changes in flow and sediment

could be expected to include changes in bedforms, bed and bank scour, sediment grain size, channel slope, and planform, mediated by local geomorphic controls such as valley width or constriction (Knighton, 1998; Rasmussen, 2011). This seems especially plausible as the Sprague River has been observed to develop meander cutoffs relatively rapidly in the historic period (NewFields River Basin Services and Kondolf, 2012). Additionally, this study assumes time-invariant management schedules; however, in reality, timing, amount, source (surface or groundwater) and efficiency of irrigation as well as grazing rotations would be altered over time within a hydrologic, socioeconomic and legal context.

3.7. IMPLICATIONS AND FUTURE WORK

The primary goal of this study was to assess the basin-scale regulation of water quality provided by variable wetland extent under current and future climatic conditions in the Sprague River watershed for the mid-21st century. Specific objectives of the study were to evaluate the effects of wetland loss and gain under present-day climate on stream water quality at the watershed scale; to identify direction and magnitude of potential changes in stream flow, sediment, and nutrient loads under future climate and baseline wetland conditions; and to determine how wetland gain or loss might exacerbate or ameliorate climate-induced changes in future water quality.

Results suggest that present-day wetlands in Upper Klamath Lake tributaries may have substantially ameliorated nutrient loads at the Sprague River outlet in the past; that the efficacy of wetlands in nutrient load reductions has distinct seasonality for TN and TP; and that stream water quality at the watershed scale may be somewhat resilient to changes in wetland extent, but that a threshold of wetland loss may exist beyond which large increases in nutrient fluxes could occur.

This study implies that flows at the Sprague River outlet under future climate and baseline wetland conditions could decrease in spring and summer, a pattern which is observed in hydrologic simulations forced both with warmer-and-drier and warmer-and-wetter climate projections but

statistically significant in only two of six climate projections. Previous studies in the Pacific Northwest have noted that climate impacts to water resources could potentially be mitigated with flow regulations (e.g., Mote et al., 2003). Therefore, it may be possible that storage of higher winter flows in Upper Klamath Lake (whose outlet is regulated) and lakeside wetlands followed by releases during the growing season could moderate effects on lake endangered species and downstream users (e.g., the Klamath Irrigation Project). In contrast, under a drier future climate, reduced stream flow could occur throughout much of the year (as demonstrated by the INMCM4 RCP 8.5 scenario, although we note that mean monthly and annual flows were not significantly different from the historic period). This could put additional strain on water resources already in high demand from multiple sectors. Flow decreases during the growing season in the Sprague River watershed, which is upstream of any large reservoir or regulated lake, could have substantial implications for cattle production which has historically occurred along the stream corridor and relied predominantly on flood irrigation from rivers and streams; and could impact riparian ecology and species composition (U.S. Department of Agriculture Natural Resources Conservation Service, 2009; Perry et al., 2012). Potential effects of changes in flow must also be considered in a social and legal context. The Klamath Tribes and basin irrigators are part of the Klamath Basin Restoration Agreement (KBRA), which provides for sharing of water in dry periods. Recent adjudication in the Upper Klamath River Basin determined that Klamath Tribes water rights have seniority, which means irrigation withdrawals could be restricted in droughts (Times-Standard 2013).

To the authors' knowledge this is the first publication to assess potential effects of future climate on nutrient fluxes in an American Western watershed where shifts from snowmelt dominated to rainfall-dominated hydrology may occur in the 21st century, and one of the few to date to assess future hydroclimatic impacts on sediment loads in such systems. Results of this study may therefore shed light on potential changes in stream nutrient and sediment dynamics in other watersheds of the Western United States.

In a wetter future climate, increases in sediment disproportionate to increases in flow could increase sedimentation in Upper Klamath Lake, which in turn could contribute to further internal TP loading within the lake as has been observed in the past (Boyd et al., 2002). Additionally, increased sediment and nutrient loads from October through March combined with an extended growing season under warmer climate could provide a longer period favorable to growth in Upper Klamath Lake of cyanobacteria, whose blooms peak in summer and which may currently be P-limited early in the growing season (Boyd et al., 2002). However, changes in lake inflow and in air temperature may also alter lake turnover, residence time, and nutrient dynamics, complicating interpretation of impacts of altered flow, sediment and nutrient inputs to the lake (Whitehead et al., 2009). Increasing air temperature, seasonal low flows, and elevated nutrient levels additionally have the potential to alter stream temperature, dissolved oxygen, and cyanobacterial growth, which may in turn impact stream fish species (Whitehead et al., 2009; Beechie et al., 2012).

Previous studies evaluating the impacts of conservation practices aimed at ameliorating water quality conditions under future climate have generally assumed that the practice will persist or may reasonably be implemented under future hydroclimatic conditions. These assumptions may not hold for wetlands under a warmer future with uncertain changes in precipitation, particularly for riparian zones in the semi-arid Western United States which may be substantially impacted by future climate and climate-induced changes in stream flow (Perry et al., 2012). This study attempted to elucidate how climate-induced or anthropogenic changes in wetlands might exacerbate or ameliorate future stream water quality. Simulations under two very different climate projections indicate that large loss of present-day wetlands could significantly increase TP loads above historic baseline, but that additional gains in wetlands may not substantially ameliorate climate-induced nutrient load increases.

Similar to the findings of this work, other case studies have reported that simulated impacts of changing climate exceed those of altered land use or conservation practices; the efficacy of conservation practices on stream water quality at the watershed scale may not alter substantially between the historic or

future period; and that even implementation of additional conservation practices or altered land use strategies may not be sufficient to maintain nutrient fluxes at historic levels under future climate (Whitehead et al., 2006; Praskievicz and Chang, 2009, 2011; Woznicki et al., 2011; Van Liew et al., 2012). However, results and implications must be viewed in the context of the modeling framework used.

Finally, it is possible that pollutants of primary concern and thus potential strategies for mitigation or adaptation might change over time (for example, temperatures in some streams could approach lethal limits for certain fish species), emphasizing the importance of incorporating potential future climate change impacts into present-day decision-making (Beechie et al., 2012).

In this study we assessed change in annual and monthly average flow, sediment and nutrient loads at the Sprague River outlet to illustrate long-term climate change impacts on water resources at the basin scale and to assess the potential to meet annual TP load targets in the watershed in future. However, river geomorphology and ecosystems as well as agriculture and human infrastructure are influenced by flow regime characteristics (flow magnitude, frequency, duration, timing and rate of change, after Poff et al., 1997), which may alter under future climate, particularly as extreme climatic events may become more frequent (Praskievicz and Chang, 2009). Additionally, Sprague River tributaries are hydrologically distinct with varying groundwater influence, and span elevation gradients where snowpack may or may not persist under future climate (Mote, 2003; Mayer and Naman, 2011; Waibel et al., 2013; Sproles et al., 2013). Thus, the impacts of climate change on hydrology and wetlands may vary substantially among tributaries. We suggest that future work investigate climate-induced changes in flow regime variables within the Sprague River tributaries and the spatially variable impact of such changes on regional wetlands within a modeling framework accounting for overbank flooding, lateral connectivity of the channel with the riparian corridor, and detailed biogeochemical cycling within wetlands.

CHAPTER 4. CONCLUSIONS

The results of this study suggest:

1. Present-day wetlands in the Sprague River watershed result in lower nutrient (nitrogen and phosphorus) loads at the watershed outlet.
2. Both warmer and wetter and warmer and drier futures in the Sprague River watershed are possible, and annual and monthly changes in flow and fluxes of sediment and nutrients reflect this uncertainty in climate projections.
3. It is possible that average annual and monthly runoff and fluxes of sediment and nutrients for the 2040s in the Sprague watershed may be significantly different from the past. However, it is also possible that there will be no significant differences between the future and historic period.
4. It is possible that there may be future increases in stream flow during the high flow season in the Sprague River (October – March), as well as decreases in spring summer flows, with changes in sediment and nutrient fluxes following stream flow patterns.
5. The above simulated changes are significantly different from the historic period for high flow months under most climate projections used in this study, but significantly different for spring and summer in only a few simulations.
6. Nutrient loads at the Sprague River outlet under future climate and scenarios of wetland loss could vary significantly from baseline, or could be similar to the historic period. However, a threshold of wetland loss may exist beyond which large increases in nutrient loads could occur.

7. Additional wetland restoration in the Sprague River watershed could somewhat reduce nutrient loads at the outlet, but might do little to ameliorate climate impacts to stream water quality in the Sprague River watershed.

TABLES

Table 1. General Circulation Models (GCMs) and Representative Concentration Pathways (RCPs) used in scenario analysis using the Coupled Model Intercomparison Project 5 (CMIP5) Multivariate Adapted Constructed Analogs (MACA) of University of Idaho. Absolute change in average annual temperature (“ ΔT ”) and percent change in average annual total precipitation (“% Change P”) are shown between the future period 2030-2059 and historic period (1950-2005). Values are averaged from daily 4 km gridded data over the entire Sprague River watershed.

ΔT ($^{\circ}C$)	% Change P	GCM Abbreviation	Full GCM name	RCP
1.0	-0.4	INMCM4	Institute of Numerical Mathematics 4	4.5
1.4	-3.5			8.5
1.9	1.6	MIROC5	Model for Interdisciplinary Research on Climate 5	4.5
2.1	0.0			8.5
2.6	8.9	CanESM2	Canadian Earth System Model 2	4.5
3.1	11.1			8.5

Table 2. Depressional wetland model parameters, equations and sources. “Parameter” is the parameter name in the SWAT pond (.pnd) file. “Wetlands database” refers to Oregon Natural Heritage Information Center and the Wetlands Conservancy (2009), U.S. Department of Agriculture Natural Resources Conservation Service (2011), U.S. Fish and Wildlife Service (2011), and U.S. Geological Survey (2011).

Parameter	Description	Units	Sources	Value or equation
WET_FR	Fraction of subwatershed draining to wetlands	--	Wetlands database	--
WET_MXSA	Max. surface area	ha	Wetlands database	--
WET_NSA	Normal surface area	ha	Liu et al., 2008; Wu and Johnston, 2008	WET_MXSA·0.45
WET_NVOL	Normal volume	10 ⁴ m ³	Liu et al., 2008; Wu and Johnston, 2008	Average of: WET_NSA·0.1 WET_MXVOL·0.4
WET_MXVOL	Max. volume	10 ⁴ m ³	Liu et al., 2008; Wu and Johnston, 2008	WET_MXA·0.35
IFLOD1	Beginning month of non-flood season	--	Identified from 2001-2010 hydrographs for each tributary	Sycan, N. and S. Forks: Aug; Sprague mainstem: Jul.
IFLOD2	Ending month of non-flood season	--		Sycan and Sprague mainstem: Dec.; N. Fork: Feb.; S. Fork: Oct

Table 3. Calibration (C) and testing (T) statistics for Sprague River tributaries and mainstem. The calibration period is 2001-2006 and the testing period is 2007-2010, except for flow (Q) at the South Fork of the Sprague River, where calibration is for even years from October 1992 to September 2003, and testing is for odd years for the same period. All statistics are monthly except sediment and nutrient statistics for the South Fork of the Sprague River, which are daily. Numbers following tributary name correspond to numbered flow (first) and water quality sampling location (second) shown in Figure 1. Information on stream flow gages and water quality sampling locations is shown in Appendix IV, Table 13. PBIAS = percent bias; a negative (positive) value denotes an overestimate (underestimate). R^2 = coefficient of determination; and NS = Nash-Sutcliffe coefficient.

North Fork of the Sprague River (6, 5)								
Statistic	Q		Sed		TP		TN	
	C	T	C	T	C	T	C	T
PBIAS (%)	-8	-31	6	-18	1	-16	0	0
R^2	0.85	0.89	0.88	0.82	0.87	0.71	0.91	0.90
NS	0.71	0.67	0.69	0.63	0.73	0.42	0.74	0.63
South Fork of the Sprague River (8, 7)								
PBIAS (%)	21	17	11	12	22	28	94	97
R^2	0.90	0.83	0.79	0.78	0.54	0.62	0.64	0.69
NS	0.78	0.68	0.62	0.58	0.27	0.34	-0.31	-0.41
Sycan River (3, 4)								
PBIAS (%)	20	17	10	9	32	36	67	95
R^2	0.94	0.88	0.95	0.89	0.88	0.85	0.72	0.85
NS	0.82	0.66	0.89	0.78	0.74	0.60	0.42	-0.29
Sprague River Mainstem (1, 2)								
PBIAS (%)	3	-6	-20	10	10	-26	37	19
R^2	0.93	0.85	0.94	0.81	0.85	0.63	0.81	0.70
NS	0.84	0.70	0.86	0.62	0.70	0.28	0.56	0.45

FIGURES

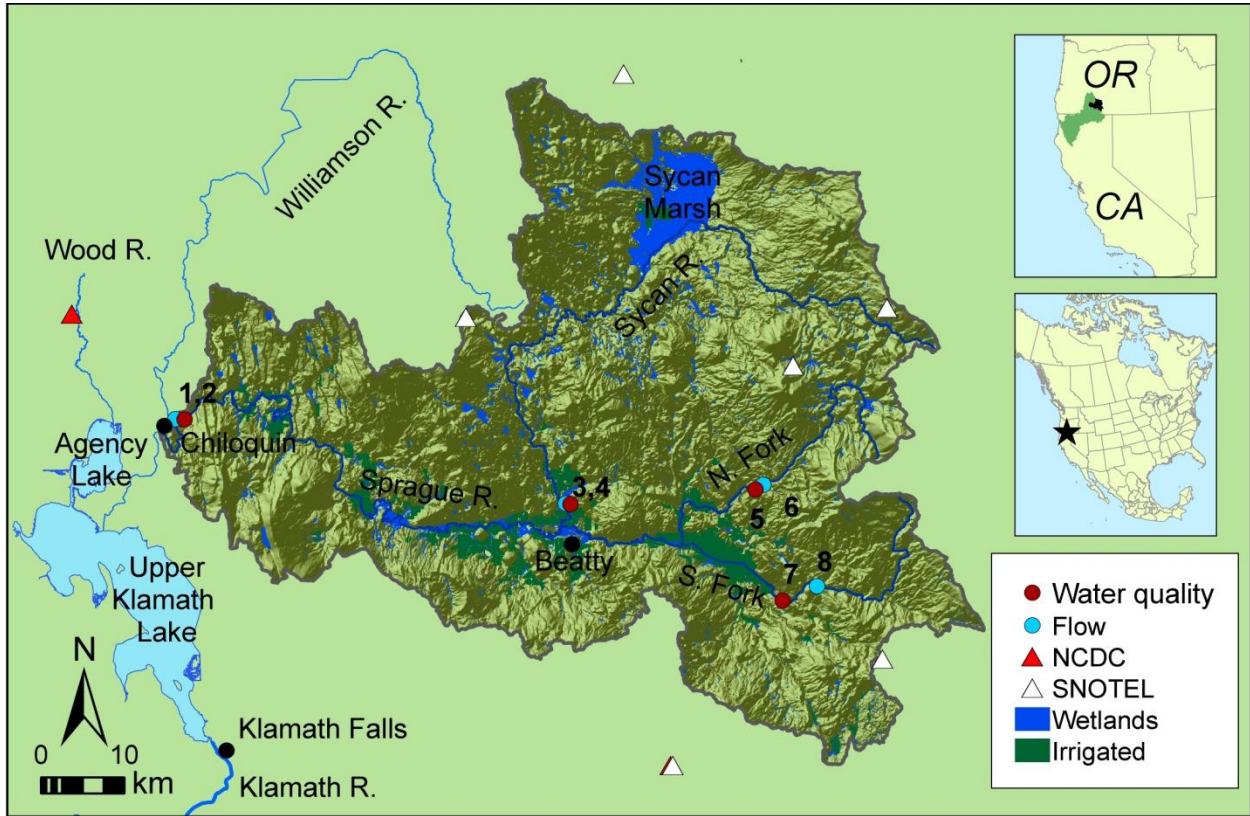


Figure 1. Sprague River watershed, Oregon, USA. Numbers of calibration and testing sites (circles) correspond to site information in Table 3 and Appendix IV, Table 13. Wetlands are derived from four Oregon wetlands databases: Oregon Natural Heritage Information Center and the Wetlands Conservancy (2009), U.S. Department of Agriculture Natural Resources Conservation Service (2011), U.S. Fish and Wildlife Service (2011), and U.S. Geological Survey (2011). Irrigated sites are those designated for agricultural irrigation by the Oregon Water Resources Department (2008). In the upper inset map, the Sprague River watershed (entire Klamath River Basin) is shown in black (green). In the lower map, the study area is denoted by a star.

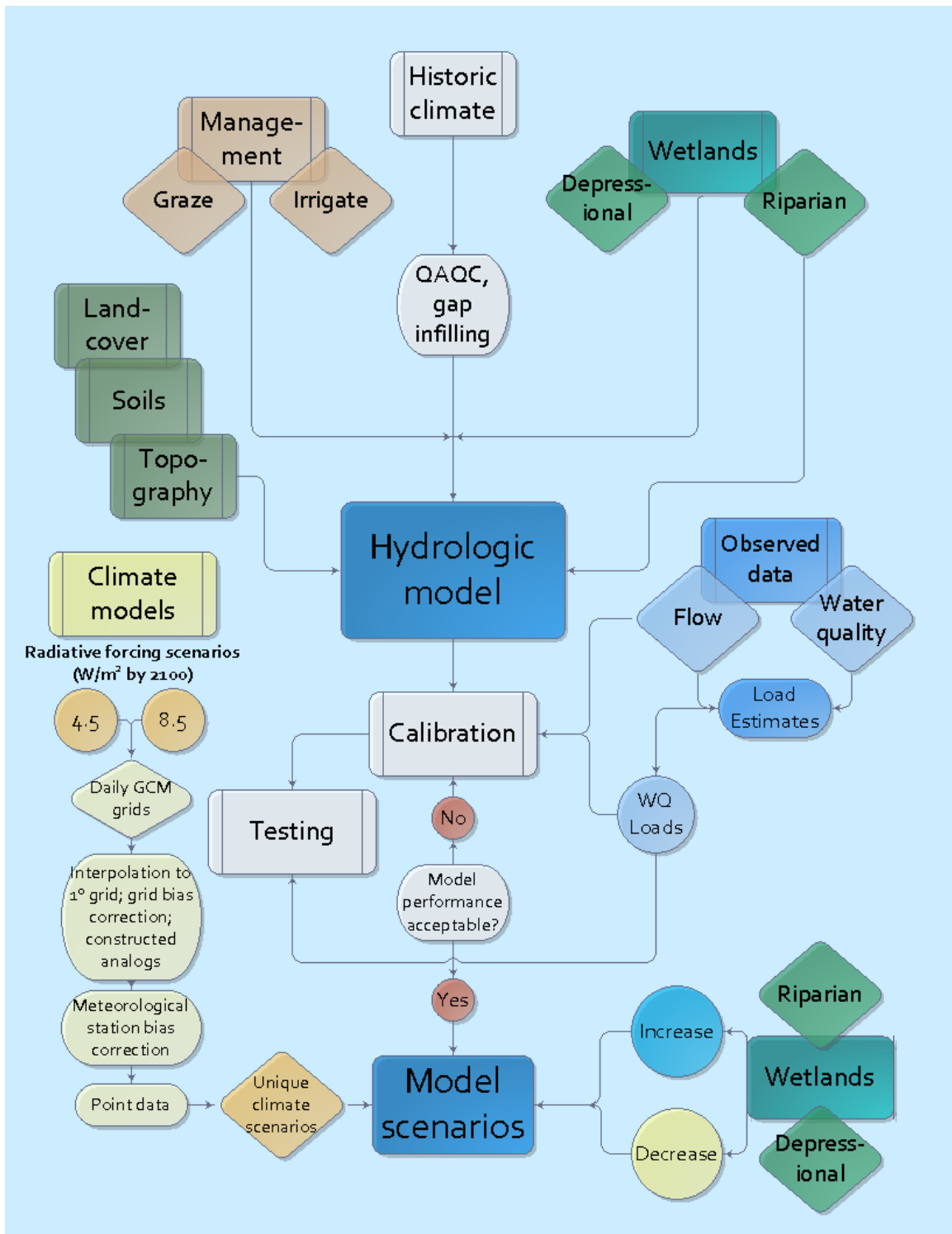


Figure 2. Schematic of SWAT hydrologic model setup and scenario analysis.

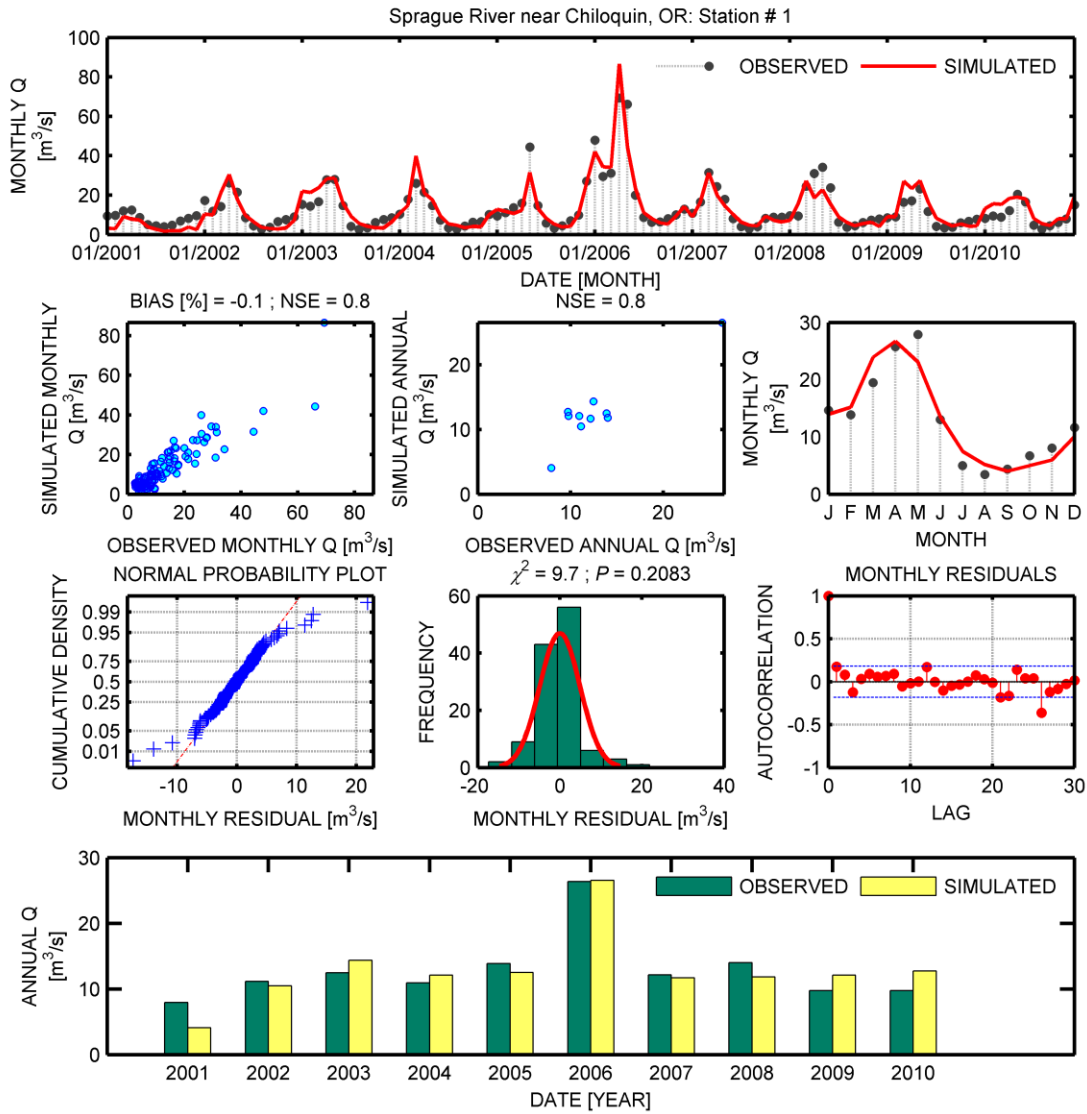


Figure 3. Time series of monthly calibration (2001-2006) and testing (2007-2010) periods for the mainstem of the Sprague River for stream flow. Stream flow time series is at the U.S. Geological Survey gauge Sprague River near Chiloquin, Oregon (site 1 in Figure 1 and Table 3; and in Appendix IV, Table 13).

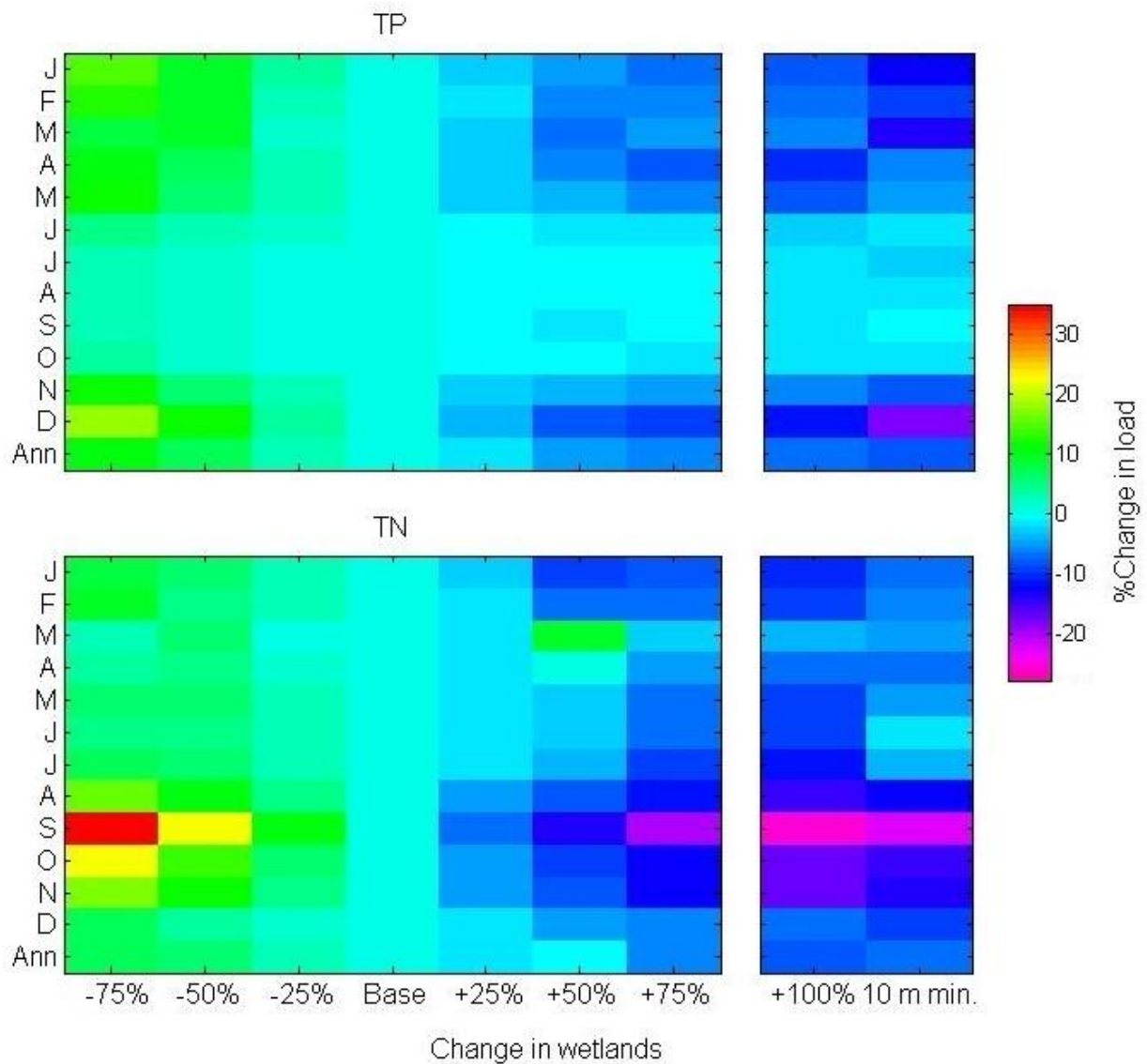


Figure 4. Simulated percent change in 2001-2010 average monthly and annual TP and TN loads at the outlet of the Sprague River, Oregon under scenarios of loss and gain of riparian and depressional wetlands. “Base” represents baseline wetland extent under present-day conditions. Scenarios of +/-25, 50, 75 and +100% are applied to all wetlands in the Sprague watershed and represent a change in width for riparian buffers and a change in surface area and volume for depressional wetlands. “10 m min” shows a scenario of a riparian buffer of a minimum 10 m width throughout the watershed, with depressional wetland extent unaltered from baseline.

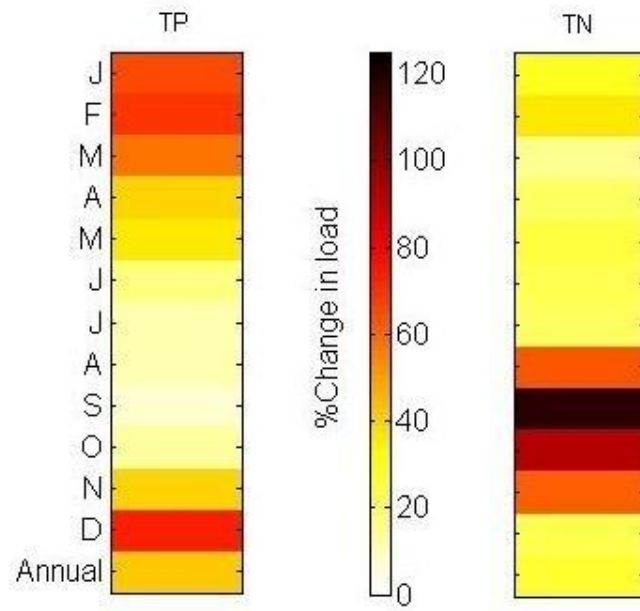


Figure 5. As for Figure 4, but only for a scenario of 100% loss of riparian and depressional wetlands.

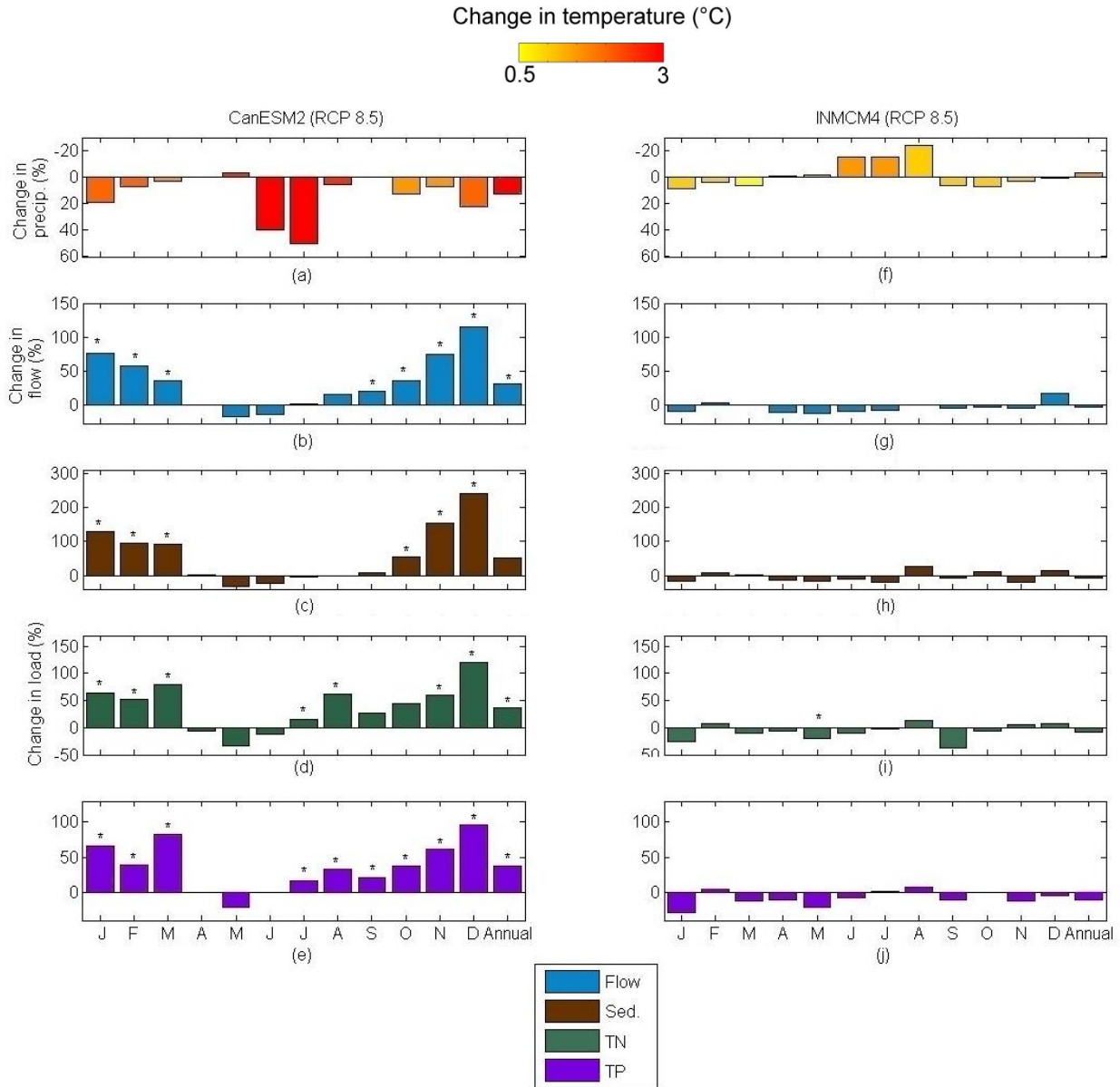


Figure 6. Annual and monthly average warming and percent change in precipitation, stream flow, sediment and nutrients for two climate projections. The two projections represent extremes in temperature and precipitation change from baseline for the six climate projections utilized in this study. Length of bars in (a) and (f) show percent change in precipitation from baseline, while colors of bars show change in average temperature, rounded to the nearest 0.5°C. Percent change is shown for stream flow (b and g) in blue; sediment (c and h) in brown; total nitrogen (d and i) in green; and total phosphorus (e and j) in purple. Percent changes are between averages for 2030-2059 and 1954-2005. Historic and future averages are also shown as mean monthly discharge and loads in Appendix V, Figure 23.

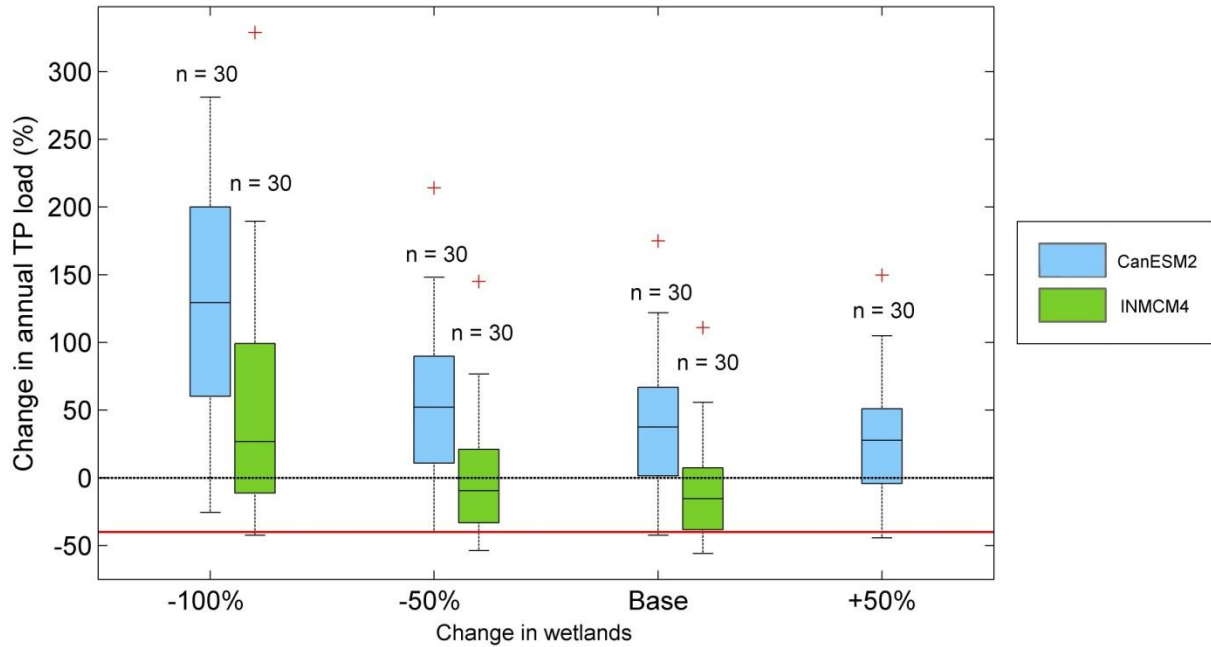


Figure 7. Change in average annual total phosphorus load between 2030-2059 relative to 1954-2005 averages under scenarios of loss and gain of riparian and depressional wetlands for Representative Concentration Pathway (RCP) 8.5, General Circulation Models (GCMs) CanESM2 and INMCM4. These GCMs and RCP represent extremes in precipitation and temperature changes for the six climate projections utilized in this study. The central mark of the box is the median; box lower (upper) edges represent the 25th and 75th percentiles, respectively, whiskers extend to the most extreme data points not considered outliers, and outliers are plotted individually as red crosses. Base” represents baseline wetland extent under present-day conditions. Scenarios of +/- 50 and -100% change are applied to all wetlands in the Sprague watershed and represent a change in width for riparian buffers and a change in surface area and volume for depressional wetlands. As precipitation decreased under INMCM4 (RCP 8.5), only scenarios of wetland loss were simulated for this GCM and RCP. The red line denotes a 40% reduction in annual TP loads (the targeted condition for total phosphorus external loads to Upper Klamath Lake in the Lake’s Total Maximum Daily Load), using GCM-driven simulations of 1954-2005 annual average loads as reference.

REFERENCES

- Abatzoglou, J.T. 2013. Development of gridded surface meteorological data for ecological applications and modelling. *Int. J. Climatol.* 33(1): 121–131.
- Abatzoglou, J.T., and T.J. Brown. 2012. A comparison of statistical downscaling methods suited for wildfire applications. *Int. J. Climatol.* 32(5): 772–780.
- Abbaspour, K. C., M. Faramarzi, S. S. Ghasemi, and H. Yang. 2010. Assessing the impact of climate change on water resources in Iran, *Water Resour. Res.*, 45:1-16.
- Ahmadi, M., R. Records, and M. Arabi. 2013. Impact of climate change on diffuse pollutant fluxes at the watershed scale. *Hydrol. Process.* Published online. doi: 10.1002/hyp.9723
- American Society of Agricultural and Biological Engineers. 2006. ASAE D384.2 MAR2005 Manure Production and Characteristics. St. Joseph, MI.
- Anderson, J.K. 1998. A management model for determining optimal watershed management strategies for reducing lake total phosphorus concentration: Application to Upper Klamath Lake, Oregon. M.S. Thesis, Humboldt State University, Arcata, CA 120 pp.

Arnold, J.G., J.R. Kiniry, R. Srinivasan, J.R. Williams., E.B. Haney, and S.L. Neitsch. 2011. Soil and Water Assessment Tool input/output file documentation, Version 2009, Report No. 365. College Station, TX.

Arnold, J.G., R. Srinivasan, R.S. Muttiah, and J.R. Williams. 1998. Large area hydrologic modeling and assessment, Part I: Model development. *J. Am. Water Resour. Assoc.* 34(1): 73–89.

Arora, V.K. 2002. The use of the aridity index to assess climate change effect on annual runoff. *J. Hydrol.* 265(1-4): 164–177.

Barnett, T.P., D.W. Pierce, H.G. Hidalgo, C. Bonfils, B.D. Santer, T. Das, G. Bala, A.W. Wood, T. Nozawa, A.A. Mirin, D.R. Cayan, and M.D. Dettinger. 2008. Human-induced changes in the hydrology of the western United States. *Science* 319: 1080–1083.

Baron, J.S., T.M. Schmidt, and M.D. Hartman. 2009. Climate-induced changes in high elevation stream nitrate dynamics. *Glob. Chang. Biol.* 15(7): 1777–1789.

Bates, B.C., Z.W. Kundzewicz, S. Wu and J.P. Palutikof, Eds. 2008. *Climate change and water*. Technical Paper of the Intergovernmental Panel on Climate Change, IPCC Secretariat, Geneva, 210 pp.

Beechie, T., H. Imaki, J. Greene, A. Wade, H. Wu, G. Pess, P. Roni, J. Kimball, J. Stanford, P. Kiffney, and N. Mantua. 2012. Restoring salmon habitat for a changing climate. *River Res. Appl.*

Published online. doi:10.1002/rra.2590

Bosch, N.S. 2008. The influence of impoundments on riverine nutrient transport: An evaluation using the Soil and Water Assessment Tool. *J. Hydrol.* 355(1-4): 131–147.

Bouraoui, F., L. Galbiati, and G. Bidoglio. 2002. Climate change impacts on nutrient loads in the Yorkshire Ouse catchment (UK). *Hydrol. Earth Syst. Sci.* 6(2): 197–209.

Boyd, M., S. Kirk, M. Wiltsey, and B. Kasper. 2002. Upper Klamath Lake Drainage Total Maximum Daily Load (TMDL) and Water Quality Management Plan (WQMP). State of Oregon Department of Environmental Quality, Portland, OR.

Bracmort, K.S., M. Arabi, J.R. Frankenberger, B.A. Engel, and J.G. Arnold. 2006. Modeling long-term water quality impact of structural BMPs. *Trans. ASABE* 49(2): 367–374.

Brown, C., and R.L. Wilby. 2012. An alternate approach to assessing climate risks. *Eos, Trans. Am. Geophys. Union* 92(41): 92–94.

- Burkett, V., and J. Kusler. 2000. Climate change: potential impacts and interactions in wetlands of the United States. *J. Am. Water Resour. Assoc.* 36(2): 313–320.
- Cahoon, J. 1985. Soil survey report of Klamath County, Oregon, southern part. U.S. Soil Conservation Service, Oregon State University, and Agricultural Experiment Station, Washington, D.C.
- Candela, L., W. von Igel, F. Javier Elorza, and G. Aronica. 2009. Impact assessment of combined climate and management scenarios on groundwater resources and associated wetland (Majorca, Spain). *J. Hydrol.* 376(3-4): 510–527.
- CH2MHill. 2012. Approaches to water quality treatment by wetlands in the Upper Klamath Basin. Prepared for PacifiCorp Energy, Portland, OR.
- Chaplot, V. 2007. Water and soil resources response to rising levels of atmospheric CO₂ concentration and to changes in precipitation and air temperature, *J. Hydrol.*, 337:159– 171.
- Cho, J., G. Vellidis, D.D. Bosch, R. Lowrance, and T. Strickland. 2010b. Water quality effects of simulated conservation practice scenarios in the Little River Experimental Watershed. *J. Soil Water Conserv.* 65(6): 463–473.

Cho, J., R. R. Lowrance, D. D. Bosch, T. C. Strickland, Y. Her, and G. Vellidis. 2010a. Effect of watershed subdivision and filter width on SWAT simulation of a coastal plain watershed, *J. Am. Water Resour. Assoc.*, 46(3):586–602.

Ciotti, D.C. 2005. Water quality of runoff from flood irrigated pasture in the Klamath Basin, Oregon. M.S. Thesis, Oregon State University, Corvallis, OR. 160 pp.

Colorado River Basin Water Supply and Demand Study Team. 2011. Colorado River Basin water supply and demand study. Request for ideas. Phase 4: Development and evaluation of opportunities for balancing water supply and demand. U.S. Bureau of Reclamation, Boulder City, NV.

Deb, K., A. Pratap, S. Agarwal, and T. Meyarivan (2002), A Fast and elitist multiobjective genetic algorithm: NSGA-II, *IEE Trans. Evol. Comput.*, 6(2), 182–197.

Diffenbaugh, N.S., M. Scherer, and M. Ashfaq. 2012. Response of snow-dependent hydrologic extremes to continued global warming. *Nat. Clim. Chang.* 2(11): 1–6.

Duff, J.H., K.D. Carpenter, D.T. Snyder, K.K. Lee, R.J. Avanzino, and F.J. Triska. 2009. Phosphorus and nitrogen legacy in a restoration wetland, Upper Klamath Lake, Oregon. *Wetlands* 29(2): 735–746.

- Durre, I., M.J. Menne, B.E. Gleason, T.G. Houston, and R.S. Vose. 2010. Comprehensive automated quality assurance of daily surface observations. *J. Appl. Meteorol. Climatol.* 49(8): 1615–1633.
- Eldridge, B.D., S.L.C. Eldridge, L.N. Schenk, D.Q. Tanner, and T.W. Wood. 2012a. Water-quality data from Upper Klamath and Agency Lakes, Oregon, 2009-10 Open-File Report 2012-1142. U.S. Geological Survey, Reston, VA.
- Eldridge, S.L.C., T.W. Wood, and K.R. Echols. 2012b. Spatial and temporal dynamics of cyanotoxins and their relation to other water quality variables in Upper Klamath Lake, Oregon , 2007 – 09. Scientific Investigations Report 2012-5069. U.S. Geological Survey, Reston, VA.
- Engel, B., D. Storm, M. White, J. Arnold, and M. Arabi. 2007. A hydrologic/water quality model application protocol. *J. Am. Water Resour. Assoc.* 43(5): 1223–1236.
- Ficklin, D.L., Y. Luo, E. Luedeling, S.E. Gatzke, and M. Zhang. 2010. Sensitivity of agricultural runoff loads to rising levels of CO₂ and climate change in the San Joaquin Valley watershed of California. *Environ. Pollut.* 158(1): 223–234.
- Ficklin, D.L., I.T. Stewart, and E.P. Maurer. 2013. Effects of climate change on stream temperature, dissolved oxygen, and sediment concentration in the Sierra Nevada in California. *Water Resour. Res.* 49(5): 2765–2782.

- Ficklin, D. L., Y. Luo, E. Luedeling, S. E. Gatzke, and M. Zhang. 2010. Sensitivity of agricultural runoff loads to rising levels of CO₂ and climate change in the San Joaquin Valley watershed of California, *Environ. Pollut.*, 158(1):223–234.
- Fisher, J., and M.C. Acreman. 2004. Wetland nutrient removal: a review of the evidence. *Hydrol. Earth Syst. Sci.* 8(4): 673–685.
- Foy, C.R. 2010. Impacts of climate change on the hydrologic response of headwater basins in Colorado, M.S. Thesis, Colorado State University, Fort Collins CO. 140 pp.
- Gannett, M.W., K.E. Lite Jr., J.L. La Marche, B.J. Fisher, and D.J. Polette. 2007. Ground-water hydrology of the Upper Klamath Basin, Oregon and California. Scientific Investigations Report 2007 – 5050. U.S. Geological Survey, Reston, VA.
- Gannett, M.W., B.J. Wagner, and K.E. Lite Jr. 2012. Groundwater simulation and management models for the Upper Klamath Basin, Oregon and California Scientific Investigations Report 2012 – 5062. U.S. Geological Survey, Reston, VA.
- Gassman, P.W., M.R. Reyes, C.H. Green, and J.G. Arnold. 2007. The Soil and Water Assessment Tool: Historical development, applications, and future research directions. *Trans. ASABE* 50(4): 1211–1250.

- Gearheart, R.A., J.K. Anderson, M.G. Forbes, M. Osburn, and D. Oros. 1995. Watershed strategies for improving water quality in Upper Klamath Lake, Oregon. Volumes I, II and III. Humboldt State University, Arcata, CA.
- Graham, S.A., C.B. Craft, P. V. McCormick, and A. Aldous. 2005. Forms and accumulation of soil P in natural and recently restored peatlands—Upper Klamath Lake, Oregon, USA. *Wetlands* 25(3): 594–606.
- Graham Matthews & Associates. 2007. Sprague River watershed: Stream flow, sediment transport and a preliminary sediment budget, WY2004-2006. Prepared for Then Klamath Tribes, Weaverville, CA.
- Gu, A.Z., L. Liu, J.B. Neethling, H.D. Stensel, and S. Murthy. 2011. Treatability and fate of various phosphorus fractions in different wastewater treatment processes. *Water Sci. Technol.* 29(10): 804–810.
- Hamlet, A.F., P.W. Mote, M.P. Clark, and D.P. Lettenmaier. 2007. Twentieth-century trends in runoff, evapotranspiration, and soil moisture in the Western United States. *J. Clim.* 20(8): 1468–1486.
- Hattermann, F. F., V. Krysanova, A. Habeck, and A. Bronstert. 2006. Integrating wetlands and riparian zones in river basin modelling, *Ecol. Modell.*, 199:379–392.

Hay, L.E., S.L. Markstrom, and C. Ward-Garrison. 2011. Watershed-scale response to climate change through the twenty-first century for selected basins across the United States. *Earth Interact.* 15(17): 1–37.

Helsel, D.R., and R.M. Hirsch. 2002. Chapter A3: Statistical methods in water resources. In *Techniques of water-resources investigations of the United States Geologic Survey: Book 4, Hydrologic analysis and interpretation*. U.S. Geological Survey, Reston, VA.

Homer, C., J. Dewitz, J. Fry, M. Coan, N. Hossain, C. Larson, N. Herold, A. McKerrow, J.N. VanDriel, and J. Wickham. 2007. Completion of the 2001 National Land Cover Database for the conterminous United States. *Photogramm. Eng. Remote Sensing* 73(4): 337–341.

Homer, C., C. Huang, L. Yang, B. Wylie, and M. Coan. 2004. Development of a 2001 National Landcover Database for the United States. *Photogramm. Eng. Remote Sensing* 70(7): 829–840.

Jefferson, A.J. 2011. Seasonal versus transient snow and the elevation dependence of climate sensitivity in maritime mountainous regions. *Geophys. Res. Lett.* 38(16): 1–7.

Jeppesen, E., B. Kronvang, M. Meerhoff, M. Søndergaard, K.M. Hansen, H.E. Andersen, T.L. Lauridsen, L. Liboriussen, M. Beklioglu, A. Ozen, and J.E. Olesen. 2007. Climate change effects on runoff, catchment phosphorus loading and lake ecological state, and potential adaptations. *J. Environ. Qual.* 38(5): 1930–41.

- Jha, M.K., P.W. Gassman, and J.G. Arnold. 2007. Water quality modeling for the Raccoon River Watershed using SWAT. *Trans. ASABE* 50(2): 479–494.
- Johnston, C.A., N.E. Detenbeck, G.J. Niemi, S. Biogeochemistry, and N. Jul. 1990. The cumulative effect of wetlands on stream water quality and quantity: A landscape approach. *Biogeochemistry* 10(2): 105–141.
- Klamath Tribes. 2008. Quality Assurance Project Plan (QAPP) Project: Baseline water quality monitoring project. Chiloquin, OR.
- Knighton, D. 1998. *Fluvial forms and processes: A new perspective*. Second Edition, Hodder Education, London.
- Lam, Q.D., B. Schmalz, and N. Fohrer. 2011. The impact of agricultural Best Management Practices on water quality in a North German lowland catchment. *Environ. Monit. Assess.* 183(1-4): 351–79.
- Lettenmaier, D.P., A.W. Wood, R.N. Palmer, E.F. Wood, and E.Z. Stakhiv. 1999. Water resources implications of global warming: A US regional perspective. *Clim. Change* 43(3): 537–579.

- Li, Y., B.-M. Chen, Z.-G. Wang, and S.-L. Peng. 2011. Effects of temperature change on water discharge, and sediment and nutrient loading in the lower Pearl River basin based on SWAT modelling, *Hydrol. Sci. J.*, 56(1):68–83.
- Van Liew, M.W., S. Feng, and T.B. Pathak. 2012. Climate change impacts on stream flow, water quality, and best management practices for the Shell and Logan creek watersheds in Nebraska. *Int. J. Agric. Biol. Eng.* 5(1): 13–34.
- Lind, P. 2009. Holocene floodplain development of the lower Sycan River, Oregon. M.S. Thesis, Oregon State University, Corvallis, OR. 203 pp.
- Liu, Y., W. Yang, and X. Wang. 2008. Development of a SWAT extension module to simulate riparian wetland hydrologic processes at a watershed scale. *Hydrol. Process.* 22(16): 2901– 2915.
- Liu, Y., W. Yang, and X. Wang. 2007. GIS-based integration of SWAT and REMM for estimating water quality benefits of riparian buffers in agricultural watersheds, *Trans. ASABE*, 50(5):1549–1563.
- Mackun, P., S. Wilson, T. Fischetti, and J. Goworowska. 2011. Population distribution and change: 2000 to 2010. 2010 Census Briefs. U.S. Dep. Commer. Econ. Stat. Adm. U.S. Census Bur. (March): 12

pp. Available at <http://www.census.gov/prod/cen2010/briefs/c2010br-01.pdf> (Accessed 11 November 2012).

Mayer, T.D., and S.W. Naman. 2011. Stream flow response to climate as influenced by geology and elevation. *J. Am. Water Resour. Assoc.* 47(4): 724–738.

McCormick, P., and S.G. Campbell. 2007. Evaluating the potential for watershed restoration to reduce nutrient loading to Upper Klamath Lake, Oregon. U.S. Geological Survey Open-File Report 2007-1168. U.S. Geological Survey, Reston, VA.

Merot, P., H. Squidadant, P. Arousseau, M. Hefting, T. Burt, V. Maitre, M. Kruk, A. Butturini, C. Thenail, and V. Viaud. 2003. Testing a climato-topographic index for predicting wetlands distribution along a European climate gradient. *Ecol. Modell.* 163(1-2): 51–71.

Meyer, J.L., M.J. Sale, P.J. Mulholland, and N.L. Poff. 1999. Impacts of climate change on aquatic ecosystem functioning and health. *J. Am. Water Resour. Assoc.* 35(6): 1373–1386.

Mitsch, W.J., and J.G. Gosselink. 2000. *Wetlands*. Third Edition. John Wiley and Sons, Inc., New York, NY.

Moradkhani, H., R.G. Baird, and S.A. Wherry. 2010. Assessment of climate change impact on floodplain and hydrologic ecotones. *J. Hydrol.* 395(3-4): 264–278.

- Moriasi, D.N., J.G. Arnold, M.W. Van Liew, R.L. Bingner, R.D. Harmel, and T.L. Veith. 2007. Model evaluation guidelines for systematic quantification of accuracy in watershed simulations. *Trans. ASABE* 50(3): 885–900.
- Moriasi, D.N., J.L. Steiner, and J.G. Arnold. 2006. Sediment measurement and transport modeling: impact of riparian and filter strip buffers. *J. Environ. Qual.* 40(3): 807–14.
- Morris, M.D. 1991. Factorial sampling plans for preliminary computational experiments. *Technometrics* 33(2): 161–174.
- Mote, P.W. 2003. Trends in snow water equivalent in the Pacific Northwest and their climatic causes. *Geophys. Res. Lett.* 30(12).
- Mote, P.W., E.A. Parson, A.F. Hamlet, W.S. Keeton, D. Lettenmaier, N. Mantua, E.L. Miles, D.W. Peterson, D.L. Peterson, R. Slaughter, and A.K. Snover. 2003. Preparing for climatic change: The water, salmon and forests of the Pacific Northwest. *Clim. Change* 61: 45–88.
- Mote, P.W., and E.P. Salathé Jr. 2010. Future climate in the Pacific Northwest. *Clim. Change* 102: 29–50.

Mulholland, P.J., and M.J. Sale. 2011. Impacts of climate change on water resources: Findings of the IPCC Regional Assessment of Vulnerability for North America. *J. Contemp. Water Res. Educ.* 112(1): 10–15.

Murdoch, P.S., J.S. Baron, and T.L. Miller. 2000. Potential effects of climate change on surface-water quality in North America. *J. Am. Water Resour. Assoc.* 36(2): 347–366.

Naik, P.K., and D. A. Jay. 2011. Distinguishing human and climate influences on the Columbia River: Changes in mean flow and sediment transport. *J. Hydrol.* 404(3-4): 259–277.

Park, J. Y., M. J. Park, S. R. Ahn, G. A. Park, J. E. Yi, G. S. Kim, R. Srinivasan, and S. J. Kim. 2011. Assessment of future climate change impacts on water quantity and quality for a mountainous dam watershed using SWAT, *Trans. ASABE*, 54(2004): 1725–1737.

Neitsch, S.L., J.G. Arnold, J.R. Kiniry, and J.R. Williams. 2009. Soil & Water Assessment Tool theoretical documentation version 2009, Texas Water Resources Institute Technical Report No. 406. Texas A&M University, College Station, TX.

Neitsch, S.L., J.G. Arnold, J.R. Kiniry, and J.R. Williams. 2005. Soil & Water Assessment Tool theoretical documentation version 2005, Grassland, Soil and Water Research Laboratory,

Agricultural Research Service and Blackland Research Center, Texas Agricultural Experiment Station, Temple, TX.

NewFields River Basin Services and G.M. Kondolf. 2012. Evaluating stream restoration projects in the Sprague River Basin. Prepared for Klamath Watershed Partnership.

Nicks, A.D. 1971. Stochastic generation of the occurrence, pattern and location of maximum amount of daily rainfall. In Proceedings of the Symposium on Statistical Hydrology, Arizona University, Tucson, August 31-September 2, 1971. Miscellaneous Publication No. 1275. U.S. Government Print Office, Washington, D.C.

Nolin, A.W., and C. Daly. 2006. Mapping “at risk” snow in the Pacific Northwest. *J. Hydrometeorol.* 7(5): 1164–1171.

Novotny, V. 2003. *Water quality: diffuse pollution and watershed management*. Second Edition. Hoboken, NJ: J. Wiley.

Oregon Natural Heritage Information Center and the Wetlands Conservancy. 2009. Oregon Wetland Geodatabase vector digital data. Available at <http://spatialdata.oregonexplorer.info/> (Accessed 28 July 2012).

Oregon Water Resources Department. 2008. Oregon water rights Places of Use (POUs), by administrative basin vector digital data. Available at <http://www.oregon.gov/owrd/pages/wr/index.aspx> (Accessed 22 July 2011).

Parker, G.T., R.L. Droste, and K.J. Kennedy. 2008. Modeling the effect of agricultural best management practices on water quality under various climatic scenarios. *J. Environ. Eng. Sci.* 7(1): 9–19.

Perry, L.G., D.C. Andersen, L. V. Reynolds, S.M. Nelson, and P.B. Shafroth. 2012. Vulnerability of riparian ecosystems to elevated CO₂ and climate change in arid and semiarid western North America. *Glob. Chang. Biol.* 18(3): 821–842.

Poff, N.L., J.D. Allan, M.B. Bain, J.R. Karr, K.L. Prestegard, B.D. Richter, R.E. Sparks, and J.C. Stromberg. 1997. The natural flow regime: A paradigm for river conservation and restoration. *Bioscience* 47(11): 769–784.

Portland State University. 2012. Atlas of Oregon Lakes. Available at <http://aol.research.pdx.edu/> (Accessed 9 September 2012).

Praskievicz, S., and H. Chang. 2009. A review of hydrological modelling of basin-scale climate change and urban development impacts. *Prog. Phys. Geogr.* 33(5): 650–671.

Praskievicz, S., and H. Chang. 2011. Impacts of climate change and urban development on water resources in the Tualatin River Basin, Oregon. *Ann. Assoc. Am. Geogr.* 101(2): 249–271.

PRISM Climate Group at Oregon State University. 2012. United States Average Monthly or Annual Precipitation, Maximum Temperature, and Minimum Temperature. 1981 - 2010 ARC/INFO ASCII Grid. Available at <http://prism.nacse.org/normals/> (Accessed 22 February 2013).

Rabe, A., and C. Calonje. 2009. Lower Sprague-Lower Williamson Watershed Assessment. Prepared for Klamath Watershed Partnership, Klamath Falls, OR.

Rasmussen, C.G. 2011. Geomorphology, hydrology and biology of floodplain vegetation in the Sprague Basin, OR: History and potential for natural recovery. PhD Dissertation, Oregon State University, Corvallis, OR. 105 pp.

Risley, J., L.E. Hay, and S. Markstrom. 2012. Watershed scale response to climate change--Sprague River Basin, Oregon: U.S. Geological Survey Fact Sheet 2011-3120. Denver, CO.

Risley, J.C., and A. Laenen. 1999. Upper Klamath Lake basin nutrient-loading study— Assessment of historic flows in the Williamson and Sprague Rivers. U.S. Geological Survey Water-Resources Investigations Report 98-4198. U.S. Geological Survey, Portland, OR.

- Runkel, R.L., C.G. Crawford, and T.A. Cohn. 2004. Load Estimator (LOADEST): A FORTRAN program for estimating constituent loads in streams and rivers. Techniques and Methods Book 4, Chapter A5. U.S. Geological Survey, Reston, VA.
- Rupp, D.E., J.T. Abatzoglou, K.C. Hegewisch, and P.W. Mote. 2013. Evaluation of CMIP5 20th century climate simulations for the Pacific Northwest USA. *J. Geophys. Res. Atmos.* Accepted. doi: 10.1002/jgrd.50843.
- Sahu, M., and R.R. Gu. 2009. Modeling the effects of riparian buffer zone and contour strips on stream water quality. *Ecol. Eng.* 35(8): 1167–1177.
- Salathé, E.P., W. Mote, and M.W. Wiley. 2007. Review of scenario selection and downscaling methods for the assessment of climate change impacts on hydrology in the United States Pacific Northwest. *Int. J. Climatol.* 27: 1611–1621.
- Salmi, T., A. Maatta, P. Anttila, T. Ruoho-Airola, and Amnell. 2002. Detecting trends of annual values of atmospheric pollutants by the Mann-Kendall test and Sen's slope estimates - the Excel template application MAKESENS, Publications on Air Quality No. 31. Finnish Meteorological Institute, Helsinki.

Santhi, C., J.G. Arnold, J.R. Williams, W.A. Dugas, R. Srinivasan, and L.M. Hauck. 2001. Validation of the SWAT model on a large river basin with point and nonpoint sources. *J. Am. Water Resour. Assoc.* 37(5): 1169–1188.

Serreze, M.C., M.P. Clark, R.L. Armstrong, D.A. Mcginnis, and R.S. Pulwarty. 1999. Characteristics of the western United States snowpack from snowpack telemetry (SNOTEL) data. *Water Resour.* 35(7): 2145–2160.

Sheffield, J., A. Barrett, B. Colle, D.N. Fernando, R. Fu, K.L. Geil, Q. Hu, J. Kinter, S. Kumar, B. Langenbrunner, K. Lombardo, L.N. Long, E. Maloney, A. Mariotti, J.E. Meyerson, K.C. Mo, J.D. Neelin, S. Nigam, Z. Pan, T. Ren, A. Ruiz-Barradas, Y.L. Serra, A. Seth, J.M. Thibeault, J.C. Stroeve, Z. Yang, and L. Yin. 2013. North American climate in CMIP5 Experiments. Part I: Evaluation of historical simulations of continental and regional climatology. *J. Clim.* Published online. doi: 10.1175/JCLI-D-12-00592.1

Shrestha, R. R., Y. B. Dibike, and T. D. Prowse. 2012. Modeling climate change impacts on hydrology and nutrient loading in the Upper Assiniboine Catchment1, *J. Am. Water Resour. Assoc.*, 48(1):74–89.

Snyder, D.T., and J.L. Morace. 1997. Nitrogen and phosphorus loading from drained wetlands adjacent to Upper Klamath and Agency Lakes, Oregon, Water-Resources Investigations Report 97-4059. U.S. Geological Survey, Portland, OR.

- Solheim, A.L., K. Austnes, T.E. Eriksen, I. Seifert, and S. Holen. 2010. Climate change impacts on water quality and biodiversity: Background report for EEAA European Environment State and Outlook Report 2010 ETC Water Technical Report 1/2010. Prague, Czech Republic.
- Sproles, E.A., A.W. Nolin, K. Rittger, and T.H. Painter. 2013. Climate change impacts on maritime mountain snowpack in the Oregon Cascades. *Hydrol. Earth Syst. Sci.* 17(7): 2581–2597.
- Stewart, I.T., D.R. Cayan, and M.D. Dettinger. 2005. Changes in snowmelt runoff timing in western North America under a ‘business as usual’ climate change scenario. *Clim. Change.* 62: 217-232.
- Taylor, K.E., R.J. Stouffer, and G.A. Meehl. 2012. An overview of CMIP5 and the experiment design. *Bull. Am. Meteorol. Soc.* 93(4): 485–498.
- Thorsteinson, L., S. VanderKooi, and W. Duffy. 2011. Proceedings of the Klamath Basin Science Conference, Medford, Oregon, February 1–5, 2010. U.S. Geological Survey, Reston, VA.
- Times-Standard. 2013. Oregon backs Klamath Tribes water rights; effects on Lower Klamath Basin unclear. 10 March, 2013. Eureka Times-Standard, Eureka, CA. Available at http://www.times-standard.com/ci_22759422/oregon-backs-klamath-tribes-water-rights-effect-lower (Accessed 15 October 2013).

Tolson, B.A., and C.A. Shoemaker. 2007. Dynamically dimensioned search algorithm for computationally efficient watershed model calibration. *Water Resour. Res.* 43(1): 1–16.

U.S. Department of Agriculture Agricultural Research Service. 2011. ArcSWAT 2009.93.7b. Available at <http://swat.tamu.edu/>.

U.S. Department of Agriculture Natural Resources Conservation Service. 2009. Sprague River CEAP Study Report. Portland, OR.

U.S. Department of Agriculture Natural Resources Conservation Service. 2011. The National Easement Dataset vector digital data, U.S. Department of Agriculture, Natural Resources Conservation Service, National Cartography and Geospatial Center, Fort Worth, TX.

U.S. Fish and Wildlife Service. 2011. Classification of wetlands and deepwater habitats of the United States vector digital data. U.S. Fish and Wildlife Service Division of Habitat and Resource Conservation, Washington, D.C. Available at <http://www.fws.gov/wetlands/data/DataDownload.html> (Accessed 19 February 2011).

U.S. Geological Survey. 2009. 1-Arc Second National Elevation Dataset SDE raster digital data. Available at <http://seamless.usgs.gov> (Accessed 20 May 2010).

- U.S. Geological Survey. 2010a. NHDWaterbody vector digital data. Available at <ftp://nhdftp.usgs.gov/DataSets/Staged/SubRegions/FileGDB/HighResolution/> (Accessed 8 August 2011).
- U.S. Geological Survey. 2010b. NHDFlow line vector digital data. NHD High Resolution pre-staged by sub-basin. Available at <ftp://nhdftp.usgs.gov/DataSets/Staged/SubRegions/FileGDB/HighResolution/> (Accessed 28 March 2012).
- U.S. Geological Survey. 2012. USGS 11501000 Sprague River near Chiloquin, OR. Peak stream flow Oregon. Available at http://nwis.waterdata.usgs.gov/or/nwis/peak?site_no=11501000&agency_cd=USGS&format=brief_list (Accessed 10 October 2012).
- Vaché, K.B., J.M. Eilers, and M. V Santelmann. 2003. Water quality modeling of alternative agricultural scenarios in the U.S. Corn Belt. *J. Am. Water Resour. Assoc.* 38(3): 773–787.
- Verhoeven, J.T.A., B. Arheimer, C. Yin, and M.M. Hefting. 2006. Regional and global concerns over wetlands and water quality. *Trends Ecol. Evol.* 21(2): 96–103.

- Vrac, M., P. Drobinski, A. Merlo, M. Herrmann, C. Lavaysse, L. Li, and S. Somot. 2012. Dynamical and statistical downscaling of the French Mediterranean climate: uncertainty assessment. *Nat. Hazards Earth Syst. Sci.* 12(9): 2769–2784.
- Wade, A.A., T.J. Beechie, E. Fleishman, N.J. Mantua, H. Wu, J.S. Kimball, D.M. Stoms, and J. A. Stanford. 2013. Steelhead vulnerability to climate change in the Pacific Northwest. *J. Appl. Ecol.* 50(1093-1104).
- Waibel, M.S., M.W. Gannett, H. Chang, and C.L. Hulbe. 2013. Spatial variability of the response to climate change in regional groundwater systems – Examples from simulations in the Deschutes Basin, Oregon. *J. Hydrol.* 486: 187–201.
- Wang, X., S. Shang, Z. Qu, T. Liu, A.M. Melesse, and W. Yang. 2010. Simulated wetland conservation-restoration effects on water quantity and quality at watershed scale. *J. Environ. Manage.* 91(7): 1511–25.
- Whitehead, P.G., R.L. Wilby, R.W. Battarbee, M. Kernan, and A.J. Wade. 2009. A review of the potential impacts of climate change on surface water quality. *Hydrol. Sci.* 54(1): 101–123.
- Whitehead, P.G., R.L. Wilby, D. Butterfield, and A.J. Wade. 2006. Impacts of climate change on in-stream nitrogen in a lowland chalk stream: An appraisal of adaptation strategies. *Sci. Total Environ.* 365(1-3): 260–73.

Wong, S.W., M.J. Barry, A.R. Aldous, N.T. Rudd, H.A. Hendrixson, and C.M. Doehring. 2011. Nutrient release from a recently flooded delta wetland: Comparison of field measurements to laboratory results. *Wetlands* 31(2): 433–443.

Wood, A.W., L.R. Leung, V. Sridhar, and D.P. Lettenmaier. 2004. Hydrologic implications of dynamical and statistical approaches to downscaling climate model outputs. *Clim. Change* 62(1-3): 189–216.

Woznicki, S.A., A.P. Nejadhashemi, and C.M. Smith. 2011. Assessing best management practice implementation strategies under climate change scenarios. *Trans. ASABE* 54(1): 171–190.

Wu, K., and C.A. Johnston. 2008. Hydrologic comparison between a forested and a wetland/lake dominated watershed using SWAT. *Hydrol. Process.* 22: 1431–1442.

APPENDIX I:
DETAILED METHODS FOR CALIBRATION AND TESTING

Calibration parameters were selected using a Morris sensitivity analysis for flow, sediment, TN and TP at the sites shown in Appendix IV, Table 13 for 2001-2010 (Morris, 1991) and supplemented with additional parameters from the SWAT literature. Ranges of parameter values for sensitivity analysis and calibration were identified from the SWAT literature and are shown in Appendix IV, Table 14. Several parameters were identified specifically from regional data: Precipitation and temperature lapse rates with elevation were calculated from Parameter-elevation Regressions on Independent Slopes Model (PRISM) 1981-2010 800 m gridded climate normals and a 30 m NED raster dataset and calibrated within a 95% confidence interval around the resulting regression slopes (U.S. Geological Survey, 2009; PRISM Climate Group at Oregon State University, 2012). The estimated background concentration of TP in Upper Klamath River Basin baseflow is $77 \mu\text{g} \cdot \text{L}^{-1}$ with a standard deviation of $22 \mu\text{g} \cdot \text{L}^{-1}$ (Boyd et al., 2002). During auto- and manual calibration, we calibrated the parameters GWSOLP (concentration of soluble P in groundwater contribution to stream flow) and LAT_ORGP (organic P in the baseflow) so that their sum was within the standard deviation of the estimated background TP concentration.

Calibration performance criteria are detailed in section 2.4 and included the Nash-Sutcliffe coefficient (NS statistic) and percent bias (PBIAS). Both are described further in Moriasi et al. (2007).

The NS statistic ranges from $-\infty$ to 1.0, with 1.0 indicating a perfect fit between observed and simulated data plotted on a 1:1 line. Values ≤ 0 indicate that the mean of observations is a better predictor than the model. The statistic is calculated as:

$$NS = 1 - \frac{[\sum_{i=1}^n (Y_i^{obs} - Y_i^{sim})^2]}{[\sum_{i=1}^n (Y_i^{obs} - Y_i^{mean})^2]} \quad \text{Eqn. 5}$$

Where Y_i^{obs} is the i th observation, Y_i^{sim} is the corresponding i th simulated value, Y^{mean} is the mean of the observations, and n is the total number of observations (Moriasi et al., 2007).

The PBIAS statistic measures the average tendency of simulated values to be lesser or greater than the corresponding observed values. Positive (negative) values indicate a model bias to underestimation (overestimation) (Moriassi et al., 2007). PBIAS is calculated as

$$PBIAS = \frac{[\sum_{i=1}^n (Y_i^{obs} - Y_i^{sim}) \cdot 100]}{[\sum_{i=1}^n (Y_i^{obs})]} \quad \text{Eqn. 6}$$

We initially attempted calibration of flow, sediment, TN and TP at the sites shown in Appendix IV, Table 13 using a multiobjective genetic algorithm and a single SWAT model for the entire Sprague River and using NS as the objective function. The algorithm, nondominated sorting genetic algorithm II (NSGA-II), is detailed in Deb et al. (2002). NSGA-II scripts were written by Mehdi Ahmadi, then at Colorado State University Department of Civil and Environmental Engineering, and were executed in a MATLAB platform using the MATLAB Global Optimization Toolbox (The MathWorks 2011, MATLAB Global Optimization Toolbox, User's Guide, R2011b, available from: http://www.mathworks.com/help/pdf_doc/gads/gads_tb.pdf; MATLAB R2011b, MathWorks, Natick, MA).

However, the above calibration approach resulted in negative NS values for most constituents, likely because no single parameter set could optimize the distinct hydrology of the tributaries and mainstem. Therefore, we calibrated separate models for the North Fork of the Sprague River, South Fork of the Sprague River, and Sycan River. We then read the daily outputs of flow, sediment and nutrients from the outlets of the three separate calibrated and tested tributary models as inflows to a model for the Sprague River mainstem, and calibrated the mainstem model by altering parameters only for subbasins and HRUs within the Sprague River mainstem.

We adopted an iterative approach to calibration in which we first autocalibrated using Dynamically Dimensioned Search (DDS) algorithms developed at Colorado State University and

executed in a MATLAB platform (Tolson and Shoemaker, 2007; MATLAB R2010b, MathWorks, Natick, MA). Initially, we selected as objective functions the NS statistic for flow and sediment. Where autocalibration did not yield NS statistics meeting acceptance criteria (section 2.4), we autocalibrated only for flow, then manually calibrated the autocalibrated parameter sets to fine-tune model performance. We then autocalibrated using as the DDS objective functions NS statistics for flow, sediment, TN and TP, utilizing as initial values for flow parameters the final calibrated parameters from the previous step, and setting the calibration range for flow parameters to vary within approximately 10-20% of the previously calibrated values. If results were poor for sediment or nutrients, we repeated this approach calibrating only for flow and sediment. Autocalibration results were subsequently adjusted using manual calibration to optimize the NS statistics for the calibrated constituents.

For sediment calibration we followed recommendations by Arnold et al. (2011) and initially varied only parameters controlling upslope erosion, such as those in the modified universal soil loss equation (e.g., USLE C and USLE K, cover and erodibility factors) and those controlling surface runoff (e.g., curve numbers and soil available water capacity). Once model performance for sediment could not be improved using these parameters, we calibrated further by allowing parameters controlling channel processes (e.g., peak rate adjustment factor and channel erodibility and cover factors) to vary.

Once flow and sediment were calibrated, and if autocalibration for flow, sediment and nutrients simultaneously had not been successful, we calibrated for TN and TP simultaneously, following autocalibration with manual calibration. Again based on recommendations by Arnold et al. (2011), we calibrated first by varying initial soil nutrient concentrations and organic residue and upland erosion (since organic nutrient loadings are a function of erosion), followed by nutrient percolation and partitioning coefficients, and finally, in-stream nutrient processes. Hydrologic parameters were not altered in this step.

Autocalibration using NS objective functions typically resulted in acceptable PBIAS, the second statistic we used in model performance criteria. However, where NS autocalibration results were acceptable for a given constituent but PBIAS was large, we repeated autocalibration using NS as a more heavily weighted objective function and relative error (RE) as a less heavily weighted objective function. PBIAS was not included as an objective function in the DDS autocalibration script, so RE was used instead during autocalibration and PBIAS performance for the calibrated model was checked following autocalibration.

RE was calculated as

$$RE = \frac{(Y_i^{mean} - Y_i^{sim})}{(Y_i^{mean})} \cdot 100 \quad \text{Eqn. 7}$$

Calibration and testing were repeated until model performance for NS and PBIAS could not be improved, using criteria defined in section 2.4

APPENDIX II:
DETAILED METHODS FOR DOWNSCALING OF FUTURE CLIMATE PROJECTIONS

(This section was adapted from a description of methods by Katherine Hegewisch, Department of Geography, University of Idaho)

Bias correction from the gridded data described above to meteorological stations was performed by University of Idaho staff. Daily data were extracted for each station (shown in Figure 1) from the corresponding 4 km grid cell of the statistically downscaled CMIP5 model output. This was repeated for the selected General Circulation Models (GCMs) for the historical (1950-2005) period and for both Representative Concentration Pathways (RCPs). Climate data input to the hydrologic model for each station were prepared by bias correcting the daily 4 km gridded Multivariate Adapted Constructed Analogs (MACA) data to the station observations. Station observations were those pre-processed following methods outlined in section 2.2, but not yet in-filled. This bias correction was accomplished with a quantile-mapping method similar to the CDF-t method (Vrac et al., 2012) utilizing the empirical cumulative distribution functions (CDFs) for a 45 day window and all years of data from (1) the historical downscaled data, (2) the future downscaled data and (3) the station observations. Values at each quantile of the GCM historical and future data were mapped to the corresponding station value with the same quantile. The initial difference (ratio) between the historical and future GCM data at each quantile was preserved by adding (multiplying) this difference (ratio) onto the quantile-mapped future GCM data for temperature (precipitation) variables.

APPENDIX III:
LITERATURE REVIEW OF ROLE OF WETLANDS IN NUTRIENT CYCLING IN THE
UPPER KLAMATH RIVER BASIN

Gearhart et al. (1995) concluded that wetland restoration, particularly of former wetlands surrounding Upper Klamath Lake, was key to reductions of TP loads to the lake. Using a spreadsheet-based optimization approach, Anderson (1998) determined that restoration in tributary deltas to Upper Klamath Lake (the Wood and Williamson Rivers and Sevenmile Creek) was the most effective of a suite of management practices in reducing TP loads to Upper Klamath Lake. However, Wong (2011) and Duff (2009) recorded seasonal or short-term benthic releases of N and P into the overlying water column from recently re-flooded lakeside wetlands in the Williamson River Delta and Wood River, respectively. Duff found that a wetland mass balance indicated a net loss of N and P during the study period, and Wong suggested that release of P was short-term. Inflow and outflow measurements at Sycan Marsh at separate time periods suggest that the marsh may act both as a source and sink of N and P (Wong and Bienz, 2011, as cited in CH2MHill, 2012). In SWAT, riparian wetland buffers are always modeled as nutrient sinks whose removal rates of sediment and nutrients vary exponentially with filter strip width. However, research conducted outside of the Klamath River Basin suggests that the role of riparian wetlands as sources or sinks of nutrients may fluctuate over seasonal or longer time periods, and that riparian wetlands may be a sink for one species of N or P but a source for another (Mitsch and Gosselink, 2000; Fisher and Acreman, 2004).

APPENDIX IV:
SUPPLEMENTARY TABLES

Table 4. Flow characteristics for calibration and testing periods at Sprague tributary and mainstem gages. Calibration (testing) periods are 2001-2006 (2007-2010), with the exception of South Fork of the Sprague River at Brownsworth, which was calibrated (tested) for even (odd) years of the period 1992-2003. Site numbers correspond to numbers in Figure 1 and in Appendix IV, Table 13. "SD" = standard deviation; "Avg" = mean.

Site	No.	Avg. annual vol. (m ³)	SD of avg. annual vol. (m ³)	Avg. daily flow (m ³ ·s ⁻¹)	SD of avg. daily flow (m ³ ·s ⁻¹)
Sprague R. near Chiloquin, OR					
Calibration	1	4.3·10 ⁸	2.0·10 ⁸	13.8	14.2
Testing		3.6·10 ⁸	6.6·10 ⁷	11.4	8.9
Sycan River below Snake Creek near Beatty					
Calibration	3	1.0·10 ⁸	9.6·10 ⁷	3.3	7.0
Testing		7.6·10 ⁷	2.2·10 ⁷	2.4	3.9
South Fork of Sprague River at Brownsworth					
Calibration	8	4.3·10 ⁷	2.4·10 ⁷	1.3	1.8
Testing		5.2·10 ⁷	2.0·10 ⁷	1.5	2.1
North Fork of the Sprague River at Power Plant near Bly, OR					
Calibration	6	5.2·10 ⁷	1.9·10 ⁷	1.6	2.2
Testing		5.1·10 ⁷	1.3·10 ⁶	1.6	1.8

Table 5. Attributes of meteorological stations used in the SWAT hydrologic model. “Lat” = latitude; “Long” = longitude. “NCDC” = National Climatic Data Center, Global Historical Climatology Network (GHCN); “SNOTEL” = Natural Resources Conservation Service Snow Telemetry.

Model code	Source	Name	Agency Code	Elevation (m)	Lat.	Long.
NCHIEN	NCDC	Chiloquin 7 NW	351574	1274	42.7	-122.0
NGERB	NCDC	Gerber Dam	353232	1478	42.2	-121.1
SCRAZ	SNOTEL	Crazyman Flat	1010	1884	42.6	-120.9
SGERB	SNOTEL	Gerber Reservoir	945	1490	42.2	-121.1
SQUAR	SNOTEL	Quartz Mountain	706	1743	42.3	-120.8
SSILV	SNOTEL	Silver Creek	756	1750	43.0	-121.2
SSUMM	SNOTEL	Summer Rim	800	2158	42.7	-120.8
STAYL	SNOTEL	Taylor Butte	810	1533	42.7	-121.4

Table 6. Results of chi-square goodness-of-fit test of daily observed precipitation data following data gap in-filling. The chi-square goodness-of-fit test was used to test the null hypothesis, h , that the cumulative gamma distributions fitted to unfilled precipitation data for each calendar month are a random sample from a cumulative gamma distribution fitted to filled precipitation data for the same calendar month. The test was performed for filled and unfilled daily precipitation data for the period January 1, 1950 to December 31, 2010. The test result, h , is unity if the null hypothesis can be rejected at the 5% significance level and 0 if the null hypothesis cannot be rejected. Significance level of the test is denoted by p . Station abbreviations and attributes are noted in Appendix IV, Table 5. The data in-filling procedure is described in the text.

Station	Jan		Feb		Mar		Apr		May		Jun		Jul		Aug		Sep		Oct		Nov		Dec	
	h	p																						
NCHIEN	0	0.38	1	0.00	1	0.00	1	0.00	1	0.00	1	0.00	0	0.27	1	0.00	1	0.01	0	1.00	0	0.81	1	0.01
NGERB	1	0.00	1	0.00	1	0.00	1	0.00	1	0.00	1	0.04	1	0.00	1	0.04	1	0.00	0	0.66	1	0.00	1	0.00
SCRAZ	1	0.01	0	0.62	0	0.72	1	0.00	1	0.03	0	0.98	0	0.41	1	0.00	0	1.00	1	0.00	0	0.52	0	0.18
SGERB	1	0.00	1	0.00	1	0.00	1	0.00	1	0.00	1	0.00	1	0.00	1	0.00	1	0.00	0	0.46	1	0.00	1	0.00
SQUAR	1	0.00	0	0.14	1	0.00	0	0.07	0	0.93	1	0.00	1	0.00	1	0.00	1	0.00	1	0.00	1	0.00	1	0.00
SSILV	1	0.00	0	0.65	0	0.13	0	0.69	0	0.31	1	0.00	1	0.01	0	1.00	1	0.00	1	0.00	0	0.16	1	0.02
SSUMM	1	0.00	1	0.00	1	0.00	1	0.00	1	0.00	1	0.00	0	0.85	1	0.00	1	0.00	1	0.00	1	0.00	1	0.00
STAYL	0	0.08	1	0.00	1	0.01	1	0.00	0	0.12	0	1.00	0	0.99	0	1.00	0	1.00	0	0.44	1	0.02	1	0.00

Table 7. Results of the two-sample Kolmogorov-Smirnov test for daily observed precipitation data following data gap in-filling. The two-sample Kolmogorov-Smirnov test was used to test the null hypothesis, h , that filled and unfilled precipitation data are from the same continuous distribution for each calendar month. The test was performed for filled and unfilled daily precipitation data for the period January 1, 1950 to December 31, 2010. The test result, h , is unity if the null hypothesis can be rejected at the 5% significance level and 0 if the null hypothesis cannot be rejected. Significance level of the test is denoted by p . Station abbreviations and attributes are noted in Appendix IV, Table 5. The data in-filling procedure is described in the text.

Station	Jan		Feb		Mar		Apr		May		Jun		Jul		Aug		Sep		Oct		Nov		Dec	
	h	p																						
NCHIEN	0	0.57	1	0.00	1	0.00	1	0.00	1	0.00	1	0.01	0	0.49	1	0.00	0	0.12	0	1.00	0	1.00	0	0.08
NGERB	1	0.00	1	0.00	1	0.00	1	0.00	1	0.00	0	0.21	1	0.00	0	0.16	1	0.00	0	0.82	1	0.00	1	0.00
SCRAZ	0	0.11	0	0.86	0	0.91	1	0.01	0	0.26	0	1.00	0	0.60	1	0.00	0	1.00	0	0.08	0	0.79	0	0.53
SGERB	1	0.00	1	0.00	1	0.00	1	0.00	1	0.00	1	0.00	1	0.00	1	0.03	1	0.00	0	0.93	1	0.00	1	0.00
SQUAR	0	0.34	0	0.57	0	0.07	0	0.43	0	1.00	1	0.00	1	0.01	1	0.00	1	0.00	1	0.00	0	0.34	0	0.24
SSILV	1	0.02	0	0.91	0	0.39	0	0.93	0	0.72	1	0.00	0	0.07	0	1.00	0	0.05	0	0.09	0	0.43	0	0.18
SSUMM	1	0.00	1	0.00	1	0.00	1	0.00	1	0.01	1	0.00	0	0.95	1	0.00	1	0.00	1	0.00	1	0.00	1	0.00
STAYL	0	0.36	1	0.00	0	0.12	1	0.02	0	0.28	0	1.00	0	1.00	0	1.00	0	1.00	0	0.68	0	0.16	1	0.04

Table 8. Results of the two-sample Kolmogorov-Smirnov test for daily observed minimum temperature data following data gap in-filling. The two-sample Kolmogorov-Smirnov test was used to test the null hypothesis, h , that filled and unfilled data are from the same continuous distribution for each calendar month. The test was performed for filled and unfilled daily minimum temperature data for the period January 1, 1950 to December 31, 2010. The test result, h , is unity if the null hypothesis can be rejected at the 5% significance level and 0 if the null hypothesis cannot be rejected. Significance level of the test is denoted by p . Station abbreviations and attributes are noted in Appendix IV, Table 5. The data in-filling procedure is described in the text.

Station	Jan		Feb		Mar		Apr		May		Jun		Jul		Aug		Sep		Oct		Nov		Dec			
	h	p																								
NCHIEN	0	0.45	0	0.06	0	0.13	1	0.02	0	0.61	0	0.86	1	0.00	1	0.00	1	0.00	1	0.00	1	0.00	1	0.00	1	0.00
NGERB	0	0.19	1	0.00	1	0.00	0	0.26	1	0.00	1	0.00	1	0.00	1	0.00	1	0.00	1	0.00	1	0.00	1	0.00	1	0.00
SCRAZ	1	0.01	1	0.00	1	0.00	1	0.00	1	0.00	1	0.00	1	0.00	1	0.00	1	0.00	1	0.04	0	0.12	0	0.05		
SGERB	1	0.00	1	0.00	1	0.01	1	0.02	1	0.00	1	0.00	1	0.00	1	0.00	1	0.00	1	0.00	1	0.00	1	0.00	1	0.00
SQUAR	1	0.00	1	0.00	1	0.00	1	0.00	1	0.00	1	0.00	1	0.00	1	0.00	1	0.00	1	0.00	1	0.00	1	0.00	1	0.00
SSILV	1	0.00	1	0.03	1	0.00	1	0.00	0	0.16	0	0.77	1	0.00	1	0.00	1	0.00	1	0.00	1	0.00	1	0.00	1	0.00
SSUMM	1	0.00	1	0.00	1	0.00	1	0.00	1	0.00	0	0.08	1	0.00	1	0.00	1	0.00	1	0.00	1	0.00	1	0.00	1	0.00
STAYL	0	0.11	0	0.05	1	0.00	1	0.00	1	0.00	1	0.00	0	0.12	1	0.00	1	0.00	1	0.00	1	0.00	1	0.00	1	0.00

Table 9. Results of the two-sample Kolmogorov-Smirnov test for daily observed maximum temperature data following data gap in-filling. The two-sample Kolmogorov-Smirnov test was used to test the null hypothesis, h , that filled and unfilled data are from the same continuous distribution for each calendar month. The test was performed for filled and unfilled daily minimum temperature data for the period January 1, 1950 to December 31, 2010. The test result, h , is unity if the null hypothesis can be rejected at the 5% significance level and 0 if the null hypothesis cannot be rejected. Significance level of the test is denoted by p . Station abbreviations and attributes are noted in Appendix IV, Table 5. The data in-filling procedure is described in the text.

Station	Jan		Feb		Mar		Apr		May		Jun		Jul		Aug		Sep		Oct		Nov		Dec			
	h	p																								
NCHIEN	1	0.00	1	0.00	1	0.00	1	0.02	0	0.46	0	0.07	1	0.00	1	0.00	1	0.00	1	0.00	1	0.00	1	0.00	1	0.00
NGERB	1	0.03	1	0.03	1	0.00	1	0.00	0	0.26	0	0.05	1	0.00	1	0.00	0	0.31	1	0.00	0	0.45	0	0.06		
SCRAZ	0	0.06	1	0.00	1	0.00	1	0.00	1	0.00	1	0.00	1	0.00	1	0.00	1	0.00	1	0.00	1	0.00	1	0.00	1	0.00
SGERB	1	0.00	1	0.00	1	0.00	1	0.00	1	0.02	1	0.01	1	0.04	1	0.00	1	0.00	1	0.00	1	0.00	1	0.00	1	0.00
SQUAR	1	0.00	1	0.00	1	0.00	1	0.00	1	0.00	1	0.00	1	0.00	1	0.00	1	0.00	1	0.00	1	0.00	1	0.00	1	0.00
SSILV	1	0.00	1	0.00	1	0.00	1	0.00	1	0.00	1	0.00	1	0.00	1	0.00	1	0.00	1	0.00	1	0.00	1	0.00	1	0.00
SSUMM	1	0.00	1	0.00	1	0.00	1	0.00	1	0.00	1	0.00	1	0.00	1	0.00	1	0.00	1	0.00	1	0.00	1	0.00	1	0.00
STAYL	1	0.01	1	0.00	1	0.00	1	0.00	0	0.11	1	0.00	1	0.00	1	0.01	1	0.00	1	0.00	1	0.00	1	0.00	1	0.00

Table 10. Pond model parameters, equations and sources. “Parameter” is the parameter name in the SWAT pond (.pnd) file. “Wetlands database” refers to Oregon Natural Heritage Information Center and the Wetlands Conservancy (2009), U.S. Department of Agriculture Natural Resources Conservation Service (2011), U.S. Fish and Wildlife Service (2011), and U.S. Geological Survey (2011).

Parameter	Description	Units	Sources	Value or equation
PND_FR	Fraction of subwatershed draining to ponds	--	Wetlands database	--
PND_ESA	Max. surface area	ha	Wetlands database	--
PND_PSA	Normal surface area	ha	Wu and Johnston, 2008	PND_PSA·0.8
PND_EVOL	Maximum volume	10 ⁴ m ³	PND_PSA, median depth of Klamath County natural lakes (Portland State University, 2012)	PND_PSA·3.6
PND_PVOL	Normal volume	10 ⁴ m ³	Wu and Johnston, 2008	PND_EVOL·0.8

Table 11. Performance of LOADEST model for predicting monthly loads at Sprague River water quality observation locations. Site numbers correspond to locations in Figure 1 and in Appendix IV, Table 13. 2 = Sprague River at Power Plant; 4 = Sycan River at Drew’s Road; 5 = North Fork of the Sprague River at #3411 Rd. LOADEST model numbers are described by Runkel et al. (2004). PPCC = probability plot correlation coefficient. A value of 1 indicates a perfect linear relation between the log-transformed load and model residuals. The coefficient of determination (R^2) shows the percent of variation in log load that can be explained by the model regression equation.

Site No.	Sediment			TN			TP		
	Model	R^2	PPCC	Model	R^2	PPCC	Model	R^2	PPCC
2	7	0.90	0.973	8	0.92	0.990	8	0.95	0.974
4	6	0.92	0.98	6	0.98	0.962	8	0.96	0.927
5	9	0.84	0.973	4	0.72	0.992	9	0.91	0.978

Table 12. Water quality characteristics for calibration and testing periods at Sprague River tributary and mainstem sampling locations. All values are in mg L⁻¹. “NF” = North Fork; “SF” = South Fork. Sampling locations are shown in Figure 1 and in Appendix IV, Table 13. Calibration (testing) periods are 2001-2006 (2007-2010). “Avg” = mean; “SD” = standard deviation.

Site	Sediment		TP		TN		Mineral P		Nitrate-N	
	Avg	SD	Avg	SD	Avg	SD	Avg	SD	Avg	SD
NF Sprague R. at 3411 Rd										
Calibration	2.52	3.71	0.050	0.008	0.113	0.080	0.039	0.009	0.014	0.008
Testing	2.71	1.99	0.049	0.009	0.110	0.066	0.040	0.010	0.019	0.007
SF Sprague R. at Picnic Area										
Calibration	5.61	10.4	0.040	0.018	0.160	0.109	0.025	0.006	0.011	0.012
Testing	4.50	4.62	0.037	0.010	0.138	0.072	0.025	0.006	0.008	0.007
Sprague R. at Power Plant										
Calibration	11.1	16.0	0.073	0.029	0.366	0.143	0.045	0.014	0.017	0.017
Testing	16.5	20.6	0.065	0.025	0.317	0.147	0.039	0.009	0.011	0.013
Sycan R. at Drew's Road										
Calibration	5.43	7.79	0.061	0.043	0.404	0.148	0.035	0.016	0.028	0.018
Testing	4.98	5.92	0.050	0.016	0.380	0.123	0.029	0.011	0.046	0.037

Table 13. Stream flow gage and water quality sampling locations in the Sprague River watershed. “USGS” = U.S. Geological Survey; “OWRD” = Oregon Water Resources Department; “USFS” = Fremont Winema National Forest. Drainage areas are those calculated by the SWAT model; water quality monitoring locations are within 2 river km of a stream gage except in the case of site 6 (see explanation in section 2.4). “Q” = Stream flow gage; “WQ” = water quality monitoring location. “C” = calibration period; “T” = testing period. Numbers (“No.”) correspond to labels in Figure 1.

No.	Name	Type	Agency	Drainage area (km ²)	Lat.	Long.	Timestep	C	T
1	Sprague River near Chiloquin, OR	Q	USGS	4081	42.59	-121.85	Monthly	2001-2006	2007-2010
2	Sprague River at Power Plant	WQ	Klamath Tribes	4080	42.58	-121.84	Monthly	2001-2006	2007-2010
3	Sycan River Below Snake Creek near Beatty	Q	OWRD	1433	42.49	-121.28	Monthly	2001-2006	2007-2010
4	Sycan River at Drew's Road	WQ	Klamath Tribes	1433	42.49	-121.28	Monthly	2001-2006	2007-2010
5	North Fork of the Sprague River at #3411 Rd	WQ	Klamath Tribes	201	42.50	-121.01	Monthly	2001-2006	2007-2010
6	North Fork of the Sprague River at Power Plant near Bly, OR	Q	USGS	173	42.50	-120.99	Monthly	2001-2006	2007-2010
7	South Fork of the Sprague River at Picnic Area	WQ	Klamath Tribes	274	42.38	-120.97	Daily	2001-2006	2007-2010
8	South Fork of the Sprague River at Brownsworth	Q	USFS	159	42.39	-120.91	Monthly	1992-2003, even years	1992-2003, odd years

Table 14. Calibrated model parameters and values for Sprague River tributaries and mainstem (“Main”).

Parameter	Description	File	Units	North Fork	South Fork	Sycan	Main
ADJ_PKR	Peak rate adjustment factor for sediment routing in tributary channels.	.bsn	-	1.768	0.705	0.500	0.710
AI0	Ratio of chlorophyll-a to algal biomass.	.wwq	µg-chla/mg algae	10.070	0.588	1.000	17.500
AI1	Fraction of algal biomass that is N.	.wwq	mg N/mg algae	0.089	0.070	0.090	0.090
AI2	Fraction of algal biomass that is P.	.wwq	mg P/mg algae	0.011	0.010	0.010	0.010
ALPHA_BF	Base flow alpha factor.	.gw	days	0.001	0.033	0.048	0.011
BC1	Rate constant for biological oxidation of NH ₄ to NO ₂ in the reach.	.swq	day ⁻¹	0.954	0.100	0.100	0.100
BC2	Rate constant for biological oxidation of NO ₂ to NO ₃ in the reach.	.swq	day ⁻¹	1.775	0.200	0.200	0.200
BC3	Rate constant for hydrolysis of organic N to NH ₄ in the reach.	.swq	day ⁻¹	0.013	0.167	0.012	0.008
BC4	Rate constant for mineralization of organic P to dissolved P in the reach.	.swq	day ⁻¹	0.406	0.194	0.117	0.010
CANMX	Maximum canopy index.	.hru	mm	0.000	9.468	4.647	1.661
CDN	Denitrification exponential rate coefficient.	.bsn	-	1.103	1.120	1.120	3.000
CH_COV(1)	Channel erodibility factor.	.rte	-	0.108	0.681	0.953	0.673
CH_COV(2)	Channel cover factor.	.rte	-	0.130	0.375	0.024	0.028
CH_KI	Effective hydraulic conductivity in tributary channel alluvium.	.sub	mm·hr ⁻¹	1.651	148.900	58.540	146.600
CH_KII	Effective hydraulic conductivity in main channel alluvium.	.rte	mm·hr ⁻¹	10.540	0.025	3.969	0.938
CH_NI	Manning's <i>n</i> value for tributary channels.	.sub	-	0.014	0.014	0.014	0.098
CH_NII	Manning's <i>n</i> value for the main channel.	.rte	-	0.147	0.111	0.145	0.057
CMN	Rate factor for humus mineralization of active organic nutrients.	.bsn	-	0.001	0.000	0.000	0.002
CN_F	Initial SCS runoff curve number for moisture condition II.	.mgt	%	0.242	-0.237	-0.082	-0.130
DEP_IMP	Depth to impervious layer in soil profile (mm).	.hru	mm	0	0	0	1656
ERORGN	Organic N enrichment ratio.	.hru	-	0.000	5.000	4.087	1.652
ERORGP	Organic P enrichment ratio.	.hru	-	0.000	1.880	3.286	0.000
ESCO	Soil evaporation compensation factor.	.hru	-	0.010	0.978	0.996	0.309
GWQMN	Threshold depth of water in the shallow aquifer required for return flow to occur.	.gw	mm H ₂ O	0	50	109	4669
GWSOLP	Soluble P concentration in groundwater flow.	.gw	mg P L ⁻¹	0.055	0.057	0.057	0.077
HLIFE_NGW	Half-life of nitrate in the shallow aquifer.	.gw	days	365.25	365.25	365.25	291.60

Table 14 continued.

Parameter	Description	File	Units	North Fork	South Fork	Sycan	Main
ICN	Curve number calculation method.	.bsn	-	0	0	1	0
LABP	Initial soluble P concentration in soil layer.	.chm	mg P/kg soil	108.000	7.224	57.940	0.000
NPERCO	Nitrate percolation coefficient.	.bsn	-	0.258	0.085	0.085	0.010
P_N	Algal preference factor for ammonia.	.wwq	-	0.358	0.677	0.890	0.010
PHOSKD	P soil partitioning coefficient.	.bsn	$\text{m}^3 \cdot \text{Mg}^{-1}$	150	165	132	100
PLAPS	Precipitation lapse rate.	.sub	$\text{mm H}_2\text{O km}^{-1}$	698.400	708.100	699.500	712.700
PPERCO	P percolation coefficient.	.bsn	$10 \text{ m}^3 \cdot \text{Mg}^{-1}$	16.310	12.210	11.120	10.000
PRF	Peak rate adjustment factor for sediment routing in the main channel.	.bsn	-	0.812	1.908	0.690	1.666
RCHRG_DP	Deep aquifer percolation fraction.	.gw	-	0.000	0.246	0.825	0.009
RHOQ	Algal respiration rate.	.wwq	-	0.050	0.050	0.500	0.050
RS1	Local algal settling rate in the reach.	.swq	$\text{m} \cdot \text{day}^{-1}$	0.327	1.820	1.492	0.150
RS2	Sediment source rate for dissolved P in the reach.	.swq	$\text{mg P} \cdot \text{m}^{-2} \cdot \text{day}^{-1}$	3.012	0.578	0.246	0.550
RS3	Benthic source rate for $\text{NH}_4\text{-N}$ in the reach.	.swq	$\text{mg N} \cdot \text{m}^{-2} \cdot \text{day}^{-1}$	0.427	0.413	0.346	0.060
RS4	Rate coefficient for organic N settling in the reach.	.swq	day^{-1}	0.058	0.050	0.061	0.050
RS5	Organic P settling rate in the reach.	.swq	day^{-1}	0.964	0.249	0.202	0.010
RSDCO	Residue decomposition coefficient.	.bsn	-	0.599	0.100	0.319	0.109
RSDIN	Initial residue cover.	.hru	$\text{kg} \cdot \text{ha}^{-1}$	2661	10000	819	111
SDNCO	Denitrification threshold water content.	.bsn	-	0.100	0.247	0.247	0.142
SFTMP	Snowfall temperature.	.bsn	$^{\circ}\text{C}$	2.079	2.661	2.429	2.226
SLSUBBSN	Average slope length.	.hru	m	30.680	143.400	148.700	82.980
SMFMN	Melt factor for snow on December 21.	.bsn	$\text{mm} \cdot ^{\circ}\text{C}^{-1} \cdot \text{day}^{-1}$	1.838	1.800	2.052	4.022
SMFMX	Melt factor for snow on June 21.	.bsn	$\text{mm} \cdot ^{\circ}\text{C}^{-1} \cdot \text{day}^{-1}$	1.838	1.800	3.500	4.022
SMTMP	Snow melt base temperature.	.bsn	$^{\circ}\text{C}$	4.803	-1.241	-2.710	-3.392
SNO50COV	Fraction of snow volume represented by SNOCOVMX corresponding to 50% snow cover.	.bsn	-	0.307	0.010	0.180	0.412
SNOCOVMX	Minimum snow water content corresponding to 100% snow cover.	.bsn	mm	296.200	1.000	533.300	220.600

Table 14 concluded.

Parameter	Description	File	Units	North Fork	South Fork	Sycan	Main
SOL_AWC	Available water capacity of the soil layer.	.sol	fraction	-0.053	-0.194	-0.239	0.115
SOL_K	Saturated hydraulic conductivity.	.sol	fraction	-0.220	-0.199	0.019	-0.167
SOL_ORGN	Initial organic N concentration in the soil layer.	.chm	mg N/kg soil	1897	1	1717	0
SOL_ORGP	Initial organic P concentration in the soil layer.	.chm	mg P/kg soil	1.00	63.06	99.62	500.00
SOL_Z	Depth from soil surface to bottom of layer.	.sol	fraction	0.034	-0.120	0.084	0.222
SOLN	Initial NO ₃ ⁻ concentration in the soil layer.	.chm	mg N/kg soil	149.300	6.971	174.000	1.000
SPCON	Linear parameter for calculating maximum sediment reentrainment.	.bsn	-	0.000	0.009	0.005	0.002
SPEXP	Exponent parameter for calculating sediment reentrainment.	.bsn	-	1.143	1.808	1.976	1.769
SURLAG	Surface runoff lag coefficient.	.bsn	day	4.462	9.893	10.580	11.960
TIMP	Snow pack temperature lag factor.	.bsn	-	0.289	0.295	0.295	0.953
TLAPS	Temperature lapse rate.	.sub	°C/km	-3.508	-3.561	-3.563	-3.516
USLE_C	USLE equation cropping practices factor.	crop.dat	fraction	0.000	-0.216	-0.078	-0.040
USLE_K	USLE equation soil erodibility (K) factor.	.sol	fraction	-0.026	-0.332	-0.371	0.449

Table 15. Change in downscaled and bias-corrected projected precipitation and temperature, 1954-2005 and 2030-2059. Differences between historic and future climate from a given General Circulation Model (GCM) and Representative Concentration Pathway (RCP) are calculated separately for eight meteorological stations and averaged across all stations.

Change in average annual precipitation (%)						
	RCP 4.5			RCP 8.5		
	CanESM2	INMCM4	MIROC5	CanESM2	INMCM4	MIROC5
Annual	9.9	0.1	2.4	13	-3.2	2.1
Jan	14	8.4	-3.5	19	8.7	0.3
Feb	3.5	-4.8	7.1	7.0	4.4	9.3
Mar	-0.8	1.4	-1.2	3.4	6.2	1.6
Apr	3.4	1.1	-13	0.2	-0.8	-13
May	2.9	-8.4	-13	-3.5	-1.4	-5.5
Jun	38	-19	-7.2	40	-15	18
Jul	39	-15	3.0	51	-15	15
Aug	3.4	-28	5.7	5.4	-24	-4.4
Sep	-9.9	4.5	-9.3	-0.1	6.4	-17
Oct	12	-1.2	-1.5	13	7.1	8.7
Nov	5.6	-4.9	9.6	7.6	3.4	7.5
Dec	11	-2.2	5.0	22	0.7	5.6
Change in average daily maximum temperature (°C)						
Annual	2.6	1.1	2.1	3.1	1.5	2.3
Jan	1.3	0.3	0.7	1.8	0.7	1.2
Feb	1.4	0.4	0.9	2.1	0.6	1.0
Mar	1.1	0.3	1.1	1.6	0.3	1.3
Apr	1.0	0.6	1.4	1.4	0.9	1.7
May	1.8	0.9	1.2	2.6	1.4	1.7
Jun	2.0	1.4	1.3	3.1	2.3	1.7
Jul	1.8	1.6	1.4	2.7	2.2	1.8
Aug	1.4	1.3	1.4	2.4	1.5	1.9
Sep	1.6	0.6	1.2	2.0	1.2	1.7
Oct	0.7	0.4	1.1	1.6	0.8	1.6
Nov	1.0	0.6	1.2	1.7	0.9	1.6
Dec	1.1	0.5	1.0	2.0	0.9	1.5
Change in average daily minimum temperature (°C)						
Annual	2.5	0.8	1.7	3.1	1.0	1.9
Jan	1.6	0.6	0.4	2.1	1.2	1.0
Feb	1.3	0.6	0.9	1.9	1.0	1.1
Mar	0.9	0.4	0.9	1.4	0.8	1.2
Apr	0.8	0.4	0.9	1.3	0.9	1.2
May	1.5	0.5	0.9	2.1	1.0	1.4
Jun	1.9	0.6	1.1	3.1	1.1	1.7
Jul	1.8	0.4	1.2	3.1	0.9	1.8
Aug	1.5	0.4	1.1	2.6	0.8	1.7
Sep	1.2	0.1	0.8	1.9	1.0	1.3
Oct	0.8	0.4	1.0	1.6	1.2	1.5
Nov	1.2	0.8	1.1	1.8	1.2	1.5
Dec	1.4	0.7	0.9	2.4	1.1	1.5

Table 16. Average annual simulated runoff and loads of sediment, total nitrogen and total phosphorus at the Sprague River outlet for the period 2001-2010 under scenarios of depressional and riparian wetland extent (scenarios defined in section 2.6) and observed precipitation and temperature. “Base” represents baseline wetland extent under present-day conditions. Scenarios of +/-25, 50, 75 and 100% are applied to all wetlands in the Sprague watershed and represent a change in width for riparian buffers and a change in surface area and volume for depressional wetlands. “10 m min” shows a scenario of a riparian buffer of a minimum 10 m width throughout the watershed, with depressional wetland extent unaltered from baseline. “Diff” and “% Change” show absolute and percent change between a given wetland scenario and baseline wetland extent utilizing the same climate forcings for 2001-2010. “Avg” = mean; “SD” = standard deviation.

Runoff (mm · yr ⁻¹)										
	-100%	-75%	-50%	-25%	Base	+25%	+50%	+75%	+100%	10 m min
Avg	101.3	100.3	100.5	100.3	100.3	100.3	101.0	100.4	100.5	100.3
SD	50.5	50.2	50.3	50.3	50.3	50.3	50.7	50.4	50.5	50.3
Diff.	1.0	0.0	0.2	0.0	--	0.0	0.7	0.1	0.2	0.0
% Change	1.0	0.0	0.2	0.0	--	0.0	0.7	0.1	0.2	0.0
Sediment (ktons · yr ⁻¹)										
	-100%	-75%	-50%	-25%	Base	+25%	+50%	+75%	+100%	10 m min
Avg	13.7	12.7	12.8	12.6	12.5	12.5	12.4	12.4	12.4	12.0
SD	9.2	8.2	8.3	8.1	8.1	8.1	8.0	8.1	8.1	7.6
Diff.	1.2	0.1	0.3	0.1	--	0.0	-0.1	-0.1	-0.1	-0.5
% Change	9.3	1.0	2.2	0.5	--	-0.3	-0.9	-0.7	-0.8	-4.1
TN (tons · yr ⁻¹)										
	-100%	-75%	-50%	-25%	Base	+25%	+50%	+75%	+100%	10 m min
Avg	317	267	265	256	250	245	248	234	229	234
SD	359	304	305	295	289	282	293	270	265	283
Diff.	66.6	16.6	15.1	5.6	--	-5.4	-2.1	-16.3	-21.5	-16.4
% Change	27	7	6	2	--	-2	-1	-6	-9	-7
TP (tons · yr ⁻¹)										
	-100%	-75%	-50%	-25%	Base	+25%	+50%	+75%	+100%	10 m min
Avg	44	34	33	32	31	30	29	29	29	28
SD	25	17	17	16	15	15	14	14	14	14
Diff.	13.0	3.1	2.1	0.8	--	-0.7	-1.4	-1.7	-2.2	-2.4
% Change	42	10	7	2	--	-2	-5	-6	-7	-8

Table 17. Summary of annual runoff 1954-2005 ($n = 52$) observed at the U.S. Geological Survey gauge 1150100, Sprague River near Chiloquin, Oregon (“Obs”), and simulated by the calibrated and tested model using precipitation and temperature forcings under three General Circulation Models (CanESM2, INMCM4, and MIROC5) and two Representative Concentration Pathways (RCPs). Values shown are in mm; “Avg” = mean; “SD” = standard deviation; and “Diff” = the observed average less the simulated average.

	Obs.	RCP 4.5			RCP 8.5		
		CanESM2	INMCM4	MIROC5	CanESM2	INMCM4	MIROC5
Avg	143.4	154.4	156.7	152.6	154.4	156.7	152.6
SD	52.8	68.3	62.6	61.1	68.3	62.6	61.1
Diff	--	8.7	11.0	6.9	8.7	11.0	6.9

Table 18. Simulated 30-year average annual runoff, sediment and nutrient loads for the period 2030-2059 at the outlet of the Sprague River forced with precipitation and temperature data from three General Circulation Models (GCMs) and two Representative Concentration Pathways (RCPs). Absolute and percent differences are differences between the 52-year annual average for 1954-2005 and the 30-year annual average for 2030-2059, where the hydrologic model is forced with the same GCM and RCP for both time periods. Unshaded values indicate positive differences, while shaded values indicate negative differences. Bold values marked with an asterisk show future fluxes that are significantly different from the historic baseline under a Mann-Whitney-Wilcoxon two-tailed test ($\alpha = 0.1$).

“Avg” = mean; “SD” = standard deviation.

Runoff (mm · yr ⁻¹)						
	RCP 4.5			RCP 8.5		
	CanESM2	INMCM4	MIROC5	CanESM2	INMCM4	MIROC5
Avg	181	166	165	203	150	165
SD	51	66	54	55	63	49
Difference	27	10	13	48	-6.4	12
% Change	17*	6.1	8.2	31*	-4.1	7.9
Sediment (ktons · yr ⁻¹)						
Avg	27	23	24	33	21	24
SD	14	14	13	16	13	13
Difference	5.7	1.5	2.2	11	-1.3	2.0
% Change	26*	7.1	10	52*	-6.0	9.1
TN (tons · yr ⁻¹)						
Avg	180	161	165	205	142	166
SD	57	71	59	71	62	62
Difference	31	6.7	15	56	-12	16
% Change	21*	4.4	10	37*	-7.9	11
TP (tons · yr ⁻¹)						
Avg	74	64	65	84	56	67
SD	25	27	24	28	23	27
Difference	13	0.9	3.2	23	-6.8	4.6
% Change	22	1.5	5.2*	38*	-11	7.4

Table 19. Percent difference in monthly flow (“Q”), sediment load (“S”), TN load (“N”), and TP load (“P”) simulated for 30 years from 2030-2059 and 52 years from 1954-2005 under three General Circulation Models (GCMs) and two Representative Concentration Pathways (RCPs).

Differences are between the 52-year annual average for the historic period and the 30-year annual average for the future period, where the hydrologic model is forced with the same GCM and RCP for both time periods. Unshaded values indicate positive differences, while shaded values indicate negative differences. Bold values marked with an asterisk show future fluxes that are significantly different from the historic baseline under a Mann-Whitney-Wilcoxon two-tailed test ($\alpha = 0.1$).

		Jan				Feb				Mar				Apr			
GCM	RCP	Q	S	N	P	Q	S	N	P	Q	S	N	P	Q	S	N	P
CanESM2	4.5	66*	120*	70*	67*	45*	89*	44*	37*	25*	63*	38	48	-13	-17	-29	-17
	8.5	75*	129*	64*	66*	57*	96*	51*	38*	36*	93*	80*	83*	-1	1	-6	0
INMCM4	4.5	21	32*	3	-1	11	15	6	2	3	6	1	2	-10	-9	-7	-8
	8.5	-9	-18	-26	-29	3	8	7	5	-1	2	-11	-12	-11	-13	-6	-11
MIROC5	4.5	51*	60*	34*	20*	11	12	-8	-14	16	43	49*	40	-9	-12	-14	-14
	8.5	29*	34*	19*	13	29*	28*	21	9	16	38*	30	28	0	7	10	10
		May				Jun				Jul				Aug			
GCM	RCP	Q	S	N	P	Q	S	N	P	Q	S	N	P	Q	S	N	P
CanESM2	4.5	-23	-44	-26	-21	-22	-39	-13	-8	-2	-9	66*	25*	3	-16	32*	18*
	8.5	-18	-33	-33	-21	-14	-23	-13	0	1	-5	15*	17*	15	-2	62*	33*
INMCM4	4.5	-9	-13	-11	-11	-11	-22	-25	-15	-3	-11	-3	3	-1	-11	-4	2
	8.5	-13	-16	-19*	-21*	-10	-12	-11	-7	-9	-19	-3	2	-1	26	13	8
MIROC5	4.5	-23*	-39*	-40*	-33*	-23*	-38*	-21	-15	-19*	-35*	-17	-6	-3	-13	39	12
	8.5	-23*	-38*	-41*	-33*	-24	-42*	-24	-16	-15	-30*	2	0	-3	-16	16	9
		Sept				Oct				Nov				Dec			
GCM	RCP	Q	S	N	P	Q	S	N	P	Q	S	N	P	Q	S	N	P
CanESM2	4.5	12	-21*	52	23*	4	-7	-17	-1	49*	87*	65*	56*	65*	94*	47*	32
	8.5	19*	7	27	21*	36*	53*	45	37*	75*	154*	60*	62*	115*	242*	121*	97*
INMCM4	4.5	-2	-10	-27	-3	25	91	27	36	32*	35*	43*	24*	32*	29*	23*	6
	8.5	-5	-6	-37	-10	-4	10	-7	0	-6	-21	5	-13	16	13	7	-4
MIROC5	4.5	-5	-25	-7	1	-8	-25	-18	-16	13	38	14	14	52*	57*	59*	41*
	8.5	-4	-31	2	8*	12	9	24	26	15	12	17	7	30*	38*	30	21

Table 20. Results of Mann-Kendall test for trend and Sen’s slope estimator for 2030-2059 monthly average daily stream flow (“Q”, in $\text{m}^3 \cdot \text{s}^{-1}$), total sediment load (“S”, in $\text{tons} \cdot \text{month}^{-1}$), total nitrogen load (“N”, in $\text{kg} \cdot \text{month}^{-1}$), and total phosphorus load (“P”, in $\text{kg} \cdot \text{month}^{-1}$) simulated under three General Circulation Models (GCMs) and two Representative Concentration Pathways (RCPs). Blank cells are not significant; unshaded values indicate significant positive trends, while shaded values indicate significant negative trends ($\alpha = 0.1$); $n = 30$ for each month. Values show Sen’s slope estimate of rate of change (units are described above), and superscript symbol shows significance level. + = 0.1; * = 0.05; and ** = 0.01. Annual Q, S, N and P showed significant trends only for P under CanESM2 (RCP 4.5 and 8.5) ($1033 \text{ kg} \cdot \text{year}^{-1}$ and $1484 \text{ kg} \cdot \text{year}^{-1}$, respectively, $\alpha = 0.05$), and MIROC5 (RCP 8.5, $1049 \text{ kg} \cdot \text{year}^{-1}$, $\alpha = 0.01$).

GCM	RCP	Jan				Feb				Mar				Apr			
		Q	S	N	P	Q	S	N	P	Q	S	N	P	Q	S	N	P
CanESM2	4.5	--	57⁺	--	--	--	--	--	--	--	--	--	--	--	--	--	--
	8.5	--	--	--	--	1⁺	--	587⁺	220*	0.9⁺	154⁺	939*	417*	--	--	-461⁺	--
INMCM4	4.5	--	--	--	--	--	--	--	--	--	--	814*	250*	0.5⁺	--	--	152⁺
	8.5	--	--	--	--	--	--	--	--	--	--	--	--	--	-69⁺	--	--
MIROC5	4.5	--	--	--	--	--	--	--	--	--	--	--	--	--	--	--	--
	8.5	--	58⁺	792*	310**	--	--	--	--	--	--	--	--	--	--	--	--
Model	RCP	May				Jun				Jul				Aug			
		Q	S	N	P	Q	S	N	P	Q	S	N	P	Q	S	N	P
CanESM2	4.5	--	--	--	--	--	--	--	--	--	--	--	16⁺	--	--	--	--
	8.5	--	--	--	--	--	--	--	--	--	--	--	--	--	--	37⁺	--
INMCM4	4.5	--	--	--	--	0.2⁺	--	--	--	0.1*	--	42**	26*	--	--	--	--
	8.5	-0.5⁺	-69⁺	-468*	--	--	--	--	--	--	-8*	--	--	-0.1⁺	-9⁺	--	--
MIROC5	4.5	--	--	--	--	--	--	--	--	--	--	--	--	--	--	--	--
	8.5	--	--	--	--	--	--	111*	--	--	--	--	--	--	--	--	16⁺
Model	RCP	Sep				Oct				Nov				Dec			
		Q	S	N	P	Q	S	N	P	Q	S	N	P	Q	S	N	P
CanESM2	4.5	0.1⁺	4⁺	--	--	--	--	--	--	--	--	--	--	--	--	--	--
	8.5	--	--	--	--	--	--	--	--	--	--	--	--	--	--	--	--
INMCM4	4.5	--	--	--	--	--	--	--	--	--	--	--	--	--	--	--	123⁺
	8.5	--	-5⁺	--	--	--	--	--	--	--	--	--	--	--	--	--	--
MIROC5	4.5	--	--	--	--	--	--	--	--	--	--	--	--	--	--	--	--
	8.5	--	--	--	--	0.1⁺	4*	--	--	0.2⁺	19*	--	178*	--	--	496**	--

Table 21. Average annual simulated runoff and loads of sediment, TN and TP at the Sprague River for the period 2030-2059 under scenarios of depressional and riparian wetland extent (scenarios defined in section 2.6) and two General Circulation Models (RCP 8.5). “Base” represents baseline wetland extent under present-day conditions. Scenarios of +/- 50 and -100% are applied to all wetlands in the Sprague watershed as a change in width for riparian buffers and in surface area and volume for depressional wetlands. “Fut. Change” and “Fut % Change” are between a given wetland scenario and baseline wetland extent utilizing the same General Circulation Model forcing for 2030-2059; “Hist. Diff” and “Hist % Change” are between the 2030-2059 scenario and 1954-2005 baseline wetland extent. “Avg” = mean; “SD” = standard deviation.

Q (mm · year ⁻¹)								
	Base		-100%		-50%		+50%	
	CanESM	INMCM	CanESM	INMCM	CanESM	INMCM	CanESM	INMCM
Avg	203	150	203	151	203	150	203	--
SD	55	63	55	62	55	63	55	--
Fut. Change.	--	--	0.2	0.3	0.0	0.1	0.0	--
Fut. % Change	0.0	0.0	0.1	0.2	0.0	0.1	0.0	--
Hist. Change	48	-6.4	49	-6.1	49	-6.3	49	--
Hist. % Change	31	-4.1	32	-3.9	31	-4.0	31	--
Sediment (ktons · year ⁻¹)								
Avg	33	21	34	21	33	21	33	--
SD	16	13	18	13	17	13	16	--
Fut. Change.	--	--	1.4	0.4	0.3	0.1	-0.2	--
Fut. % Change	0.0	0.0	4.3	2.0	0.9	0.4	-0.7	--
Hist. Change	11	-1.3	13	-0.9	12	-1.2	11	--
Hist. % Change	52	-6.0	59	-4.2	54	-5.6	51	--
TN (tons · year ⁻¹)								
Avg	205	142	251	177	216	151	195	--
SD	71	62	86	76	75	66	68	--
Fut. Change.	--	--	46	35	11	8.6	-10	--
Fut. % Change	0.0	0.0	23	24	5.6	6.0	-4.8	--
Hist. Change	56	-12	102	23	67	-3.6	46	--
Hist. % Change	37	-7.9	68	15	45	-2.4	31	--
TP (tons · year ⁻¹)								
Avg	84	56	143	92	93	62	78	--
SD	28	23	57	50	33	28	25	--
Fut. Change.	--	--	59	36	9	5.7	-6	--
Fut. % Change	0.0	0.0	70	64	11	10	-7.3	--
Hist. Change	84	56	143	92	93	62	78	--
Hist. % Change	38	-11	135	47	53	-1.7	28	--

Table 22. Percent of riparian wetland area within a 30 m buffer of streams in the Sprague River watershed, sorted by Strahler stream order (Knighton, 1998). Riparian wetland areas are from a wetlands database (Oregon Natural Heritage Information Center and the Wetlands Conservancy 2009, U.S. Department of Agriculture Natural Resources Conservation Service, 2011; U.S. Fish and Wildlife Service, 2011; U.S. Geological Survey 2011). Stream orders are based on classification of a high-resolution stream network (U.S. Geological Survey, 2010b). Where multi-thread channels occurred, side channels were assigned the stream order of the main channel. “Not classified” indicates canals, ditches and some bifurcating side channels where order could not be determined (most of the latter are near the confluence of the South Fork of the Sprague River with the Sprague River mainstem). Disappearing streams occur throughout the study area because of high soil permeability (Gannett et al., 2007).

Stream order	%
1	24.6
2	17.3
3	10.1
4	26.5
5	6.2
6	7.9
Not classified	4.7
Disappearing stream	2.6

APPENDIX V:
SUPPLEMENTARY FIGURES

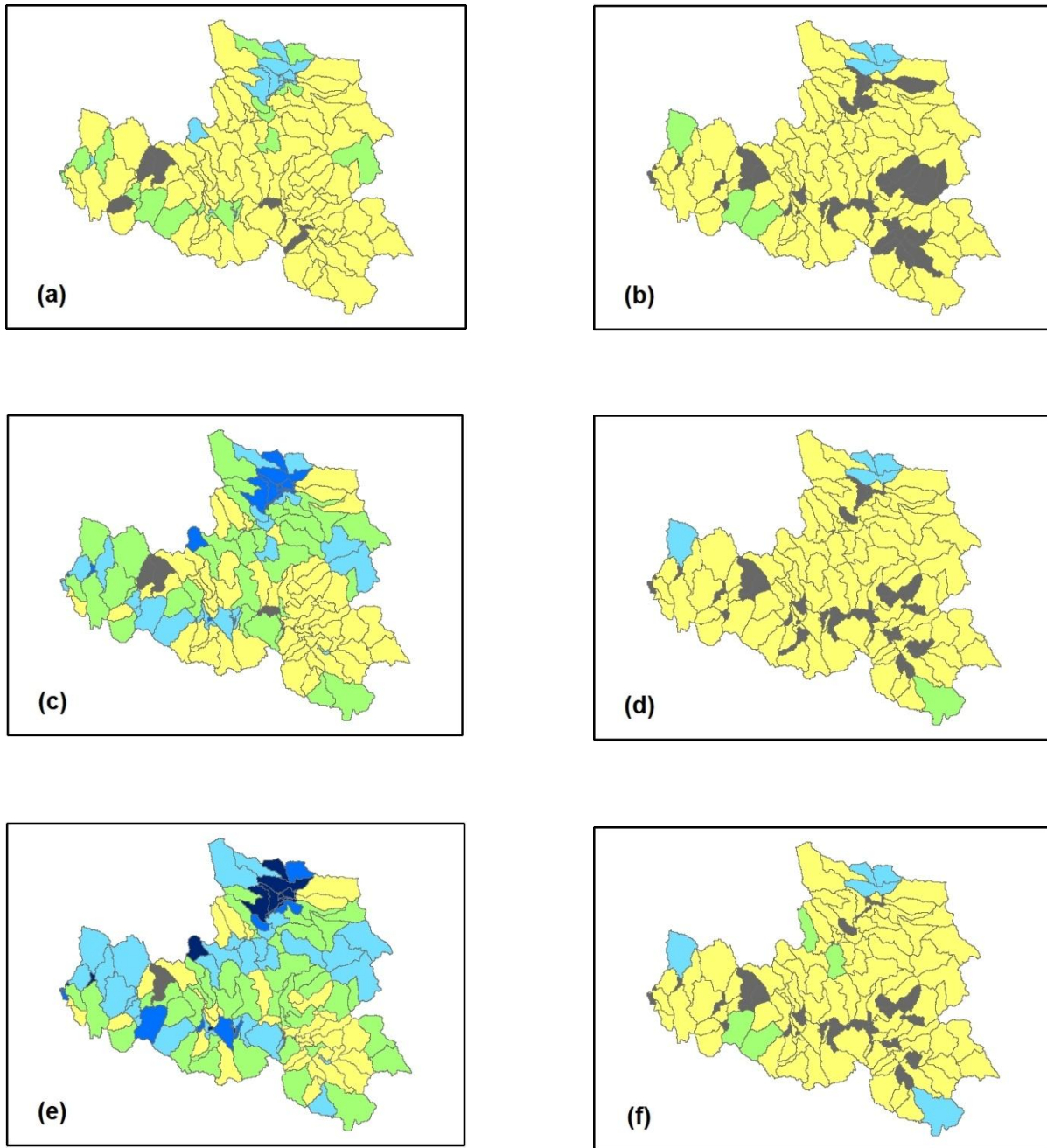


Figure 8. Map of example riparian wetland width and maximum depressional wetland volume used in SWAT model wetland scenarios. Figures 8a, c and e show riparian wetland width (FILTERW parameter in SWAT .mgt file) in m under 50% decrease in baseline width (a); baseline width (c) and 50% increase in baseline width (e). Dark grey = 0; yellow = 1 – 5; green = 6 – 10; pale blue = 11 – 20; medium blue = 21 – 30; and dark blue \geq 30. Figures 8b, d and f show the maximum depressional wetland volume (WET_MXVOL parameter in SWAT .pnd file) in 104 m³ under 50% decrease (b); baseline extent (d) and 50% increase (f). Grey = 0; yellow = 1 -25; green = 26 – 50; and pale blue \geq 50.

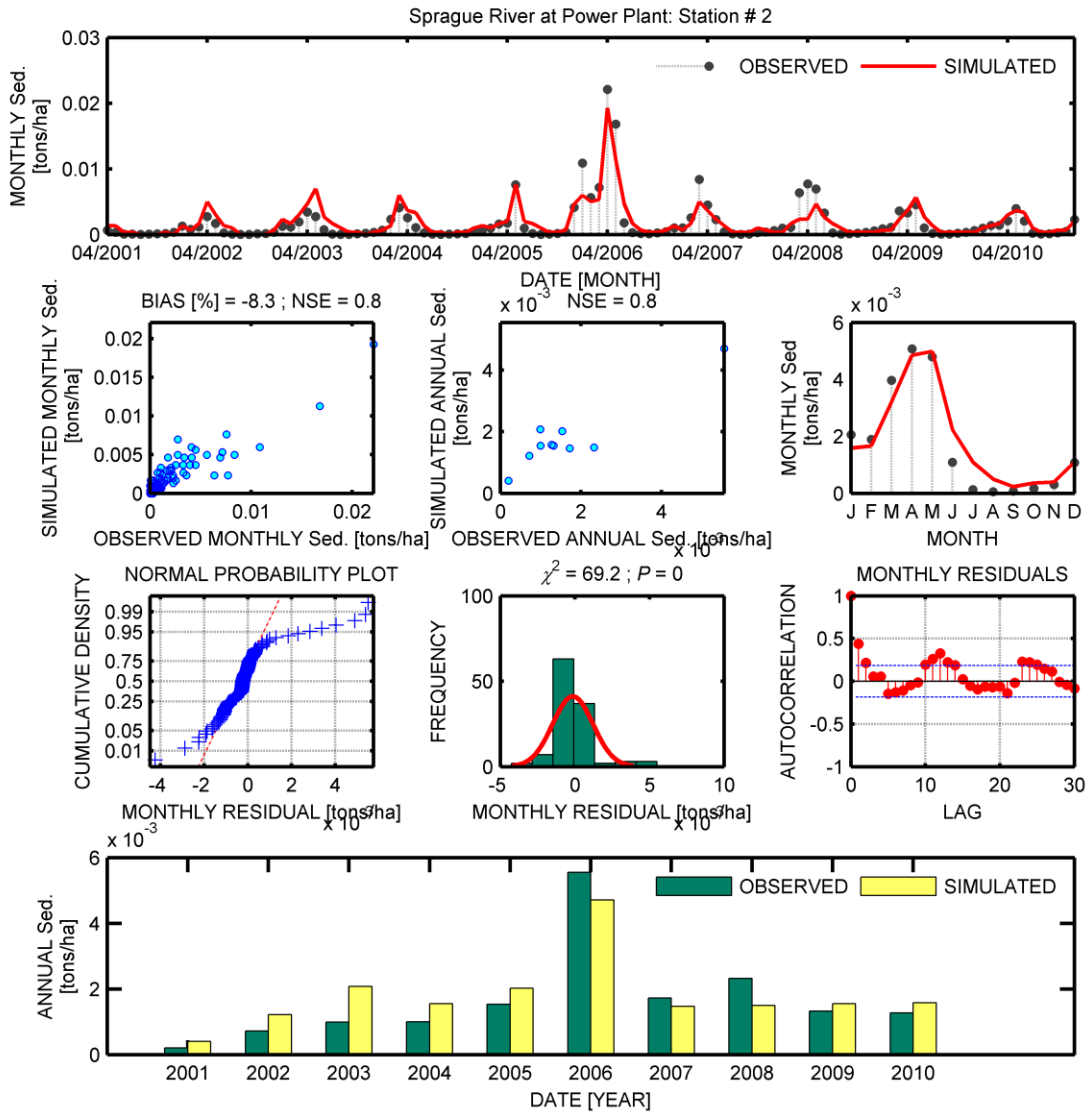


Figure 9. Time series and analysis of calibration (2001-2006) and testing (2007-2010) periods for the mainstem of the Sprague River for sediment. Time series is at site 2 (Figure 1; Table 3; Appendix IV, Table 13).

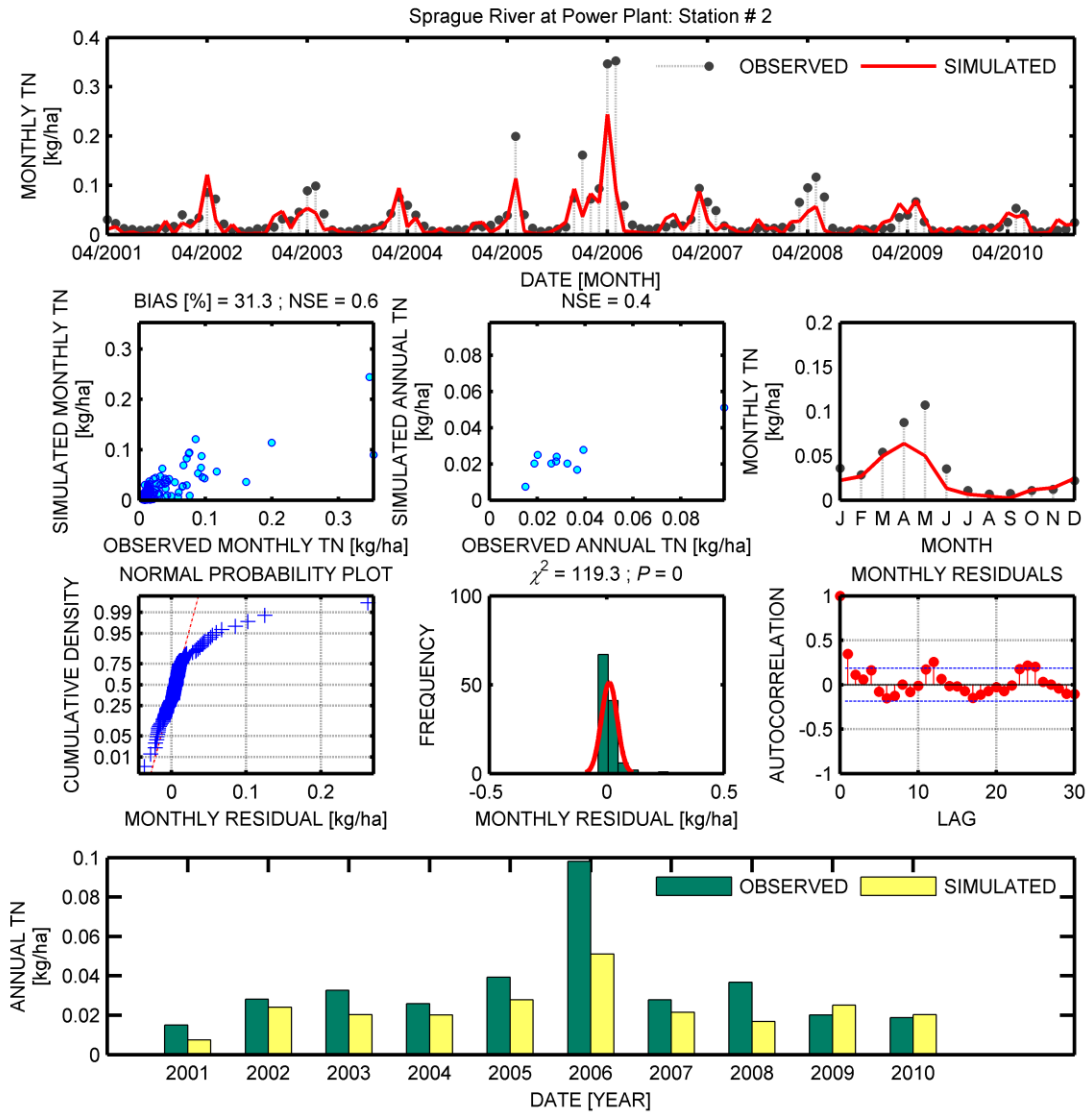


Figure 10. Time series and analysis of calibration (2001-2006) and testing (2007-2010) periods for the mainstem of the Sprague River for total nitrogen. Time series is at site 2 (Figure 1; Table 3; Appendix IV, Table 13).

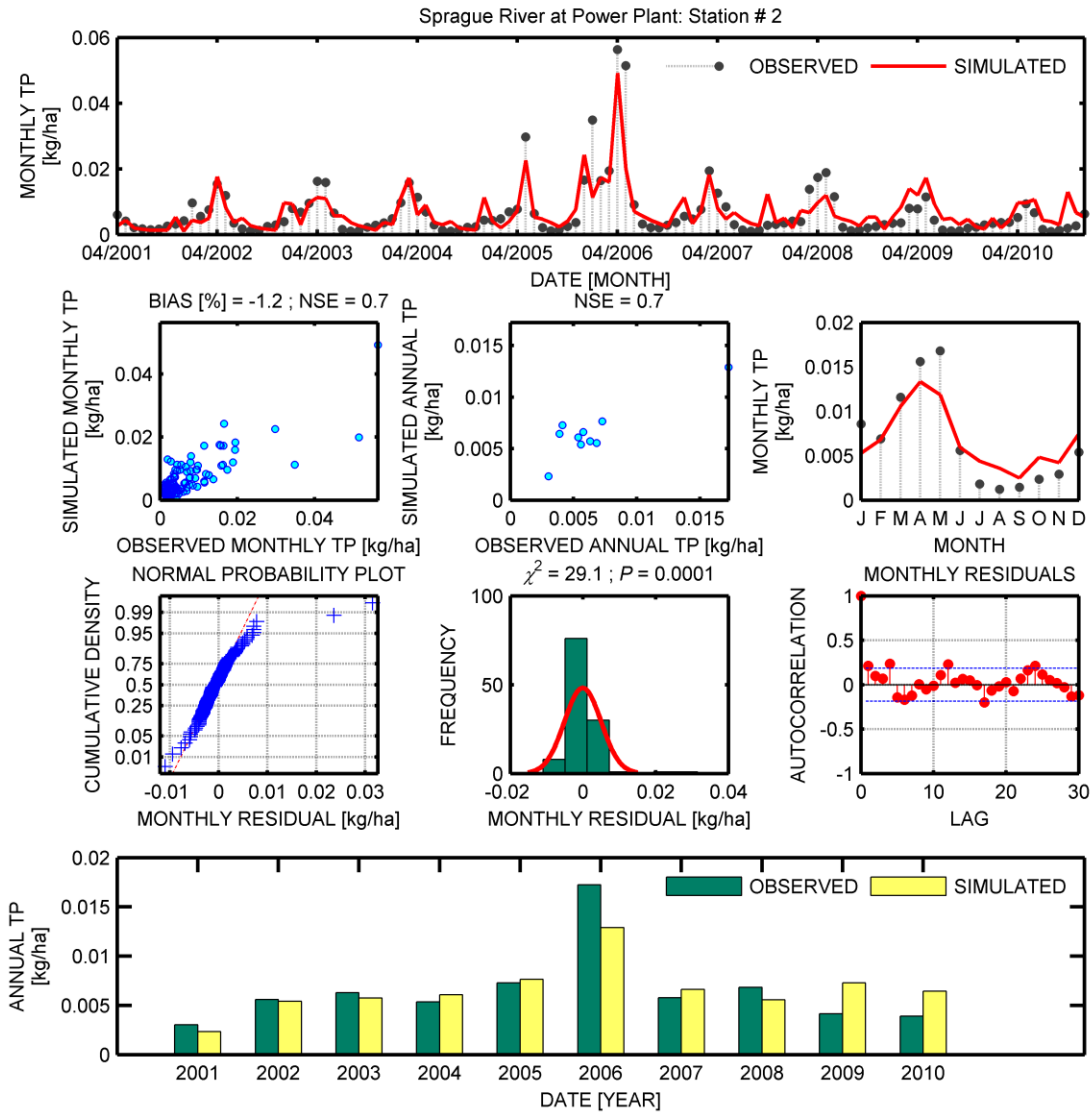


Figure 11. Time series and analysis of calibration (2001-2006) and testing (2007-2010) periods for the mainstem of the Sprague River for total phosphorus. Time series is at site 2 (Figure 1; Table 3; Appendix IV, Table 13).

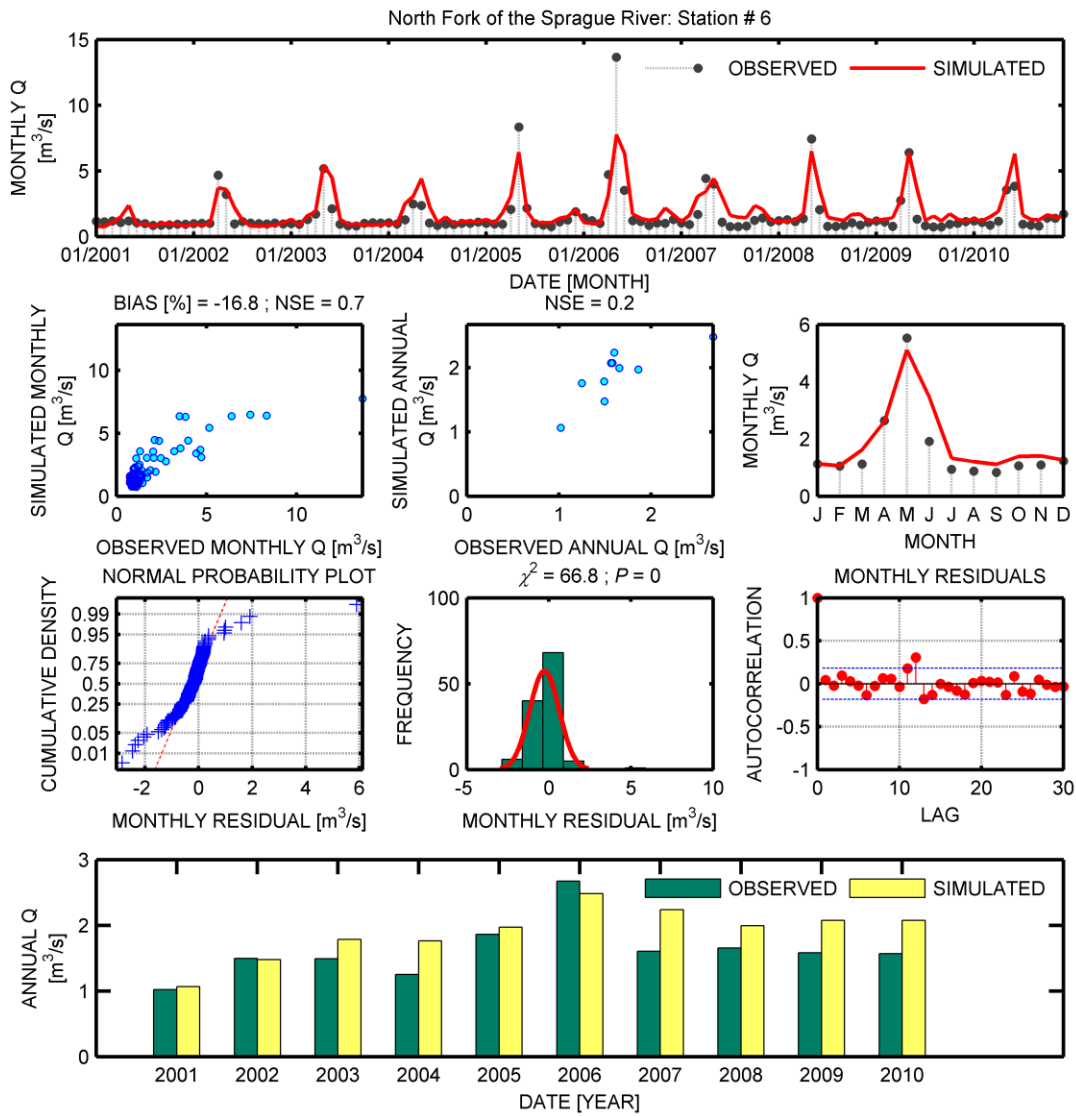


Figure 12. Time series and analysis of calibration (2001-2006) and testing (2007-2010) periods for the North Fork of the Sprague River for stream flow. Time series is at site 6 (Figure 1; Table 3; Appendix IV, Table 13).

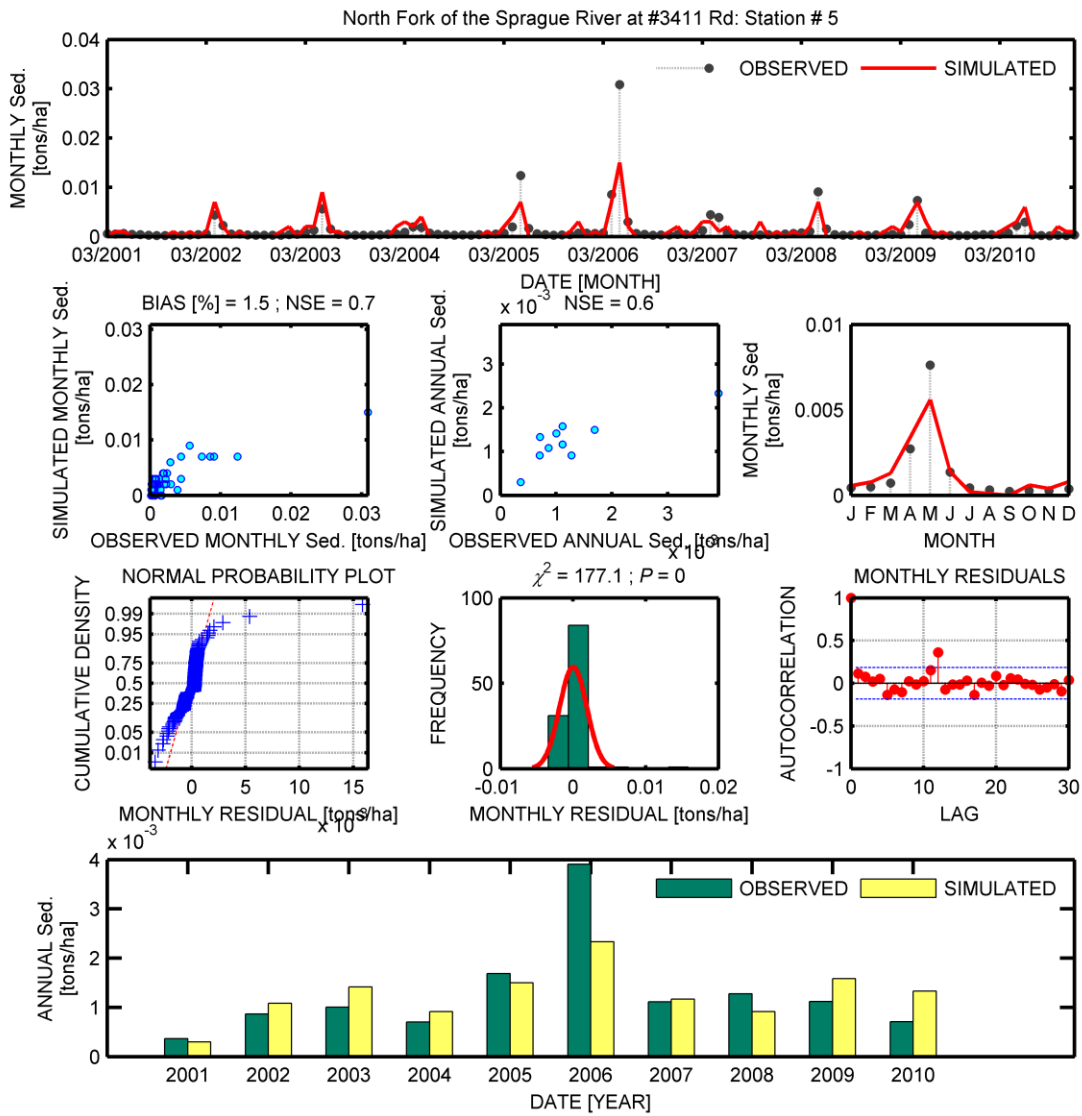


Figure 13. Time series and analysis of calibration (2001-2006) and testing (2007-2010) periods for the North Fork of the Sprague River for sediment. Time series is at site 5 (Figure 1; Table 3; Appendix IV, Table 13).

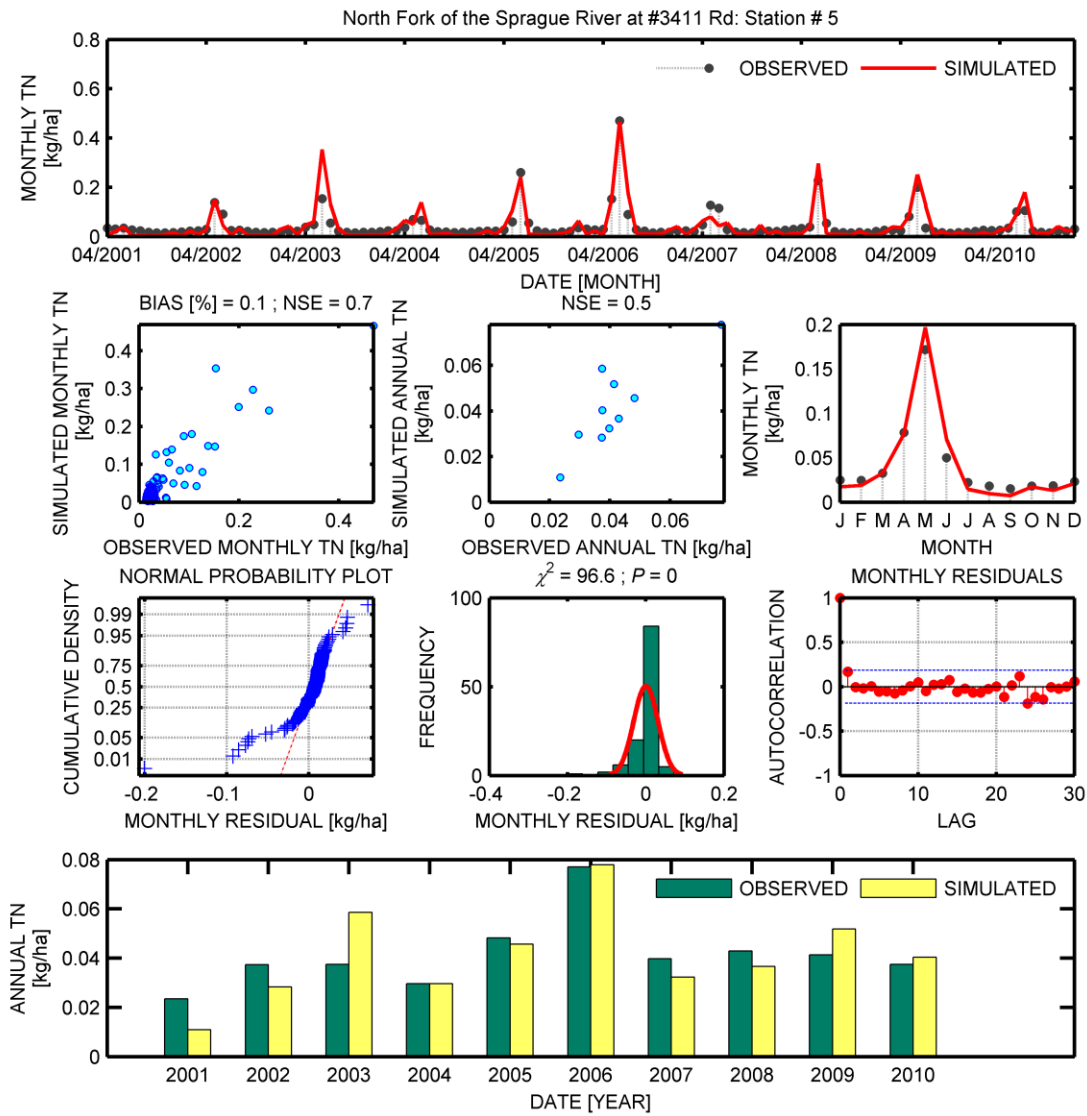


Figure 14. Time series and analysis of calibration (2001-2006) and testing (2007-2010) periods for the North Fork of the Sprague River for total nitrogen. Time series is at site 5 (Figure 1; Table 3; Appendix IV, Table 13).

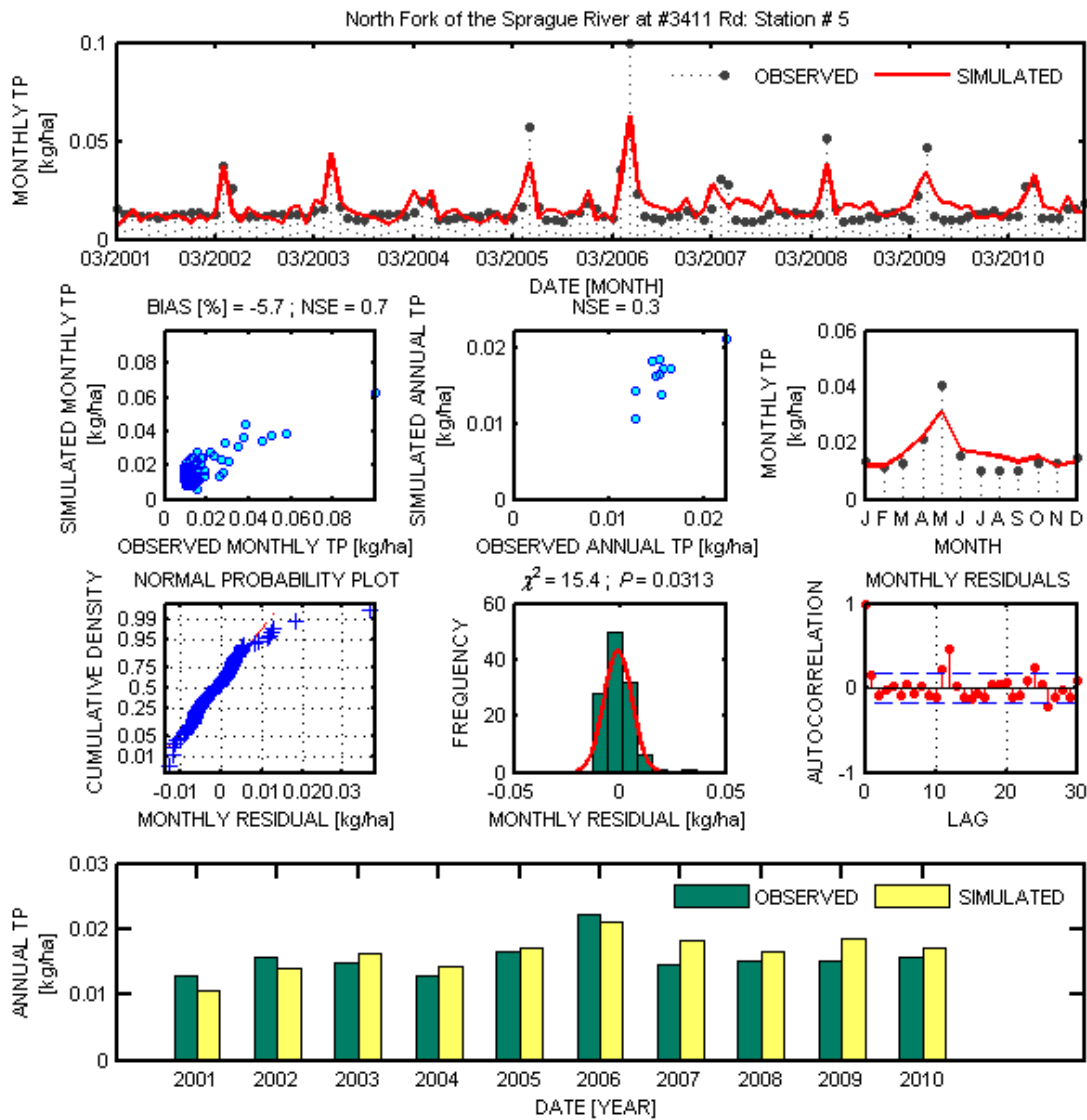


Figure 15. Time series and analysis of calibration (2001-2006) and testing (2007-2010) periods for the North Fork of the Sprague River for total phosphorus. Time series is at site 5 (Figure 1; Table 3; Appendix IV, Table 13).

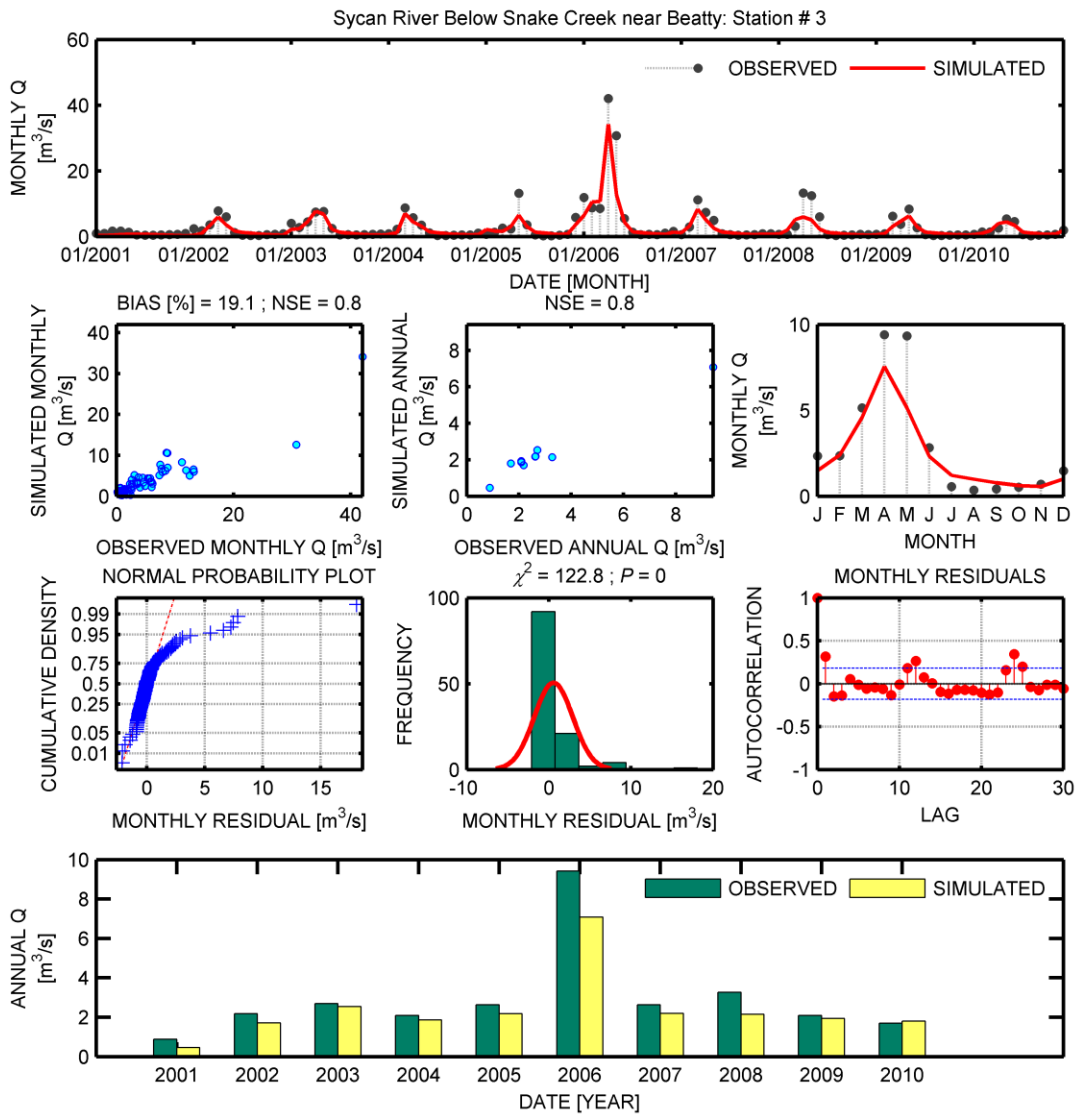


Figure 16. Time series and analysis of calibration (2001-2006) and testing (2007-2010) periods for the Sycan River for stream flow. Time series is at site 3 (Figure 1; Table 3; Appendix IV, Table 13).

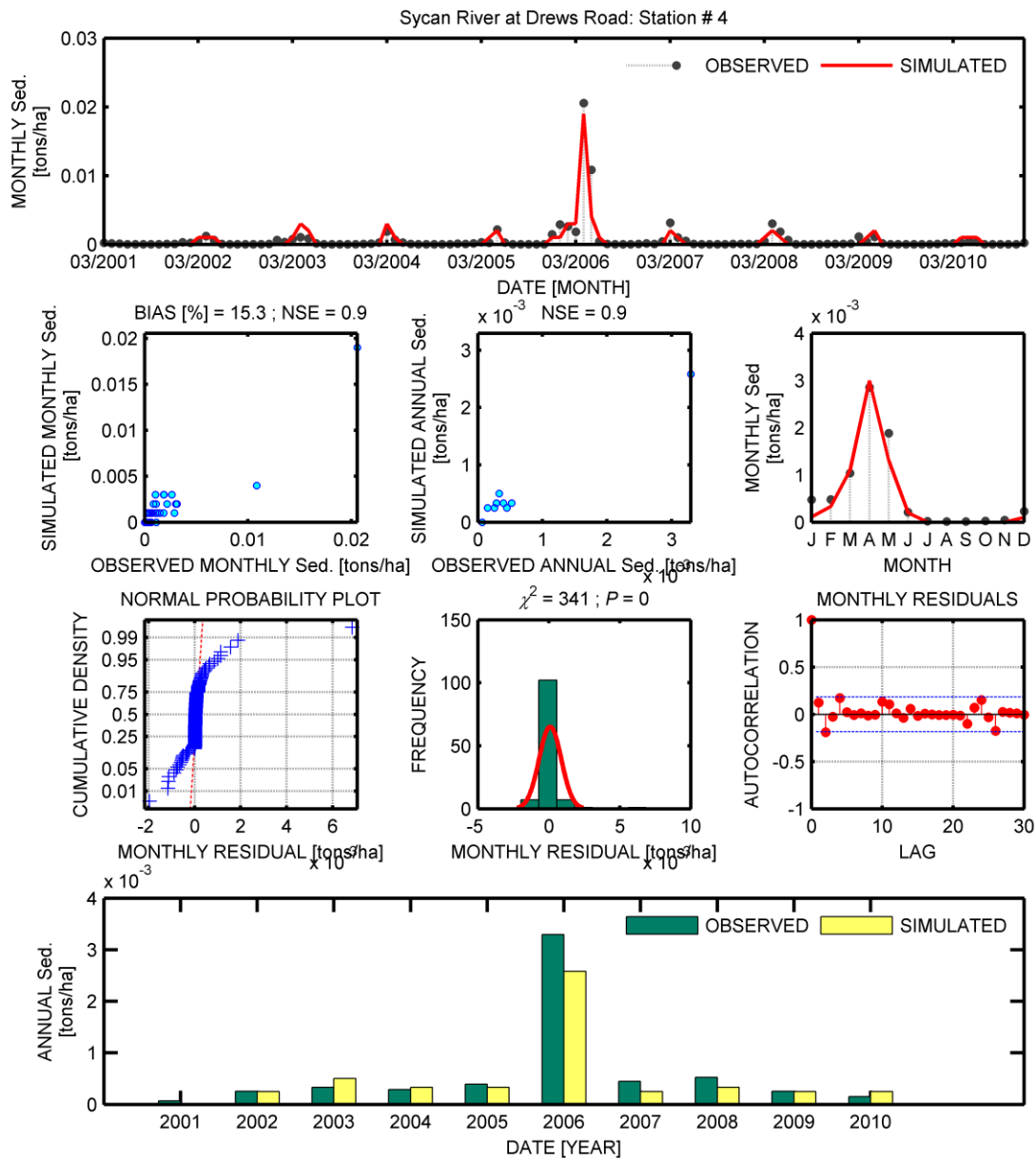


Figure 17. Time series and analysis of calibration (2001-2006) and testing (2007-2010) periods for the Sycan River for sediment. Time series is at site 4 (Figure 1; Table 3; Appendix IV, Table 13).

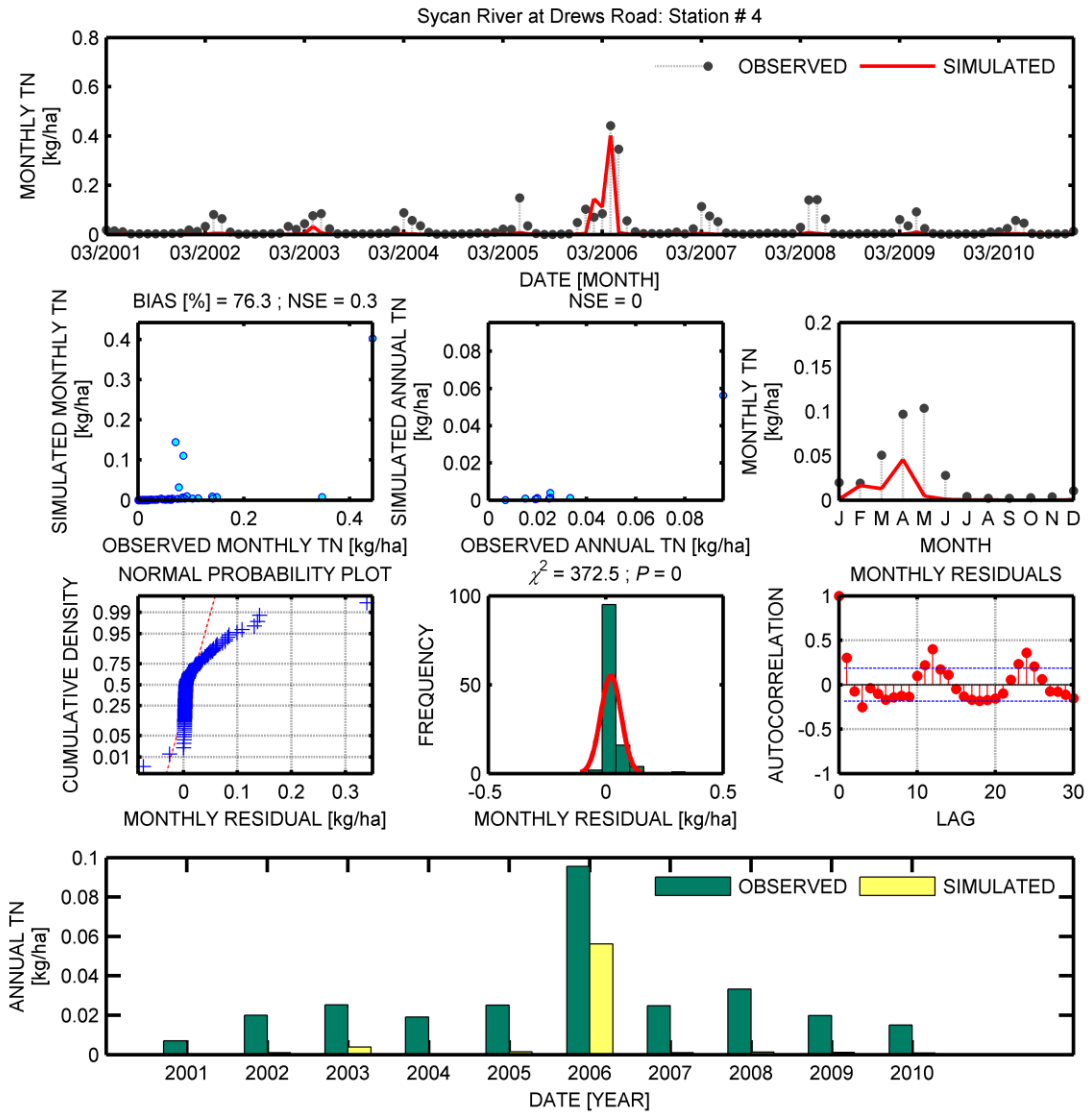


Figure 18. Time series and analysis of calibration (2001-2006) and testing (2007-2010) periods for the Sycan River for total nitrogen. Time series is at site 4 (Figure 1; Table 3; Appendix IV, Table 13).

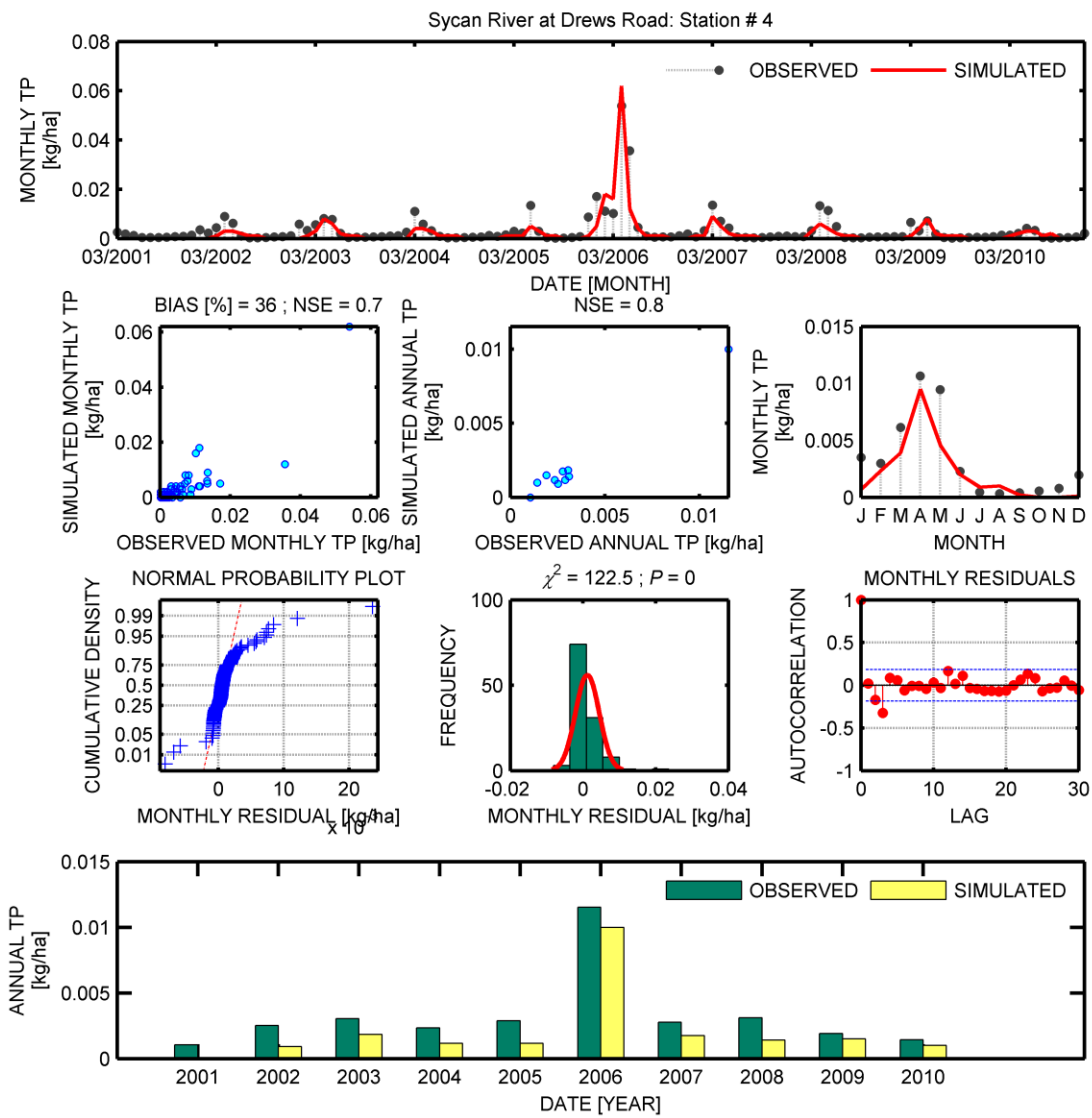


Figure 19. Time series and analysis of calibration (2001-2006) and testing (2007-2010) periods for the Sycan River for total phosphorus. Time series is at site 4 (Figure 1; Table 3; Appendix IV, Table 13).

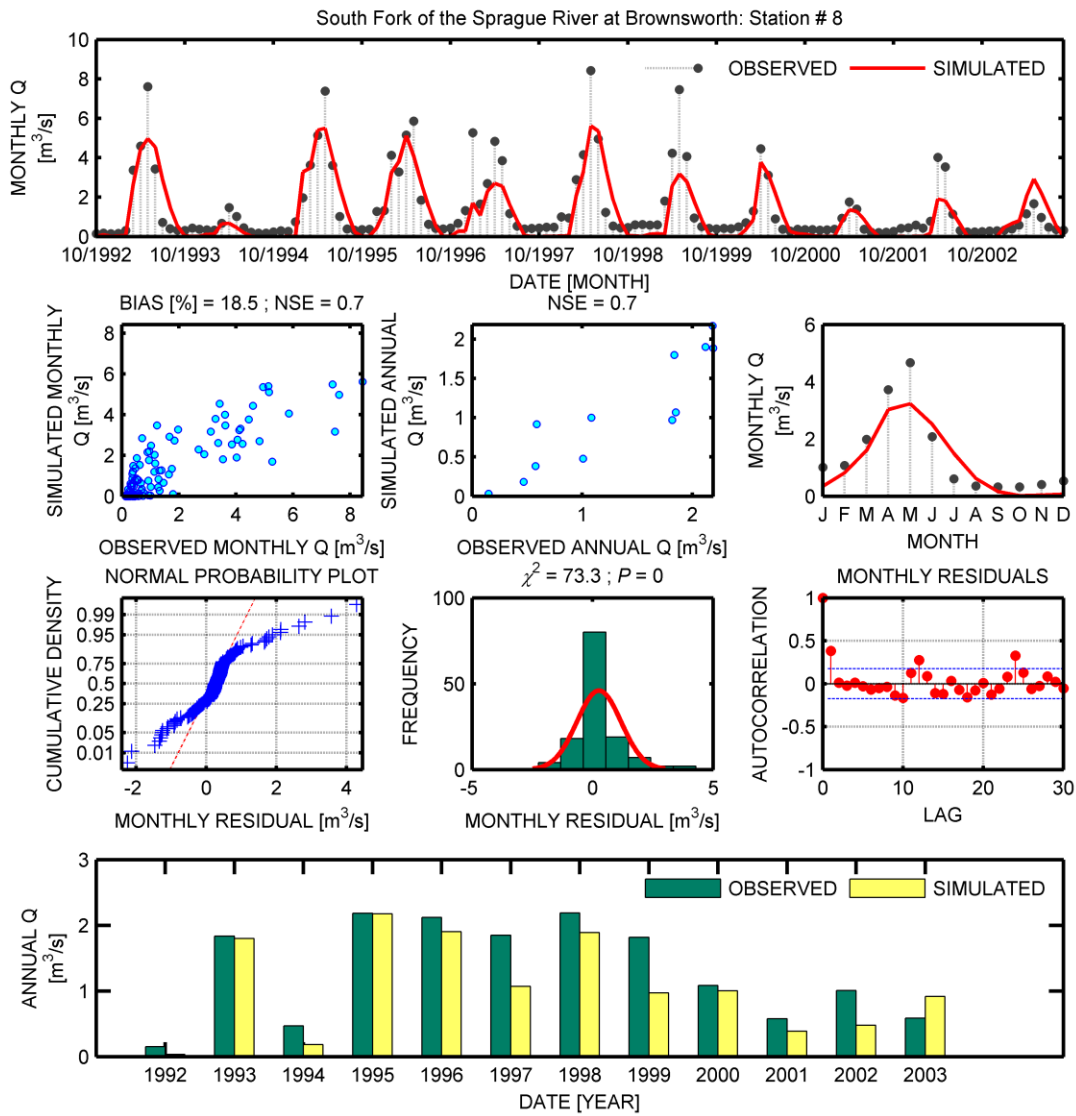


Figure 20. Time series and analysis of calibration (and testing periods for the South Fork of the Sprague River for stream flow. Calibration is for even calendar years from 1992 – 2003; testing is for odd years for the same period. Time series is at site 8 (Figure 1; Table 3; Appendix IV, Table 13).

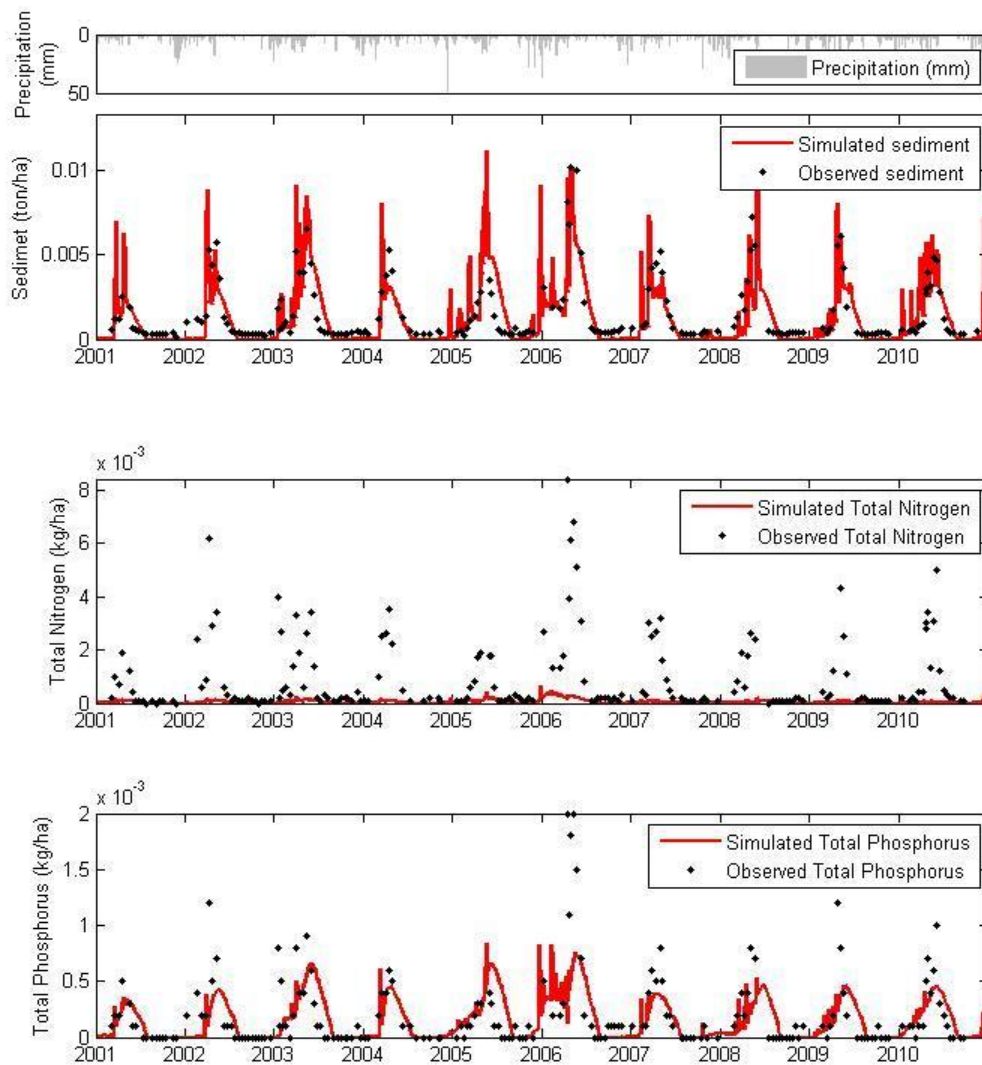


Figure 21. Time series of daily sediment, TN and TP calibration and testing periods for the South Fork of the Sprague River. Time series are at site 7 (Figure 1; Table 3; Appendix IV, Table 13).

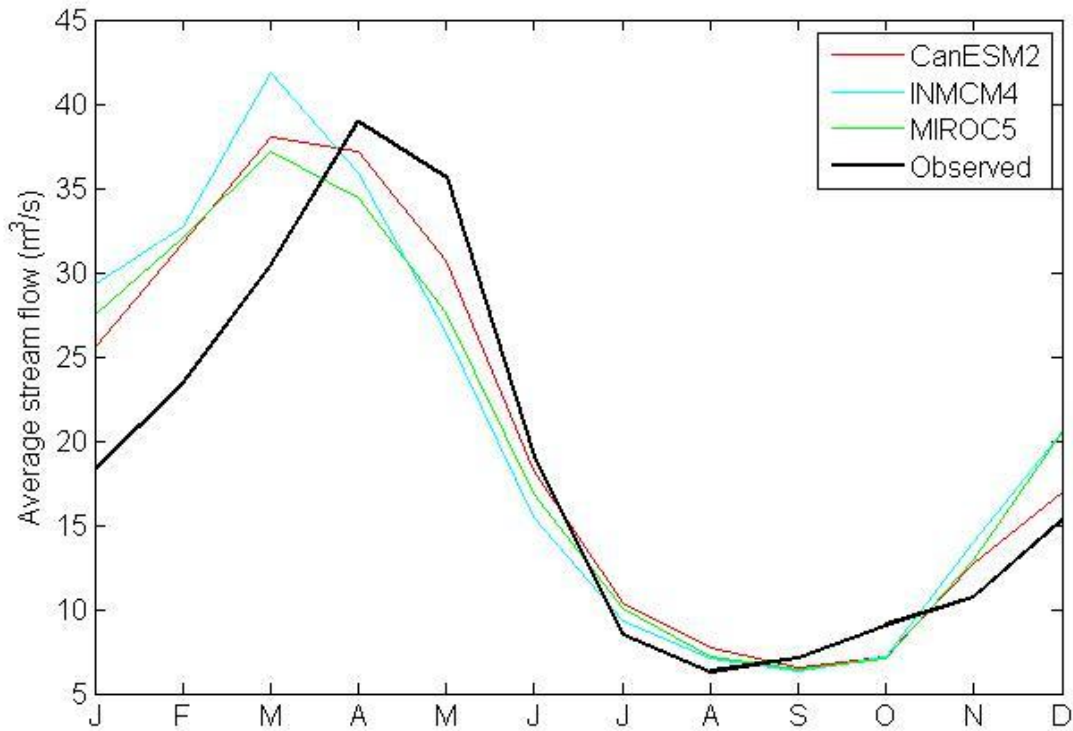


Figure 22. Graph of average monthly stream flow, 1954-2005 simulated by the SWAT hydrologic model at the Sprague River outlet using precipitation and temperature forcings from the three General Circulation Models used in this study. Averages of observations for the same time period near the Sprague River outlet at the U.S. Geological Survey stream flow gauge, Sprague River near Chiloquin, Oregon, are shown in black.

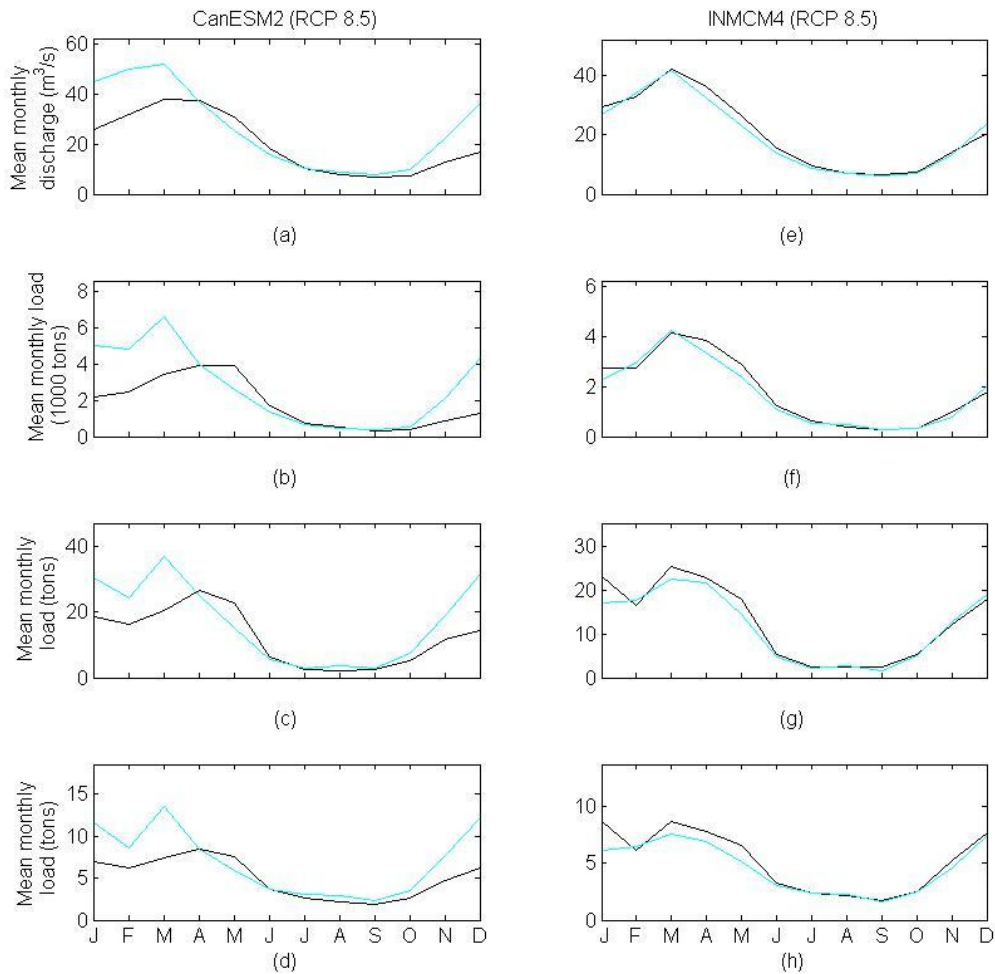


Figure 23. Simulated average monthly stream flow, sediment, and nutrient fluxes at the Sprague River outlet under the historic period (1954-2005, shown in black) and future period (2030-2059, shown in blue) under two climate projections. Figures 23a, 23b, 23c, and 23d show stream flow, sediment load, TN load and TP load, respectively under the CanESM2 RCP 8.5 projection. Figures 23e, 23f, 23g, and 23h show the same constituents for the INMCM4 RCP 8.5 projection.

LIST OF ABBREVIATIONS

CanESM2	Canadian Earth System Model 2
CEAP	Conservation Effects Assessment Project
CMIP5	Coupled Model Intercomparison Project 5
DDS	Dynamically Dimensioned Search
GCM	General Circulation Model
GHCN	Global Historical Climatology Network
HRU	Hydrologic Response Unit
INMCM4	Institute of Numerical Mathematics 4
KBRA	Klamath Basin Restoration Agreement
LOADEST	Load Estimator
MACA	Multivariate Adapted Constructed Analogs
MIROC5	Model for Interdisciplinary Research on Climate 5
N	Nitrogen
NCDC	National Climatic Data Center
NED	National Elevation Dataset
NHD	National Hydrography Dataset
NLCD	National Land Cover Dataset
NS	Nash-Sutcliffe coefficient
OWRD	Oregon Water Resources Department
P	Phosphorus
PBIAS	Percent bias
PRISM	Parameter-elevation Regressions on Independent Slopes Model
RCP	Representative Concentration Pathway

SNOTEL	Snow Telemetry
SWAT	Soil and Water Assessment Tool
TMDL	Total Maximum Daily Load
TN	Total nitrogen
TP	Total phosphorus
USDA	U.S. Department of Agriculture